2020-12-16

Development of a Highly Efficient Amidoxime Functionalized Cellulose Adsorbent for Enhanced Separation of Vanadium using Acetate as a Complexing Agent

Bakuska, Derrick C. R.

UNIVERSITY OF CALGARY

Development of a Highly Efficient Amidoxime Functionalized Cellulose Adsorbent for Enhanced Separation of Vanadium using Acetate as a Complexing Agent

by

Derrick Charles Robert Bakuska

A THESIS

SUBMITTED TO THE FACULTY OF GRADUATE STUDIES

IN PARTIAL FULFILMENT OF THE REQUIREMENTS FOR THE

DEGREE OF MASTER OF SCIENCE

GRADUATE PROGRAM IN CHEMICAL ENGINEERING

CALGARY, ALBERTA

DECEMBER, 2020

Abstract

Vanadium is a strategic alloying metal that is used in high strength steel for varying applications, from high performance tools to earthquake resistant rebar. However, most vanadium is produced as a by-product of iron ore mining and this cannot meet increasing demand. Several new vanadium deposits, such as stone coal or carbonaceous shales, are suitable for low-cost hydrometallurgical extraction, which involves dissolving metal ions into solution for recovery. Currently, purifying vanadium ions from other dissolved metals is done with solvent extraction, which utilizes organic solvents and toxic extractants.

In this work, a cellulose-based adsorbent material was developed that demonstrates high selectivity towards vanadium. Cellulose powder was functionalized with amidoxime functional groups via a simple two step heterogenous reaction, first adding nitrile groups to the surface followed by conversion to amidoxime. We developed a new hybrid approach for amidoxime functionalization on cellulose which uses fewer reagents under benign conditions, resulting in an adsorbent with high adsorption capacity for vanadium (70 mg g^{-1}). Furthermore, by dissolving acetic acid as a complexing agent, the vanadium adsorption capacity of the adsorbent was found to increase by over a factor of 4, from 70 mg g^{-1} to 330 mg g^{-1}. Additionally, the inclusion of acetate enhanced the selectivity towards vanadium over chromium, increasing from 2.0 ± 0.5 to 7.0 ± 0.2 at an acetate concentration of 0.5 M. When in competition with simple divalent metal ions such as copper or nickel, the adsorbent had a selectivity towards vanadium of more than 150, the lower bound of detectability. Following adsorption, vanadium was found to be easily recovered through elution with dilute sulfuric acid (0.5 M) which makes the adsorbent promising for future applications.

The applicability of amidoxime functionalized cellulose was further demonstrated through the synthesis and utilization of functionalized cellulose beads. Using the insights gained from functionalizing cellulose fibers, cellulose beads were functionalized to yield a similar adsorption capacity per gram of cellulose

while at the same time providing mechanical structure for use in an adsorption column. From adsorption column experiments, the kinetic performance was analyzed, and future optimizations were proposed.

Preface

This thesis is an original, unpublished, independent work by the author, Derrick Charles Robert Bakuska.

Acknowledgements

Throughout my program I received an exceptional amount of support and assistance, without which the results of this work certainly would not have had the same impact.

First of all, I would like to acknowledge my supervisor, Dr. Sathish Ponnurangam. Your willingness to allow me to pursue my own hypotheses gave me valuable experience that typically would not have been expected in a MSc. program. Your attentiveness and insights allowed us to achieve exciting results in a timely manor while at the same time identifying research gaps that could further catalyze work within our group. I am excited to see how subsequent group researchers can utilize our observations to springboard their own experimental work.

I would also like to thank my co-supervisor, Dr. Edward (Ted) Roberts. Your experience in engineering design, and general research insights, greatly helped me clarify my thoughts and determine efficient ways forward. This was clear in both experimental planning as well as communication and without a doubt, the quality of this thesis was improved by your attention to detail and useful suggestions.

I would also like to thank my fellow lab members, specifically Fernanda Pablos and Markus Ingelsson, who contributed valuable discussions and allowed me to bounce around ideas. Their companionship was greatly appreciated and the long hours in the lab were always more enjoyable when they were around.

Lastly, I would like to thank my family members as well as my external friends who provided countless hours of support and enjoyable downtime. Helping me stave off stress and keeping me invigorated undoubtably allowed this work to come to fruition, and without them, the quality of the work would not have been the same.

Table of Contents

List of Figures

List of Tables

List of Abbreviations

[A] – Concentration of species A (mol L^{-1} or mg L^{-1})

C_e – Residual or bulk metal equilibrium concentration (mg L^{-1})

C_o – Initial solution concentration (mg L^{-1})

CHN – Carbon, hydrogen, nitrogen analysis also referred to as elemental analysis

DoF – Degrees of freedom

$D.S._1$ – Degree of hydroxide group substitution following cyanoethylation (Number of cellulose hydroxide groups converted to cyanoethyl, maximum of 3)

$D.S._2$ – Degree of nitrile group substitution following amidoximation (Number of cyano groups converted to amidoxime, maximum of $D.S._1$)

k_{ad} – Adsorption rate constant

k_{de} – Desorption rate constant

K_L – Langmuir constant (L mg^{-1})

K_F – Freundlich constant ($L^{1/n}$ $mg^{1-1/n}$ g^{-1})

M_A – Molecular weight of species A

m_{ad} – Mass of adsorbent (g)

MSA – Mean square amongst

MSW – Mean square within

ppm – Parts per million on a mass basis (mg L^{-1}, mg kg^{-1})

ppb – Parts per billion on a mass basis (μg L^{-1}, μg kg^{-1})

q_e – Equilibrium adsorption capacity (mass of adsorbate per original mass of adsorbent, mg g^{-1})

q_m – Langmuir capacity (mg g^{-1})

r_{ad} – Rate of adsorption

r_{de} – Rate of desorption

RO – Reverse osmosis

R_L – Langmuir separation factor

s – Standard deviation of a sample

SSA – Sum of squares amongst

SSW – Sum of squares within

t – t-value of a student t-test

$V_{solution}$ – Volume of solution (L)

w_A – Mass fraction of species A

$\bar{x}$ – Sample mean

x_i – Resulting value of trial *i*

Chapter One: Introduction and Objectives

Vanadium is a critical metal that is used in a wide range of applications varying from metal alloying to hydrocarbon catalysis. Emerging sources of vanadium are being exploited through the application of hydrometallurgical processes that often utilize unit operations such as solvent extraction that contain toxic chemicals. Therefore, ensuring that future recovery operations are sustainable, alternative methods to substitute for this process are being developed. Due to its similar mechanism to solvent extraction, ion-exchange based technologies are often explored, specifically with regards to chelating functional groups when selective removal is required. By combining effective surface functional groups with environmentally friendly backbones, chelating adsorption may present an attractive alternative both in terms of cost and performance.

This work aims to explore the feasibility of utilizing amidoxime functional groups on the surface of cellulose as an adsorbent for the selective removal of vanadium ions from synthetic leach solutions. In the review of literature outlined in Chapters 2 and 3, several research gaps were identified and investigated. These include the following:

- The development of a hybrid synthesis pathway to reduce operational complexity and lessen inherent safety risks
- Prove that the selectivity of amidoxime towards vanadium is still apparent when using a biopolymer (cellulose) as a backbone as opposed to polypropylene
- Identify potential chelating agents that can enhance both the selectivity towards vanadium as well as the absolute sorption capacity

This work is comprised of seven chapters beginning with Chapters 2 and 3 which are dedicated to background information and literature review, respectively. This is followed by Chapter 4, which describes the experimental methodologies as well as post-experimental data processing techniques utilized in

subsequent results chapters. Chapters 5 and 6 explore experimental results and discussion, with a focus on adsorbent synthesis in Chapter 5 while Chapter 6 focuses on the applications of the adsorbent and analyses the adsorption performance. This work is concluded with Chapter 7 which further discusses the results as well as future work for the next steps of continuing this project.

Chapter Two: Background Information

To improve the accessibility of this work and to provide perspectives on the consequences and applications of the research findings, Chapter 2 provides an overview of necessary topics. These topics include: wastewater treatment technologies, with a focus on ion-exchange and adsorption processes; metallurgical processes, with a focus on hydrometallurgy; and the properties and uses of vanadium. Readers that are familiar with these topics may proceed to Chapter 3 where a more detailed review of the literature relevant to this research is discussed.

2.1 Trends in wastewater treatment and metal recovery

Throughout human history, civilizations have attempted to effectively remove ionic species from water sources. Historically, the focus of these attempts was to desalinate water so that it was suitable for human consumption. In the case of seawater, the process requires the removal of sodium (Na^{+}), calcium (Ca^{2+}), magnesium (Mg^{2+}), and their counter-ions, including chloride (Cl^{-}), and sulfate (SO_4^{2-}). Attempts at understanding the science behind desalination have been documented in the works by Aristotle as well as in the bible, by which both describe using evaporative processes to isolate pure water [1].

However, the removal of ions from aqueous solutions is not limited to the alkali and alkaline-earth metals, as rising environmental awareness has made the removal of other ionic species necessary. In the treatment of residential wastewater, the removal of nitrates and phosphates is required to inhibit eutrophication, which can have severe environmental impacts on the aqueous ecosystem. Similarly, industrial facilities face increasingly stringent effluent standards for dissolved heavy metals, with some of the most concerning metals being chromium, lead, mercury, and arsenic [2]. However, effluent concerns are not limited to these traditional elements, and metals such as copper, vanadium, and nickel are of growing interest. To meet these rising regulations, technologies are continually being developed that

allow for the efficient removal of target ions from aqueous effluent. Some of these technologies include ion-exchange, precipitation, adsorption, membrane removal, and electrodialysis.

Furthermore, while regulations have driven the need to remove problematic ions from the aqueous phase, the treatment technology typically yields a concentrated stream of the target ions, either solid or liquid, that must be either further treated or disposed of. Recently, changing perceptions around environmental sustainability has made it desirable to examine methods to recover valuable materials from these waste streams. This drive is particularly evident for industrial waste where the removed metals hold significant value. As a result, there is a need to develop treatment technologies that allow for the efficient and selective removal of ions so that subsequent recovery can be simplified.

Similarly, diminishing grades for primary metal sources have increased the prevalence of “low-grade” ore bodies being developed. Due to the high quantity of carrier rock, traditional enrichment methods such as flotation are proving uneconomic, leading to the necessity to utilize hydrometallurgical processes which begin with leaching. Subsequent to leaching, purification requires the selective removal of target ions from solution and technologies that improve the efficiency of these processes are in high demand.

The removal of ions from aqueous systems is important to human civilization and the improvement of technologies that facilitate these processes are vital to reduce society’s environmental impact and increase sustainability. In the arid regions of the world, desalination technologies are of growing importance while the development of treatment technologies for wastewater is needed throughout the world. Being able to couple the recovery of valuable products from these waste streams is vital in achieving a circular economy, decreasing the demands for primary sources of material. Key to these applications is the development of ion removal technologies that can selectively achieve separation while being comprised of environmentally sustainable materials and requiring minimal energy.

2.2 Wastewater treatment

Wastewater treatment is a primary concern when addressing the sustainability of society. Increased industrial activity, combined with increased variability in natural water abundance, has exacerbated water scarcity in much of the world. As a result, ensuring that water can be reused is critically important for these regions. Water is utilized in countless industrial processes due to its low-cost and unique physical properties. However, after use, water often contains many dissolved ions which may be hazardous to the environment if released and as a result, different technologies need to be employed to remove these contaminants before release.

In terms of dissolved metals, technologies that are often employed result in the metals being transferred to another phase which must be disposed of, typically a solid sludge. In contrast, depending on the metal recovered, alternative technologies result in a dissolved metal concentrate. Currently, the former set of technologies is most often used due to their simplicity and cost-effectiveness, typically chemical precipitation or filtration. Whereas technologies that may be directly applicable for metal recovery without additional treatment are adsorption/ion-exchange or electrodeposition.

2.2.1 Chemical precipitation

Chemical precipitation is the most widely used aqueous metal removal technology due to the benefits outlined above [3]. When the effluent does not contain organometallic complexes or uniquely soluble metals such as cadmium or mercury, the effluent can be treated to achieve nearly complete precipitation [4]. In many cases, the chemical reagent used is calcium oxide/calcium hydroxide, often referred to as lime. Through the addition of lime, the pH of the wastewater is raised, and the target metal ions will precipitate as metal hydroxides as shown below.

$$\mathrm{M}^{x+} + x\mathrm{OH}^{-} \rightarrow \mathrm{M(OH)}_{x} \downarrow$$

The low cost of lime as well as the simplicity of the process make chemical precipitation attractive for many applications. However, the process does have drawbacks, namely the generation of metal sludge which must be subsequently treated and disposed of. Furthermore, to maintain the simplicity of the process, the pH is not controlled to selectively precipitate specific metals, therefore, the sludge will contain a complex mixture of multiple metals, making it unsuitable for post-treatment metal recovery.

2.2.2 Membrane separation

Membrane separation is an emerging technology that is undergoing widespread deployment due to falling system costs [5]. Using a series of membranes, separation can be designed to remove dissolved organic molecules in addition to dissolved metal ions, a substantial advantage over chemical precipitation. Furthermore, when compared with chemical precipitation, filtration can achieve high throughputs for a given plant footprint, resulting in more efficient use of space. This attribute in particular has allowed filtration to be employed in facilities where space is valued at a premium, such as offshore oil platforms or cruise ships [6] [7]. Filtration technologies can be classified by the membrane pore size and are typically grouped into microfiltration, ultrafiltration, nanofiltration, and reverse osmosis as shown in Table 1 below [7].

Table 1 - Effective particle removal sizes for different membrane processes [7]

Filtration type	Effective filtering size
Microfiltration	0.1 - 3 µm
Ultrafiltration	0.01 - 0.1 µm
Nanofiltration	0.001 - 0.01 µm
Reverse osmosis	0.0001 - 0.001 µm

In the case of metal ion removal, semi-permeable or chemically modified membranes are required, limiting membrane-based solutions to either reverse osmosis, nanofiltration, or enhanced ultrafiltration [5]. During these processes, cross-flow filters are often used to decrease fouling and allow for continual operation with the flow field shown below.

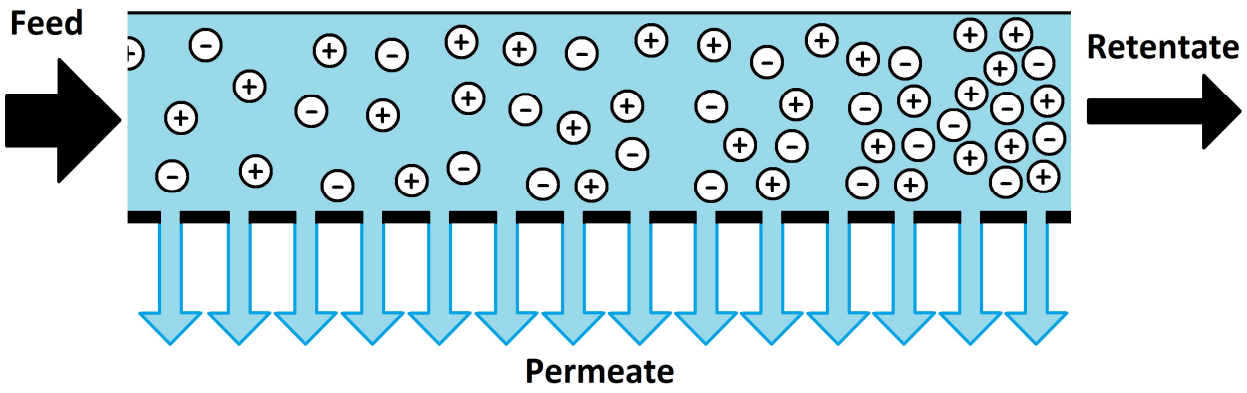

Figure 1 - Schematic of a reverse osmosis filter

While the use of filters produces a metal-free permeate, a metal-rich retentate is produced simultaneously which must be treated. However, since the ion concentration is substantially higher in the retentate than in the feed, subsequent treatment is often more economic when filtration is included. The production of a concentrated retentate also leads to a greater potential in metal recovery as selective metal recovery technologies such as ion-exchange or solvent extraction operate efficiently at high metal concentrations due to the equilibrium nature of the processes.

2.2.3 Adsorption and ion-exchange

Adsorption and ion-exchange are often utilized in wastewater treatment when low concentrations make chemical precipitation impractical [4]. Depending on the functionality of the surface, selectivity of different metal ions can be achieved which can facilitate metal recovery. Similar to membrane processes, regeneration of the ion-exchange medium produces a metal-rich solution from which recovery may be practical. The mechanisms of ion-exchange are discussed in further detail in the hydrometallurgy section later in this Chapter.

2.2.4 Electrodeposition and cementation

If a wastewater stream has a sufficiently high concentration and there are few problematic contaminants, metal ions can be directly recovered from the solution through electrodeposition or cementation. This is often used for wastewaters rich in copper, such as those coming from copper electrowinning facilities [8]. Since the mechanism of removal is strongly dependent on the concentration of the targeted contaminant in the solution, direct recovery is not suitable when the concentration of metal ions is low. Therefore, pre-treatment and concentration will be necessary to make recovery feasible.

2.3 Metal production and recovery

Metals have been utilized in human society for several millennia with some of the earliest uses of pure metal being recorded around 9,000 B.C [9]. In modern society, the use of metals still underpins the principal economic system, and they are used in countless aspects of everyday life. For convenience, metals are typically categorized on a combination of their use and relative abundance, these categories include ferrous and non-ferrous, of which subcategories of non-ferrous metals include base, noble and precious metals. Furthermore, rare-earth metals, which are also classified under non-ferrous metals, are growing in importance due to their unique physical and electrical properties. However, depending on the field of study, different categories and definitions may be adopted. For example, in the treatment of wastewater, metals are often referred to as “heavy metals” due to their aqueous toxicity. However, there is not a well agreed upon definition of heavy metals which can lead to ambiguity.

In terms of usage, ferrous metals, derived primarily from iron are the largest global application of metals. In 2018, global steel production totalled 1.8 Gt, more than 30 times the next most used metal, aluminum at 60 Mt [10] [11]. While iron is the primary component within steel, many strategic metals are utilized to form alloys which have characteristics that can be tuned to each unique application. The most common

alloying metals include manganese, nickel, chromium, molybdenum, vanadium, silicon, and boron, but niche applications can also include aluminium, cobalt, copper, and several others.

To meet the demands for metals, concentrated ore bodies must be exploited and processed to obtain pure useable metal. The complexity of the refining process is highly dependent on the metal as well as the host rock, but free metals rarely exist naturally in metallic form and most must be chemically altered to obtain a useable compound.

For most metals, mining begins with blasting and size reduction, referred to as comminution, after which the refining process can vary dramatically depending on the metal and together these processes are referred to as extractive metallurgy.

2.3.1 Extractive metallurgy

Extractive metallurgy describes the process through which valuable minerals are obtained and purified from a host rock. Extractive metallurgy is comprised of four subcategories: pyrometallurgy, hydrometallurgy, molten salt metallurgy, and vapour metallurgy. Amongst these, pyrometallurgy and hydrometallurgy are the most widely used while the other two are primarily used in niche applications.

Pyrometallurgy

When individuals think of metallurgy, pyrometallurgy is often considered first. These methods comprise of chemically reducing oxidized metal species to pure metallic form, which then naturally segregates from impurities. Iron smelting is the most common usage of pyrometallurgy, but many other metals are produced by a similar technique. Other metals produced through pyrometallurgy include; zinc, lead, and platinum group metals [12]. Currently, most copper is also produced via pyrometallurgy, but innovations within the field has led to most new projects being designed around hydrometallurgical processes.

For ores going down a pyrometallurgic pathway, enrichment above the bulk ore grade is required to improve the economic feasibility of the process. For sulfide minerals, this can be done through a process called froth floatation [13]. Froth floatation exploits the differences in hydrophobicity of different surfaces to selectively separate sulfide minerals from the residual rock. This is achieved through the addition of chemicals called collectors, surfactants that have functional groups with an affinity to the target mineral. A common collector for flotation of sulfide minerals is ethyl xanthate, whose chemical structure is shown in Figure 2 [13].

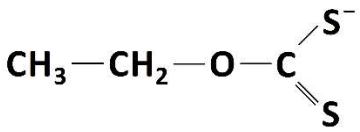

Figure 2 - Chemical structure of the collector ethyl xanthate

Upon addition to the water-rock slurry, the functional group in the collector will selectively bind with the surface of the target mineral, and with a hydrophobic tail, the surface of the mineral will become hydrophobic. Small air bubbles are passed through the slurry and minerals with hydrophobic surfaces will bind with the bubbles, floating to the surface leaving the gangue minerals to the slurry. The resulting froth at the top of the tank laden with valuable minerals is skimmed off and the material, now referred to as concentrate can be shipped to a smeltery.

The efficacy of pyrometallurgy is highly dependent on the concentrate grade which is fed into the smeltery. Due to the high temperatures required for operation, any unwanted material represents inefficiencies and wasted energy. Therefore, the continued feasibility of smelteries is dependent on the ability of flotation circuits to produce highly enriched concentrates. As the world's high-grade mines continue to be exhausted, lower grade ore bodies are being developed which is putting strain on the suitability of froth flotation. For example, for the period 2005 to 2017, average global copper grades have declined from 0.75% to reach a record low of 0.6% in 2017 [14]. As a result, many proposed copper mines

are now looking to utilize hydrometallurgical methods, which are more economic when treating large quantities of low-grade material.

Hydrometallurgy

When metals are processed with the use of water, these methods are referred to as hydrometallurgical processes and can generally be categorized into three unit processes: leaching, solution concentration and purification, and metal recovery.

Hydrometallurgy is typically utilized when several chemically similar desirable metals are held within an ore body or when a high purity product is desired, as is in the case in copper mining. In addition to primary sources, hydrometallurgy is also conducive to recycling of metallic wastes from secondary sources. Applications of secondary sourcing of metals has been rising in recent years with increased international focus on sustainability and two examples of this process can be seen in the recovery of vanadium and molybdenum from waste catalyst as well as metal recovery from printed circuit boards [15] [16]. Altogether, hydrometallurgy allows for the treatment of complex polymetallic samples through ion dissolution and purification steps.

Leaching

Leaching is the first step in hydrometallurgical processing and is designed to strip the host rock of valuable metals and dissolve them into a pregnant leach solution. Several different leaching methods have been developed and continue to be developed to reduce the environmental severity of the process. Leaching with inorganic mineral acids is the most well-known of the processes but alternatives such as leaching with organic acids or bioleaching are being researched due to the environmental impacts of using mineral acids.

Sulfuric acid is commonly used as a leaching solution due to its cost-effectiveness and ease of logistical transport. For mining operations that utilize sulfuric acid, elemental sulfur can be easily transported and stored on-site until synthesis of sulfuric acid is required.

Once synthesized, sulfuric acid can be applied in several different forms, including vat leaching, dump leaching, heap leaching, or pressure leaching. Depending on the grade of material being leached, some methods can be more economically advantageous than others. For example, when the grade is relatively high, vat leaching can be economic due to higher recoveries outweighing the cost of vat construction. Conversely, when the grade is lower, heap leaching can be more economic due to lower capital costs outweighing lower recoveries [17].

Commonly, heap leaching or dump leaching is utilized for large open pit mining operations that are designed for hydrometallurgical processing. In these processes, ore is piled on an impervious liner and is subject to acid addition. Heap and dump leaching are differentiated by the pre-treatment or lack-there-of before piling, with heap leaching ore being subject to comminution, while dump leaching ore does not undergo size reduction following blasting.

Once exposed to the leaching solution, minerals within the host rock undergo chemical reactions to solubilize them. For oxide-based minerals such as copper oxide and iron oxide, the metal cation is replaced through a single replacement reaction with hydrogen ions to form water and, in the case of sulfuric acid, a metal sulfate.

$$\mathrm{CuO} + \mathrm{H_2SO_4} \rightarrow \mathrm{CuSO_4} + \mathrm{H_2O}$$

For certain metals deemed as acid-soluble sulfides, their sulfide mineral can undergo a single replacement reaction similar to that of the oxide and the resulting reaction producing a metal sulfate as well as hydrogen sulfide [18].

Solution concentration and purification

Once the desired metal ions have been transferred to the aqueous phase, several techniques can be utilized to concentrate and purify the solution and produce pure products. Due to differences in the chemical properties of different metals, separation can occur through methods such as liquid-liquid solvent extraction, ion exchange, precipitation and cementation, adsorption, and membrane separation. Amongst these methods, liquid-liquid extraction and ion exchange can be applied to many different scenarios while the remaining methods are typically applied in niche applications that are unique to each metal [19].

Solvent extraction

Of the methods for concentrating and purifying leach solutions, solvent extraction and ion-exchange are widely used for a variety of metals. Mechanistically, both processes are similar, but instead differ in the physical properties of the process. Solvent extraction, also referred to as liquid-liquid extraction, uses two immiscible liquid phases to strip the target metal from the leach solution. Conversely, ion-exchange uses a solid exchange bed, which a leach solution is pumped through [19].

Solvent extraction consists of two immiscible liquid phases; one consisting of the leach solution discussed in previous sections, and the other, an organic phase that contains an extractant and a diluent.

While the diluent does not play a substantial role in the chemistry of the extraction process, the choice of diluent plays a large role in the overall performance of the process due to its physical properties. Diluent used in the process is typically a paraffinic organic compound such as kerosene and is necessary to dilute the extractant to decrease the viscosity of the phase. This results in improved pumpability as well as more dynamic mixing between the aqueous and organic phases, leading to improved mass transfer [19].

The extractant is categorized as one of three types: ion-exchanging, solvating, or coordinating. Amongst the three, ion-exchanging and coordinating share substantial similarities and coordinating extractants often undergo ion-exchange to stabilize a metal coordinate bond.

Solvating extractants do not undergo ion-exchange and their mechanism of interaction is to replace solvating water molecules that occupy the region around a metal ion. This allows the metal to become soluble within the organic phase and by controlling the affinity of the metal ion to each phase, the metal can be enriched into the organic phase. Since the extractant is replacing water in the hydration sphere, extractants that perform this mechanism are typically rich in oxygen groups and an example of an extractant is trioctyl phosphine oxide (TOPO) which is currently marketed by Solvay under the trade name CYANEX 923 [20].

Ion-exchange extractants contain either acidic or basic functional groups, similar to those in solid ion-exchange resins. For metals that exist as cationic species, acidic functional groups are used which include carboxylate or sulfonate. In these groups, protons exist as the counter ion and must be exchanged with a metal cation to facilitate removal from the leachate. As a result, the thermodynamics of the process is highly dependent on the pH of the solution, with there being a lower tendency for an exchange occurring at lower pH values due to the high concentration of protons within the system. For metals that exist as anionic species, the opposite is true and hydroxide ions are exchanged with typical functional groups including quaternary and tertiary amines.

Coordination extractants are highly selective due to the chelation mechanism that is employed. Lone pairs of electrons situated on nitrogen or oxygen atoms can react with metal ions to form a coordinate covalent bond and the use of electrons from two separate atoms can facilitate the formation of a cyclic structure, enhancing its stability. Due to the formation of a cyclic structure, steric effects such as the ionic radius of the metal ion can be influential in the development of the complex, leading to selectivity for the

extractant. Stability of the resulting coordinate complex can be enhanced if one of the coordinating atoms is able to deprotonate. Due to this deprotonation, the pH becomes a critical factor as in ion-exchange extraction and can be used to further enhance selectivity.

Ion exchange

In many aspects, ion-exchange is mechanistically similar to solvent extraction. Ion exchange is a two-phase phenomenon during which either cations or anions exchange bonding with functional groups on a solid surface. Ion exchange media are typically classified into four categories depending on the strength of the bond between the functional group and the mobile ions, these classifications are strong acid, weak acid, strong base, and weak base.

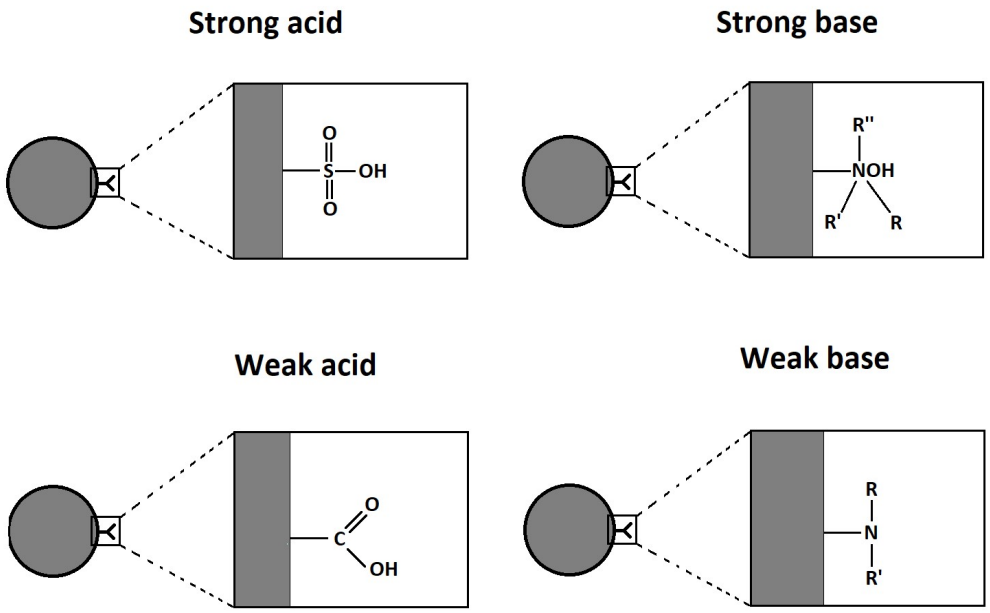

Figure 3 - Example chemistries of strong and weak, acid and base ion-exchange groups

Both strong acids and strong bases are characterized by their insensitivity to the pH of the solution for proper operation. This is a consequence of the high tendency of their functional groups to dissociate. As shown in Figure 3 above, an example of a strong acid is the sulfonate functional group, which depending on the nature of the bond with the solid surface, can have pKa values below −7, indicating deprotonation

under all realistic pH conditions [21]. Conversely, weak acid and base resins require pH control since their capacity is dependent on the pKa values of their functional groups. These weaker ionic interactions can be advantageous when attempting to selectively remove ions as various ions will interact differently with the functional groups. This is often utilized in water softening processes where the resin will exchange with calcium and magnesium but will not exchange significantly with monovalent sodium.

A further subsection of weak acid resins are chelating resins which are specifically functionalized to interact with transition metal ions, and these have the benefit of not meaningfully interacting with alkali and alkaline-earth metals such as sodium, calcium, and magnesium. Since alkali and alkaline-earth metals typically have low toxicity, their removal is not important and for resins that remove them, the effective ion exchange capacity of the resin is reduced. Thus, chelating resins can be highly effective for treating high salinity wastewater streams where decreasing the toxicity is the primary treatment objective.

Chelating adsorption

As previously mentioned, chelating adsorption is typically utilized when it is desirable to remove transition metal ions from an aqueous solution that contains a background electrolyte. This is accomplished by the selective binding of certain functional groups and transition metals over alkali and alkaline-earth metals such as sodium and calcium. Many of the functional groups that are used for chelating adsorption contain either nitrogen or oxygen atoms due to the availability of lone pair electrons.

The mechanism behind chelating adsorption is known as coordinate covalent bonding. Contrasted with covalent bonding, coordinate covalent bonding requires an electron pair to be contributed from a single atom as opposed to one single electron each being contributed by both bonded atoms in covalent bonding. As a result, the energetics of bond formation is normally between that of physical adsorption and chemisorption.

Eigen and Wilkins studied the mechanism of chelation bonding and determined that the reaction is comprised of two steps: firstly the ligand will interact with the hydrated metal complex and secondly, the ligand will replace one or more water molecules for direct bonding with the transition metals [22]. The stabilization of the ligand-metal bond often involves the deprotonation of one or more of the lone-pair donating atoms. As a result, the degree to which bond formation is favourable will depend strongly on the pH of the solution. It is often observed that the chelation affinity of transition metals will increase as the solution pH increases, and this trend can be observed in the data from Wilson et al. shown below in Figure 4 [23].

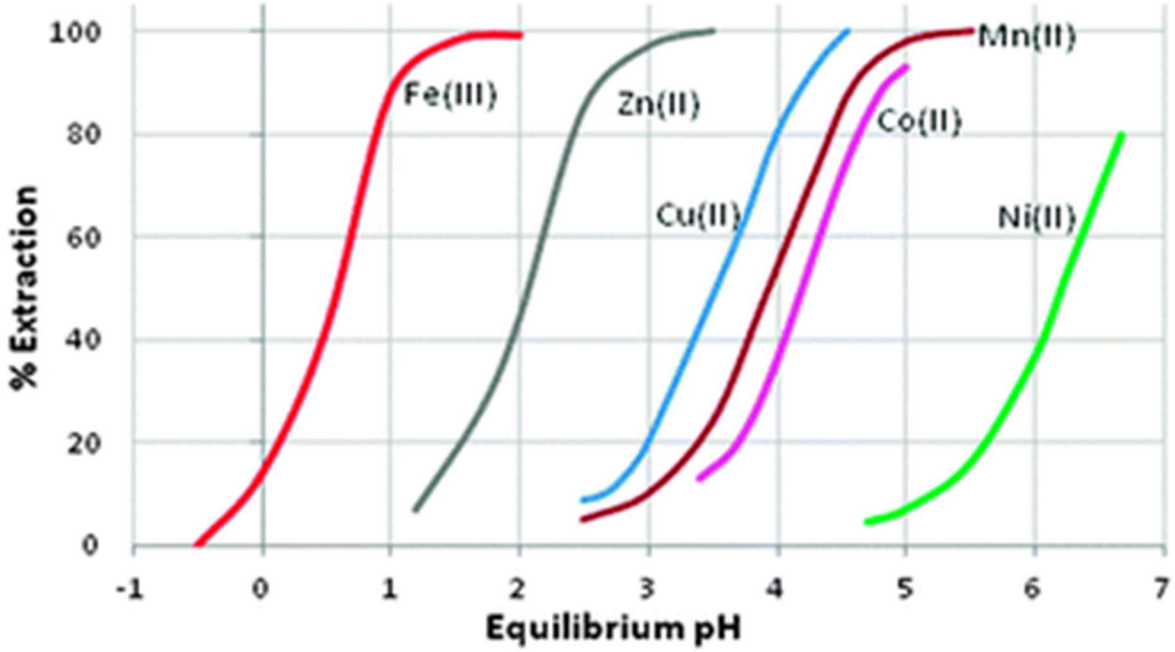

Figure 4 - Extraction efficiencies for separate metals and varying pH values. Figure reproduced from ref [23] under CC 3.0

Importantly, the solution pH not only influences the adsorption of a single transition metal but can be utilized to selectively remove specific ions from a polymetallic solution as shown in Figure 4.

Furthermore, in aqueous environments, the chelating ligand often displaces a water molecule from the hydration shell of a transition metal when a bond is formed. However, if other ligands are dissolved in

solution, different metal-ligand complexes may be formed in the solution bulk, affecting the coordination between the metal and the surface ligands. By utilizing this effect, selectivity of the surface towards particular metal ions can also be improved by appropriate addition of a soluble complexing ligand that can non-uniformly change the energetics of binding for different metals to the surfaces.

Several functional groups have been utilized for bonding with aqueous metal ions and these include; carboxylates, hydroxamates, amidoxime, and amines amongst others [24] [25] [26] [27] [28]. The performance of different functional groups is discussed in further detail in chapter 3. As with solvent extraction, once the desired metal has been chelated onto the adsorbent surface, the ions can be eluted through the application of either acid or base depending on the metal. Metals are then recovered from the concentrated and purified solution which is the final step of hydrometallurgical processing.

Metal recovery

The final operation in a hydrometallurgical process is metal recovery, which produces a saleable product. Recovery of metals from an aqueous solution typically requires reduction of cationic metal ions to the zero-valency metallic state. When starting with a metal concentrate solution, this process typically employs electrowinning to reduce the metal ions. However, depending on the metal, cementation may be a suitable approach, which was discussed previously. Alternatively, electrorefining may be used to treat the relatively impure product coming from smelting to enhance its purity [19].

Electrowinning is the principal method of metal recovery when high purity metal is desired from a concentrated solution. By applying a potential across the solution, metal ions, depending on their standard reduction potential, will be reduced and plated onto the cathode as shown in Figure 5 below. At the anode, water undergoes electrolysis to split into oxygen gas and protons, liberating electrons in the process.

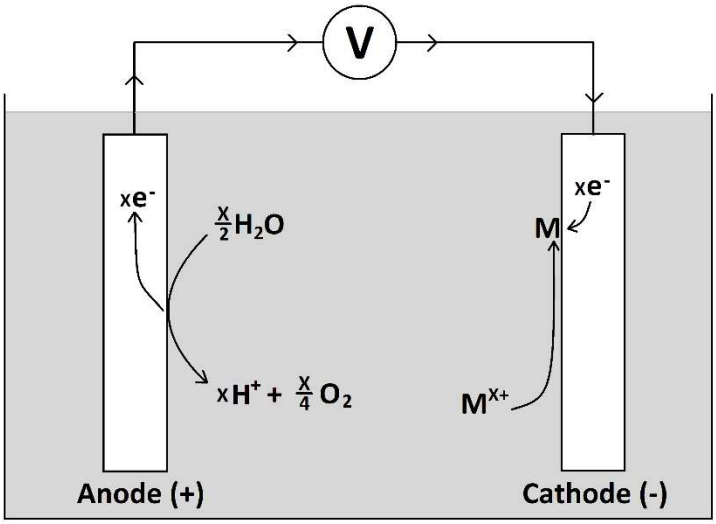

Figure 5 - Schematic of metal electrowinning

For example, during the electrowinning of zinc, the following reactions will occur.

$$\mathrm{Zn}^{2+} + 2e^- \rightarrow \mathrm{Zn} \qquad E^o = -0.76\,V$$

$$\mathrm{H_2O} \rightarrow 2\mathrm{H}^+ + 2e^- + \frac{1}{2}\mathrm{O_2} \qquad E^o = 1.23\,V$$

As seen in the above reactions, the necessary potential to initiate zinc electrowinning is dependent on the pH of the solution as well as the concentration of zinc ions, but at STP conditions, the minimum required potential is 1.99 V. Theoretically, minimizing the required potential can be achieved through increasing the zinc ion concentration as well as decreasing the proton concentration (increasing the pH). However, zinc is difficult to solubilize in high pH environments so little variability can be practically achieved in the proton concentration [19].

For all electrowinning processes, ensuring that only the desired metal undergoes reduction is important in achieving a high purity product. The importance of eliminating undesirable ions from the concentrate solution increases as the reduction of the metal becomes less favourable, i.e. the standard reduction potential of the metal decreases. Therefore, eliminating contaminant ions is substantially more important for zinc electrowinning ($E^o = -0.76\,V$) when compared with copper electrowinning ($E^o = 0.34\,V$). However, the presence of noble metals such as silver are problematic for electrowinning many metals as

their high reduction potential, ($E^0_{Ag} = 0.80\ V$), makes them favourable when compared with any base metal [19].

2.4 Ion-exchange materials

The inclusion of chelating functional groups to materials can enhance their performance, particularly with respect to metal binding affinity but other characteristics could be targeted such as the surface wettability of the material. This is commonly seen in the treatment of carbonaceous materials with acids or other oxidizers to oxidize carbon on the surface to form carboxylate groups. In addition to the chelating ability of these functional groups, having ionic groups on the surface of materials improve their wettability due to their hydrophilicity, allowing more surface area to be effectively accessed.

2.4.1 Polymeric backbones

Successfully utilizing chelating adsorbents often involves the functionalization of a polymeric backbone. While several authors have examined using raw natural materials as adsorbents, these materials are typically characterized by their low adsorption capacities when contrasted with functionalized materials. At the same time, raw materials introduce natural variability that can hamper the reproducibility of results when synthesizing materials.

Thus, the most widely used approach is functionalization of a uniform polymer such as polypropylene and polyethylene, used as a backbone, with suitable functional groups. Polyethylene and polypropylene are hydrophobic polymers and do not dissolve or swell in aqueous systems which can make their utilization simpler. However, adsorption from an aqueous system requires a minimum degree of hydrophilicity to facilitate ion transfer between the aqueous phase and the adsorbent. The addition of functional groups to these polymers serves two roles: to add chemical groups which will bind selectively with the desired metal ion, and to increase the hydrophilicity sufficiently to allow for easy mass transfer. For many

polyolefins, the addition of functional groups is difficult due to their chemical stability and as a result, grafting techniques are required.

Functionalization through grafting

For polymeric chains such as polyethylene and polypropylene, grafting is required to add functional groups to the backbone. Through polymerization grafting, the quantity of functional groups per unit of the backbone molecule can also be increased when compared to functionalizing through a chemical reaction. Grafting is performed via reaction with radicals that are created on the backbone chain and subsequently react with the desired side chain or functional group. Radicals are generally generated via two pathways: exposure to radiation, or through chemical initiators [29] [30] [31] [32].

Exposure to accelerated electrons can provide sufficient energy to generate surface radicals on polyolefins [31]. In this method the polymeric backbone is exposed to an electron beam to generate radicals on the surface and the material is subsequently exposed to the desired grafting agent to complete the reaction. Due to the absence of other chemical reagents, this method can limit the likelihood of side reactions occurring. However, the resulting material properties are highly sensitive to the length and intensity of exposures. Several authors have reported that when conducting this method, the physical properties of the bulk material can deteriorate due to over-exposure to the radiation source [33]. Furthermore, the use of radiation presents inherent process complexity and safety issues. Therefore, chemical initiators have been developed that can facilitate the generation of surface radicals while being highly tunable to desirable reaction conditions.

Chemical free-radical initiators are molecules which contain bonds that can readily deteriorate to form two radical molecules. The most well-known of these is inorganic peroxides which contain an unstable O-O bond. Free radical initiators can be split into two categories depending on the conditions under which they will form radicals: either thermo-radical initiators or photo-radical initiators.

Organic peroxides are often classified as thermo-radical initiators due to their instability, particularly at elevated temperatures. For thermo-radical initiators, their rate of deterioration can be controlled through thermal management which in turn controls the quantity of radicals present within a system. However, due to their instability, storage and utilization of these chemicals is hazardous and improper storage can lead to an exothermic runaway.

Photo-radical initiators are often comprised of aromatic functional groups that are resonance stabilized, providing a large degree of delocalization for a lone electron. As a result, the thermodynamics of radical formation is not as energetically penalizing when compared to molecules without resonance, allowing radicals to be formed under exposure to ultra-violet light. These molecules allow for easy control over the formation of radicals, but their carcinogenic toxicity often limits their application.

Functionalization through chemical reaction

Other polymers are more chemically reactive due to the presence of existing functional groups, and these can be substituted for other functional groups tailored for a specific application. For example, many natural polymers, including cellulose, contain hydroxyl groups that make them susceptible to nucleophilic addition. Similarly, nitrile groups can undergo acid or base catalysed hydrolysis to form carboxylate groups. Having a backbone that is more chemically reactive is beneficial when adding desirable functional groups. However, this comes at the cost of stability as the backbone may be more likely to undergo cleavage, or other reactions, that can result in a decrease in efficacy.

Functionalization of cellulose

A monomer unit of cellulose contains three hydroxyl functional groups that are susceptible to chemical reactions. For the addition of amidoxime functional groups, a functionalization pathway was proposed by Kubota and Shigehisa that did not require grafting through a radical based reaction [34]. The reaction pathway is shown in Figure 6 below and is comprised of two reaction steps. First, cellulose is coated with

tetramethyl ammonium chloride to serve as a swelling agent and the cellulose is reacted with neat acrylonitrile to form cyanoethyl cellulose. Secondly, the nitrile group is reacted with hydroxylamine hydrochloride at high temperatures to form amidoxime groups. By avoiding a radical pathway, the proposed method does not require the use of either peroxides or high energy electrons, reducing the complexity and improving the suitability of the process for commercialization.

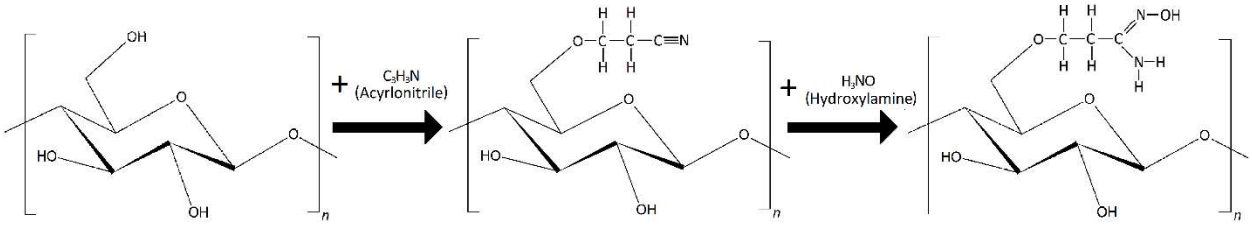

Figure 6 - Two step reaction for synthesizing amidoxime functionalized cellulose

Regardless of the method of adding nitrile functionality to cellulose, amidoximation is thought to proceed at similar reaction conditions [34]. The nitrile groups are exposed to hydroxylamine at elevated temperatures, > 70 °C, and in slightly alkaline conditions, pH 7 – 10, for eight hours or less [34] [35] [36]. The mechanism of functionalization and the importance of reaction conditions is discussed further in Chapter 3.

2.5 Vanadium properties and uses

Vanadium is a critical element that is utilized in a variety of industrial applications, including: alloy manufacturing, catalysis, and redox-flow batteries [37] [38]. With growing demand in all applications, the global market demand for vanadium is expected to grow by 4% per year through 2029 and to meet this demand, new primary sources are being examined for feasibility [39].

Currently, most vanadium is produced as a by-product due to its co-occurrence in iron ore deposits [40]. As a result, the supply from these traditional sources is largely inelastic to the demand for vanadium. This is causing for-purpose sources of vanadium to be examined. Two types of ore deposits are common:

vanadium bearing magnetite; and black shale, often referred to as “stone coal” in China. Each type of deposit requires unique processing methodologies with vanadium bearing magnetite typically following conventional pyrometallurgical processes while hydrometallurgical processes have been proposed for black shale.

Pyrometallurgical processing is performed in a blast furnace and through reduction with carbon, metallic iron is separated from the other elements which concentrate in the slag. To recover vanadium, the slag is roasted with sodium carbonate to produce water soluble vanadium metavanadates which are then leached with hot water. The vanadium rich solution can then be precipitated via the addition of ammonium to form ammonium metavanadate, which is insoluble. The final vanadium product, vanadium pentoxide, V_2O_5, is produced by roasting ammonium metavanadate, decomposing it to vanadium pentoxide, ammonia, and water.

For processing vanadium shale deposits, hydrometallurgical techniques can be utilized due to the ore body being composed of organic carbon as opposed to iron [41]. Several researchers, primarily based in China, have been investigating the optimal conditions for leaching vanadium from shale and a wide range of processes have been proposed [23] [42] [43] [44] [45]. Hydrometallurgy has several advantages over pyrometallurgy for the treatment of vanadium ores, which rarely have a grade above 2% [46].

2.5.1 Catalytic properties

Catalysis is the secondary industrial application for vanadium, in which vanadium’s easy transition between oxidation states is exploited. This property is shared with similar multivalent transition metals such as chromium, manganese, and iron, that are also used extensively in catalytic chemistry.

The most industrially important use is in the production of sulfuric acid, during which vanadium oxide oxidizes sulfur dioxide, SO_2, to sulfur trioxide, SO_3, as shown below [47].

$$V_2O_5 + \ SO_2 \rightarrow 2VO_2 + \ SO_3$$

Vanadium pentoxide is then regenerated through oxidation with oxygen.

$$2VO_2 + \frac{1}{2}O_2 \rightarrow V_2O_5$$

Vanadium has been similarly used for catalytic oxidation in a variety of other reactions, including in the production of peroxides, aldehydes, organic acids, and many others [47].

2.5.2 Redox flow batteries

A more novel application for vanadium is in the energy storage sector as the redox-active species in vanadium redox-flow batteries [48]. While the concept of a vanadium redox-flow battery first emerged in the 1980s, the technology has received increased attention due to the emergence of economically competitive renewable electricity sources. Due to the intermittency of wind and photovoltaic solar there exists a need to store excess energy during times of over-supply and release the energy during periods of under-supply. Flow batteries have risen as one of the solutions to this problem.

While vanadium redox-flow batteries have several advantages over state-of-the-art lithium ion batteries, their economics of deployment is currently hindering advancement. A large component of this is the cost of vanadium electrolyte due to it still being a niche chemical. As discussed above, most vanadium is used in either alloying of steel or chemical catalysts, both of which typically utilize pentavalent vanadium. Redox-flow batteries on the other hand start with vanadium in a tetravalent state through vanadyl sulfate. As a result, additional processing is required to transform the commodity vanadium pentoxide to vanadyl sulfate, increasing the cost of the material. Therefore, lowering the processing costs of vanadium electrolyte is of substantial importance if the economics of vanadium redox-flow batteries are to improve.

2.5.3 Aqueous properties of vanadium

Like other multivalent transition metals, vanadium forms a variety of aqueous complexes, even when only exposed to water as a possible complexing agent. The various aqueous complexes are represented in a Pourbaix diagram, which shows the major species as a function of both pH and oxidation potential of the solution.

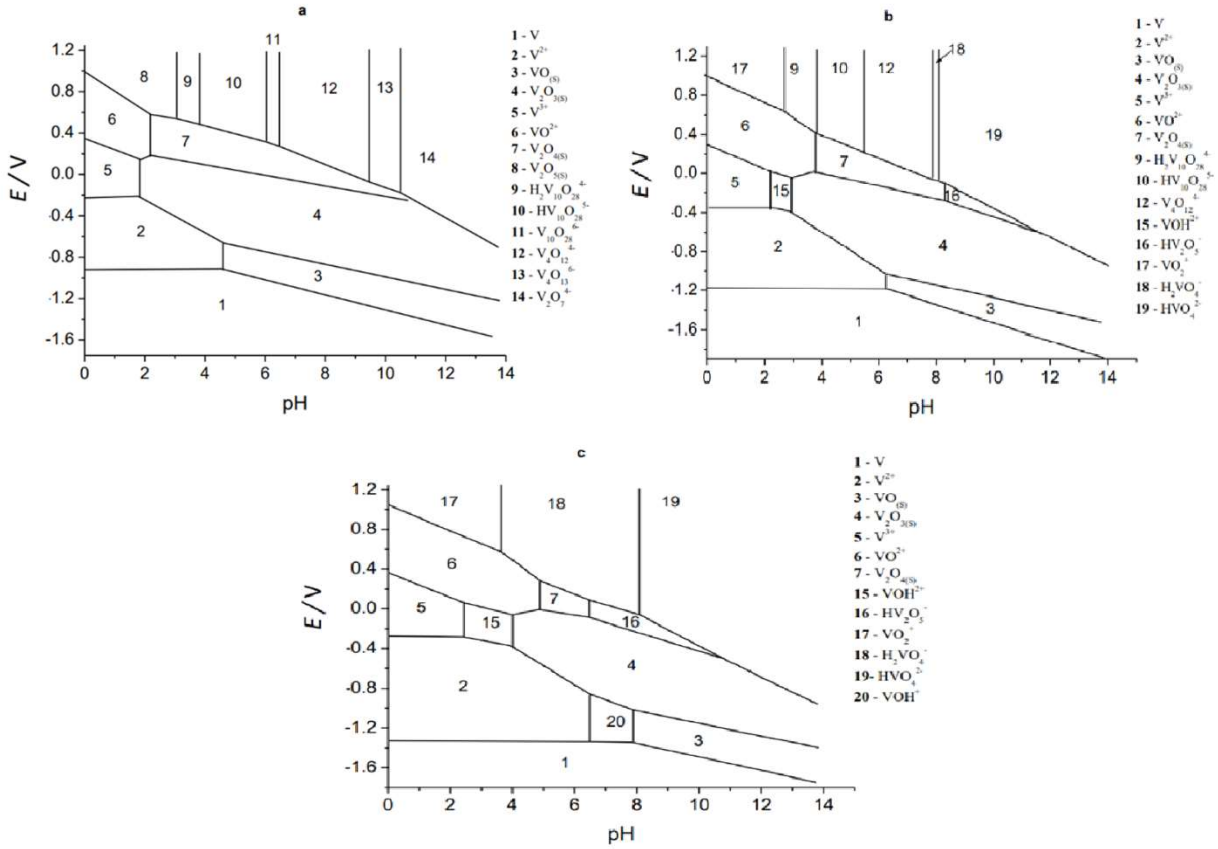

Figure 7 - Pourbaix diagrams of vanadium in water at different concentrations: a) 10 µM b) 1 mM c) 1 M. Reproduced from ref [49] under CC 4.0.

Each Pourbaix diagram is calculated for a specific metal concentration and as shown above, the prominent species will change depending on the total concentration within the solution. As expected, at lower concentrations the tendency to precipitate is lower, which is seen when comparing all three diagrams. At a concentration of 1 M, the solution at a potential of 0 V will be stable until a pH of approximately 2.3. Conversely, at a concentration of 10 µM, the solution will be stable up until a pH of approximately 4. As

mentioned above, the Pourbaix diagrams describe the equilibrium species for dissolved vanadium in water, without any additional ions present. Therefore, the inclusion of other ions, especially anions, can change the equilibrium behaviour by forming complexes which can both stabilize or destabilize dissolved vanadium ions. This is explored further in Chapter 3, where the influence of a complexing agent can have substantial impacts on the speciation and as a result, the affinity towards adsorbents or extractants can be modified.

Ultimately, the processes of metal recovery and wastewater treatment are mechanistically similar, especially with a growing trend towards hydrometallurgy. The application of selective functional groups can allow for specific metal ions to be efficiently recovered, either from leach solutions or wastewater streams. Ion-exchange materials are suitable for use in these applications and new methods for functionalizing naturally occurring biomass can increase the sustainability of the industry. For this study, vanadium was the targeted metal due to research gaps in its hydrometallurgical processes and its increasing importance in society. Altogether, the development of improved aqueous processes will be vital for the transition to a circular economy which will lead to enhanced sustainability.

Chapter Three: Literature Review

The removal of heavy metal ions from aqueous streams has been extensively studied for many years and has been discussed in the previous chapter in generic terms. However, for the context of this report, a deeper discussion of the academic research on several relevant topics is needed to understand how recent advances have contributed to the hypotheses that are examined in the subsequent chapters. These topics involve: the methodologies for functionalizing cellulose powders; the utilization of amidoxime as a functional group for heavy metal adsorption; preparation of cellulose beads; aqueous complexing agents and their influence on adsorption performance; and modelling of adsorption data and determining the suitability of isotherm models in describing experimental observations.

3.1 Cellulose as an adsorbent backbone

Cellulose is the most abundant biopolymer on Earth and has been researched significantly as an adsorbent material for the removal of both heavy metals and organic dyes. In addition, due to its unique chemical and physical characteristics, functionalized cellulose has found applications as filters (cellulose acetate) and food additives (carboxymethyl cellulose) [50] [51]. Several of these characteristics make cellulose beneficial for use in adsorption including the ability to easily undergo chemical functionalization. The ease of functionalization is due to the presence of hydroxyl groups that can easily be deprotonated, allowing electrophilic addition reactions to proceed. Furthermore, cellulose may be functionalized through polymeric grafting which greatly expands the amount of functionalization combinations that are possible. Altogether, the abundance of cellulose, combined with many avenues for functionalization, make the material an active research topic, catalysing the development of sustainable water processing technologies.

Cellulose is a complex organic polymer that is difficult to dissolve in solvents due to strong intermolecular hydrogen bonds and the overall hydrophobicity of the polymer which results from a lack of ionic

functionalities [52]. Furthermore, the structural complexities of cellulose, with several crystalline structures being documented, can result in widely varying properties, not unlike metallic crystals. Indeed, research into the crystal structures of cellulose is constantly progressing and four crystalline structures have been identified: Cellulose I, II, III, and IV [52].

As its core, cellulose is comprised of beta glucose monomers, as shown in Figure 8, which combine to form polymeric chains. The orientation of these chains with respect to each other will greatly change the properties of the material. Most importantly, the orientation of the hydroxy methyl group will influence how tight the packing of the polymeric chains will be as well as the strength of the hydrogen bonds [53].

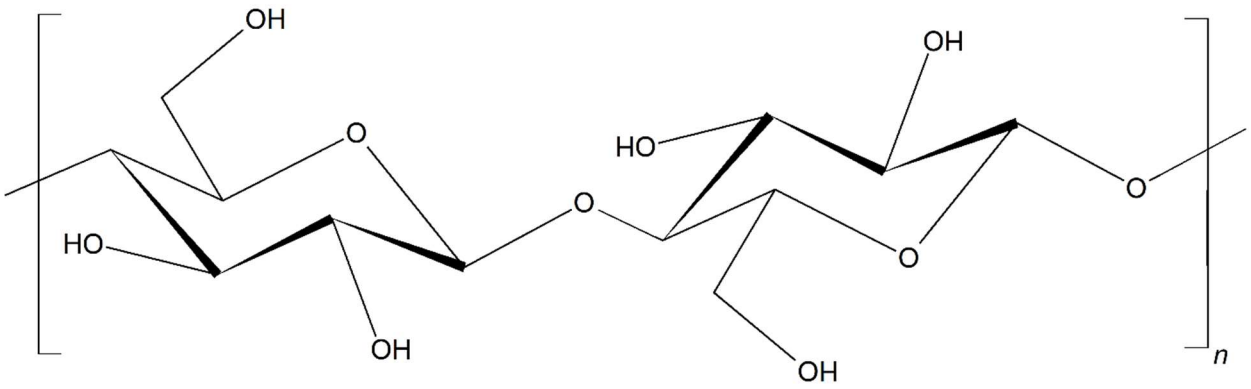

Figure 8 - Cellulose chemical monomer

In nature, cellulose is principally found as cellulose I, a structure which is controlled by the enzymic processes that form the structure of cellulose in living plants [53]. However, this structure of cellulose is not the most thermodynamically stable and several of the bonds are strained because of the enzymic process. Therefore, under conditions that relax the rigidity of the polymer, the chains may re-orient themselves to form a more stable structure, known as cellulose II, as shown in Figure 9 [53].

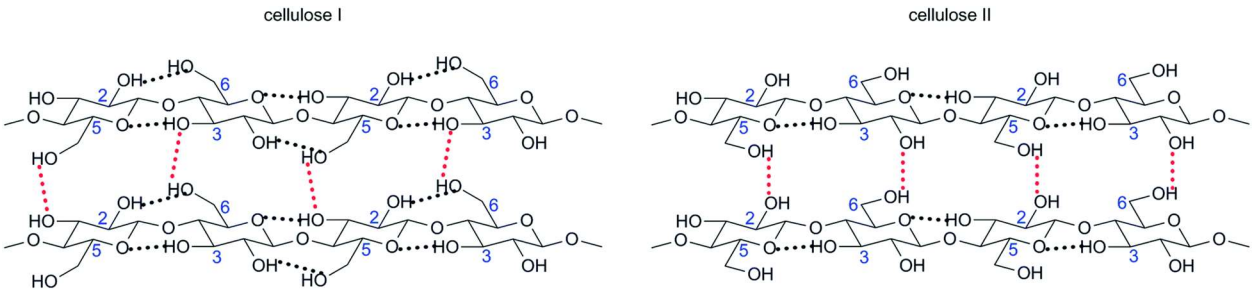

Figure 9 - Change in cellulose structure from cellulose I to cellulose II [53]

The process of changing natural cellulose I structures to cellulose II was first observed in 1844 by John Mercer, who dispersed cotton fibers in a solution of concentrated sodium hydroxide [52]. While it was unknown at the time, the immersion of cellulose fibers in concentrated sodium hydroxide allowed the hydrogen bonds to be sufficiently weakened to allow for the cellulose chains to reorganize themselves into cellulose II. The resulting cellulose structure was found to have increased tensile strength and dye uptake properties, two highly favourable characteristics for the textile industry. The increased affinity for dyes is now believed to be due to the increased availability of hydroxyl functional groups in cellulose II as opposed to cellulose I. This can be highly beneficial for adsorption as the functionalization of cellulose is often dependent on the chemical reactivity of hydroxyl groups. Therefore, it is likely that the conversion of cellulose I to cellulose II would enhance the adsorption performance of the resulting product due to the potential to increase the degree of functionalization as well as enhancing the specific surface area of the material.

While many raw, natural cellulose fibers have been shown to have adsorbent properties toward metals, these interactions are largely based on bonding between the metals and naturally present functional groups that already exist in the cellulose. For example, in a study performed by Saliba et al., wood sawdust was found to naturally have an adsorption capacity approaching 1 mmol g^{-1} for both copper and chromium [54]. To further develop the capacities of these materials, researchers have functionalized cellulose with a variety of functional groups including but not limited to: carboxylate, amino, amidoxime, amide, quaternary ammonium, hydroxamic, thiol, and imidazole. While the chemical structures of many of these

groups may vary, on a fundamental level, all of the examined groups will contain sulfur, nitrogen, or oxygen, from which lone pair electrons will be able to interact with the dissolved metal cations and immobilize them. Therefore, a further examination into the adsorption performance for each of these elemental groups is justified for understanding their suitability for adsorption applications.

3.1.1 Oxygen functionality – Carboxylate

The addition of carboxylate groups is one of the most studied functional groups for cellulose due to the ease of its addition. Carboxylate can be added to cellulose through chemical means through treatment with acids or through the electrophilic addition of compounds such as succinic anhydride [55] [56]. Due to commonalities in the functionalization process, researchers primarily differentiate their work through different biomass feedstocks on which the functionalization is performed. Due to the natural variability in the composition and structure of organic matter, these feedstocks can produce dramatically different results [57].

Alternatively, carboxylate groups can be added through polymeric grafting with carboxylic acid containing polymers, such as polyacrylic acid, using initiators, for example, UV exposure or permanganates [58]. The functionalization agent as well as the resulting adsorption capacities obtained in studies of carboxylate groups are shown in Table 2.

Table 2 - Adsorption performance for carboxylate functionalized cellulose materials with different cations

Reagent	Metal	Capacity (mmol g^{-1})	Capacity (mg g^{-1})	Reference
Grafted polyacrylic acid	Cu (II)	1.64	103.6	[58]
	Cd (II)	1.49	167.5	
	Ni (II)	1.66	97.4	
Acrylonitrile hydrolyzed to carboxylate	Cr (III)	1.71	88.9	[59]
	Cu (II)	1.31	83.6	[60]
Citric acid treated wood sawdust	Cu (II)	0.373	23.7	[55]
	Pb (II)	0.399	82.6	
Succinic anhydride reacted with mercerized cellulose	Cu (II)	2.42	153.9	[61]
	Cd (II)	2.22	250	
	Pb (II)	2.41	500	
Succinic anhydride reacted via solventless pan-milling	Pb (II)	2.03	421	[62]
Cellulose reacted with molten succinic anhydride	Co (II)	2.46	144.9	[56]
	Ni (II)	2.46	144.4	
Succinic anhydride reacted with cellulose nanocrystals	Pb (II)	1.77	367.6	[63]
	Cd (II)	2.3	259.7	

While many of the studies shown in Table 2 have utilized similar functionalization procedures, several key ideas are of importance. It can be observed that while the adsorption capacity of the materials can vary widely, carboxylate appears to have similar adsorption mechanisms regardless of the metal adsorbate. While the adsorption capacity on a mass basis varies, when normalized to molar concentration most materials perform similarly regardless of the metal. This suggests that for the metals being adsorbed, the carboxylate groups are undergoing a simple ion exchange reaction. Hence, achieving a highly selective separation using carboxylate-functionalized cellulose can be challenging.

Furthermore, it has also been observed by Gergel et al. that mercerized cellulose has enhanced adsorption capacities when compared with the other materials as shown in Table 2 [61]. This reinforces the ideas

discussed previously, that altering the cellulose structure to cellulose II can be beneficial for enhancing the adsorption capacity due to the increased availability of hydroxyl functional groups.

3.1.2 Nitrogen functionality – Amine

Amine functional groups are another possibility for interacting with aqueous metal ions. The addition of amine groups into cellulose is more difficult than adding carboxylate groups and typically requires an extra reaction step. For reactions proceeding through the hydroxyl group, typically an epoxy functional group is added, onto which the amine functionality can then react [64] [65] [66] [67]. As with the addition of carboxylate groups, amine groups can also be added through radical reactions with chemical or UV initiators [68]. Some of the resulting adsorption capacities are shown in Table 3.

Table 3 - Adsorption performance for amine functionalized cellulose materials with different cation and anions

Reagent	Metal	Capacity (mmol g^{-1})	Capacity (mg g^{-1})	Reference
Polyethyleneimine reacted with Epichlorohydrin	Hg (II)	1.44	288	[66]
Poly (N,N-dimethyl aminoethyl methacrylate	As (III)	0.12	8.96	[68]
	As (V)	0.37	27.93	
Grafting glycidyl methacrylate then reacting Tetraethylenepentamine	As (III)	0.076	5.71	[65]
	As (V)	1	75.1	
Grafting glycidyl methacrylate then reacting with ethylenediamine	Cr (VI)	3.29	171.5	[67]
Grafting allylamine	Cu (II)	0.564	35.83	[64]
	Pb (II)	0.268	55.65	
	Cd (II)	0.61	68.57	
Reacting aminopropyltriethoxysilane	Ni (II)	3.09	181.4	[69]
	Cu (II)	2.59	164.6	
	Cd (II)	3.47	390	
Addition of acrylonitrile followed by modification to amines	Cu (II)	1.47	93.6	[70]
Grafting glycidyl methacrylate followed by reaction with aminomethyl pyridine	Au (III)	2.73	537	[71]

Amine groups offer many interesting characteristics that are not seen in carboxylate groups, namely the ability to bond with anionic complexes. As seen in Table 3 above, amine groups are able to adsorb metals that typically form anionic complexes such as arsenic as well as hexavalent chromium [65] [67] [68]. This is due to the ability of amine groups to bond their lone pair with a proton at low pH values, making the surface functional group cationic. Anionic complexes are then able to interact with the functional group through charge neutralization. Therefore, nitrogen functional groups can have unique applications where a target metal forms anionic complexes as opposed to co-ions which can only exist in cationic forms, making a highly selective extraction.

3.1.3 Sulfur functionality – Thiol

Sulfur functional groups have also been investigated for use in adsorbent materials. As discussed in the background information, sulfur compounds have been used extensively in the metallurgic community due to its strong binding affinity with metals, most often as a precipitation agent because the binding strength results in an exceptionally low solubility constant. These properties can be exploited for use as an adsorbent due to the aqueous bonding complexes that can be formed. However, the cyclability of sulfur based absorbents can be problematic due to its poor chemical stability and one author that reported on cyclability showed that the capacity of the adsorbent was reduced by 90% after only 9 cycles [72].

Table 4 - Adsorption performance for thiol functionalized cellulose materials with different cation and anions

Reagent	Metal	Capacity (mmol g^{-1})	Capacity (mg g^{-1})	Reference
Thioglycolic acid followed by reduction with sodium sulfide	Cu (II)	1.41	89.5	[73]
	Pb (II)	1.01	209.5	
	Zn (II)	3.48	227.4	
	Cd (II)	2.7	303.3	
Thioglycolic acid	Pb (II)	0.22	44.8	[74]
Oxidized cellulose grafted with cysteine	Pb (II)	0.66	137.7	[75]
	Cr (VI)	1.68	87.5	
Thioglycolic acid	Hg (II)	0.055	11	[76]
Grafting of glycidyl methacrylate followed by reaction with thio-urea	Pt (IV)	0.21	40.5	[77]
Reaction with 3-mercaptopropionic acid	Hg (II)	0.95	190	[72]
Reaction with 3,3'-dithiodipropionic acid	Cu (II)	0.77	49	[78]
	Cd (II)	0.408	45.9	
	Pb (II)	0.11	22	
Oxidation to 2,3-dialdehyde cellulose followed by reductive amination with cysteine and 2-picoline-borane	Pd (II)	1.23	130.4	[79]
Oxidized cellulose reacted with (3-mercaptopropyl)-trimethoxysilane	Hg (II)	3.49	700	[80]

For many of the studies performed on the addition of thiol functionalization to cellulose, the reaction pathways are similar, often utilizing either thioglycolic acid or the amino acid, cysteine. However, as the name suggests, cysteine contain amino functionalities in addition to a carboxylate functional group. Therefore, it would be hard to differentiate the contribution for each functional group in quantifying the adsorption capacities.

In terms of adsorption performance, the results vary significantly from study to study as shown in Table 4. However, as an outlier for performance while functionalizing with thioglycolic acid, Chai et al. reduced the adsorbent with sodium sulfide following the addition of thioglycolic acid [73]. The authors speculated

that during the reaction with thioglycolic acid, two adjacent thiol groups may undergo oxidation to form disulfide bond between them as shown in Figure 10 below.

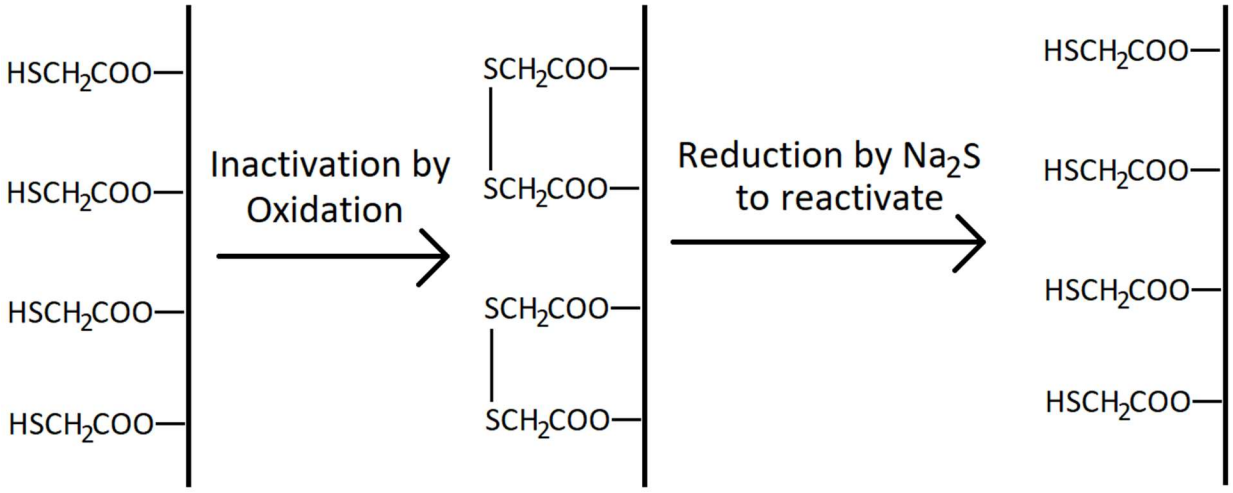

Figure 10 -Thiol functionalization reaction as proposed by Chai et al. [73]

Indeed, thioglucolic acid has been observed to easily oxidize to form dithiodiglycolic acid wherein the two sulfur atoms will bond together [81]. Therefore, it is feasible that the bonding of these sulfur atoms is inhibiting the adsorption performance of the materials synthesized by other authors that do not reduce the oxidized material. This sensitivity of oxidation, not only to dithiols but potentially further to sulfonic acids, can limit the cyclability of the materials and cause rapid degradation of capacity as observed by Ram and Chauhan [72].

Ultimately, oxygen, nitrogen, and sulfur functionalities have different selectivities when used as adsorbents as well as remarkably different stabilities. While oxygen functional groups are highly stable in a variety of environments, there is little to no selectivity with regards to different metal ions which can make applicability difficult when trying to isolate and purify different metals. On the other hand, sulfur-based functionalities have been shown to develop high selectivity towards particular metals which can be useful for industrial applications. However, sulfur groups typically have low stability due to their tendency to oxidize, forming fewer active functionalities or ultimately oxidizing to sulfonates, effectivity an oxygen

functional group. Nitrogen functional groups have been observed to provide a mix of these attributes, having demonstrable selectivity towards certain metals while also remaining stable in several different environments. These properties can be beneficial for many applications where the cyclability of an adsorbent is a key performance metric in determining the economic feasibility of the process.

3.2 Mixed oxygen and nitrogen functionality – Amidoxime

Amidoxime is a mixed oxygen and nitrogen functional group that has the structure shown below in Figure 11. Due to the presence of both oxygen and nitrogen it is expected that the functional group will have hybrid characteristics of both, including wide applicability and stability while also maintaining a degree of selectivity. Indeed, amidoxime has been demonstrated as an adsorbent for a variety of metals including; uranium, titanium, nickel, copper, vanadium, iron, silver, mercury, gallium, as well as a multitude of rare-earth elements [34] [82] [83] [84] [85]. Amidoxime has also been found to be selective towards particular metals, and one of the main research areas is its use for selective recovery of uranium from seawater [86].

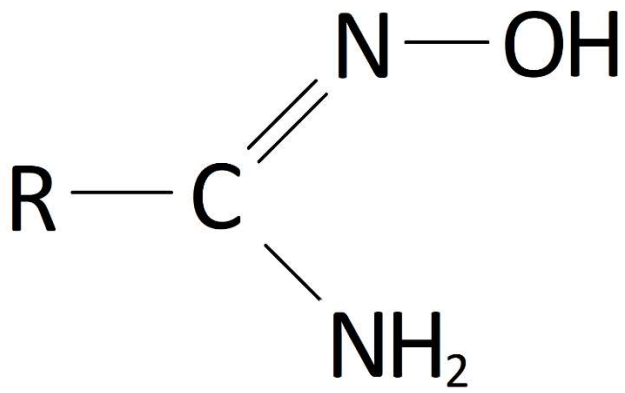

Figure 11 - Structure of the Amidoxime functional group

It has been observed that the amidoxime ligand will interact with aqueous metal ions through chelation wherein the amidoxime group will act as either a monodentate or bidentate species [82]. However, since three active chelating atoms are present in the functional group, it is feasible that a tridentate structure could be formed, although the formation of such a group would likely be unfavourable due to the steric orientation of the atoms and disruption of the carbon-nitrogen pi bond.

The nature of adsorption for different metals is being actively studied, particularly with respect to the adsorption of vanadium and uranium from seawater. Beginning in the 1980s, researchers in Japan were examining methods for recovering uranium from seawater as an alternative to traditionally mined sources, for both national security and increased sustainability [87]. After initially trying with hydrated titanium oxides, researchers identified the amidoxime functional group as a promising alternative [88]. As observed in a subsequent study, uranium was able to selectively bond with amidoxime groups and even though uranium exists in sea water at concentrations of only 3.3 ppb, the amidoxime functionalized fiber was able to achieve a loading of 0.57 mg g^{-1} [86]. This loading was reached even with other cations such as Ca^{2+} and Mg^{2+} present at concentrations over 100,000 times greater than that of uranium, and the loadings of Ca^{2+} and Mg^{2+} only reached 12.7 and 13.1 mg g^{-1} respectively.

However, another unexpected outcome was the significant adsorption of vanadium onto the fiber which reached a higher concentration factor and loading than uranium. While the concentration of vanadium in sea water is only 1.5 ppb, the loading on the fiber was 1.8 mg g^{-1} which demonstrates that amidoxime forms stable chelating bonds with vanadium. When contrasted with the adsorption capacity of uranium, the selectivity towards vanadium is further emphasized when accounting for the differences in molar mass. By normalizing with respect to the atomic mass of each element, the quantity of uranium adsorbed was 2.4 µmol g^{-1} while for vanadium it was 35.4 µmol g^{-1}, signifying that more than 10 times as many bonding sites are interacting with vanadium over uranium, assuming a similar chelate bond. Therefore, it is feasible that amidoxime will be highly selective towards vanadium in other applications, such as mining or waste recovery.

When used in uranium extraction, functionalization was often performed through graft polymerization onto a chemical inert backbone such as polypropylene or polyethylene so that the mechanical strength of the fiber can be maintained during long-term exposure in seawater [86]. Initially, acrylonitrile was grafted onto the polymeric backbone and subsequently reacted with hydroxylamine to form the amidoxime group

[89]. However, other methods were applied by authors to increase the quantity of amidoxime groups within the adsorbent. For example, utilizing a method discussed in the previous section, Kavakli et al. first grafted the epoxy glycidyl methacrylate onto the backbone and then chemically reacted 3,3'-iminodipropionitrile to yield the nitrile groups which were then converted to amidoxime via hydroxylamine [90]. By doing so two amidoxime functional groups could theoretically exist at each grafting location. However, at the time most research on this topic was applications based and as a result, comparison between different works is difficult. Regardless, the authors reported a "normalized" adsorption quantity of 2.5 mg g^{-1} and 2.6 mg g^{-1} for uranium and vanadium respectively, although the method of normalization used assumes that the quantity adsorbed is linearly proportional to the volume treated and as a result, assumes the adsorbent will never be saturated, which is erroneous [90].

Research into understanding the nature of the bonding between amidoxime and uranium or vanadium has continued through both experimental and computational studies which has allowed further insights. As expected, the oxidation state of vanadium is thought to play a substantial role in bonding with different functional groups as discussed by Ivanov et al. and Parker et al. [91] [92]. In the study by Ivanov et al. the authors examined the bonding of V(V) with different amidoxime groups, including a cyclized dioxime, glutaroimide-dioxime. Interestingly, they found that V(V) develops an exceptionally strong bond with glutaroimide-dioxime but does not interact significantly with a basic amidoxime functional group. Curiously, Parker et al. reached a similar conclusion although they were studying the interactions between V(IV) and amidoxime ligands [92]. They observed that V(IV) was able to be easily oxidized after bonding with glutaroimide-dioxime, forming the same bonding complex that was identified by Ivanov et al. This can be explained by the ease at which vanadium will change its oxidation states as exemplified through its use as a catalyst and therefore, it is possible that the reason why vanadium has been observed to bond selectively with different functional groups is that it is able to easily change its oxidation state, rapidly establishing a low energy complex that depends on the surrounding availability of ligands.

Due to its chelating abilities, amidoxime has also been investigated for removing heavy metals from wastewater and a wide variety of biomass has been examined for use in the field [36]. As discussed in the previous section, cellulosic materials have attracted many authors to explore their functionality due to their abundance and ease of functionalization. Amidoxime was added to cellulose by Kubota et al. through a method of grafting acrylonitrile in the same way as was being performed on polypropylene [34]. The authors examined the adsorbent for removal of Cu, Ni, and Cr, and found amidoxime bound with all the cations, although they did not generate adsorption isotherm data to determine the adsorption capacity of the material. Interestingly, the authors observed that at longer amidoximation times, the quantity of amidoxime groups available for bonding decreased while the nitrogen content was largely stable. They hypothesized that the amidoxime groups were undergoing a subsequent reaction to form cyclic imide dioximes (see Figure 12), whose formation has been documented in other studies [93].

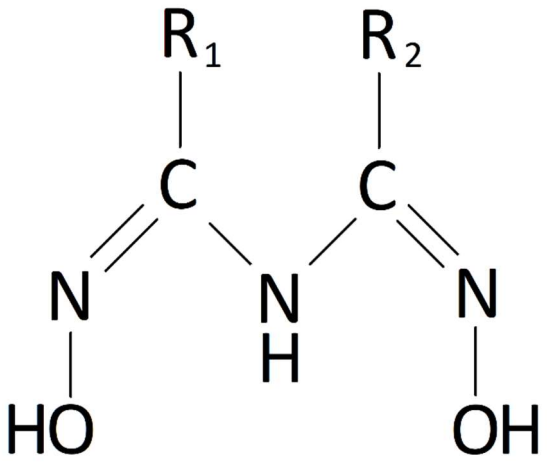

Figure 12 - Imide dioxime from the cyclicization of amidoxime functional groups.

The formation of cyclic imide dioximes can be unfavourable for certain applications since the formation of a cyclic ring will decrease the quantity of amidoxime groups available for bonding as the ring exists as only a single tridentate chelation site as opposed to two bidentate sites. Furthermore, cyclic imide dioximes have been observed to be unstable in the acidic environments used for elution of the adsorbed metals, quickly hydrolyzing to carboxylates which lose the desired selectivity [93]. Therefore, it is thought

to be desirable to minimize the formation of cyclic functional groups and attempt to maintain amidoxime groups as a bidentate bonding site. In doing so, this would both increase the quantity of bonding sites available for metal adsorption and improve the cycling stability of the material.

As an alternative to grafting, cellulose can be functionalized chemically as discussed earlier in this chapter. Due to the presence of hydroxyl functional groups, acrylonitrile can be chemically reacted with cellulose through nucleophilic addition wherein the hydroxyl functional group will react with the primary carbon of the carbon-carbon double bond, creating cyanoethyl cellulose. To accomplish this, the reaction is done in an alkaline environment where there is a high probability of the hydroxyl group being deprotonated, increasing the nucleophilicity of the atom. The mechanism of the reaction is shown in Figure 13 below.

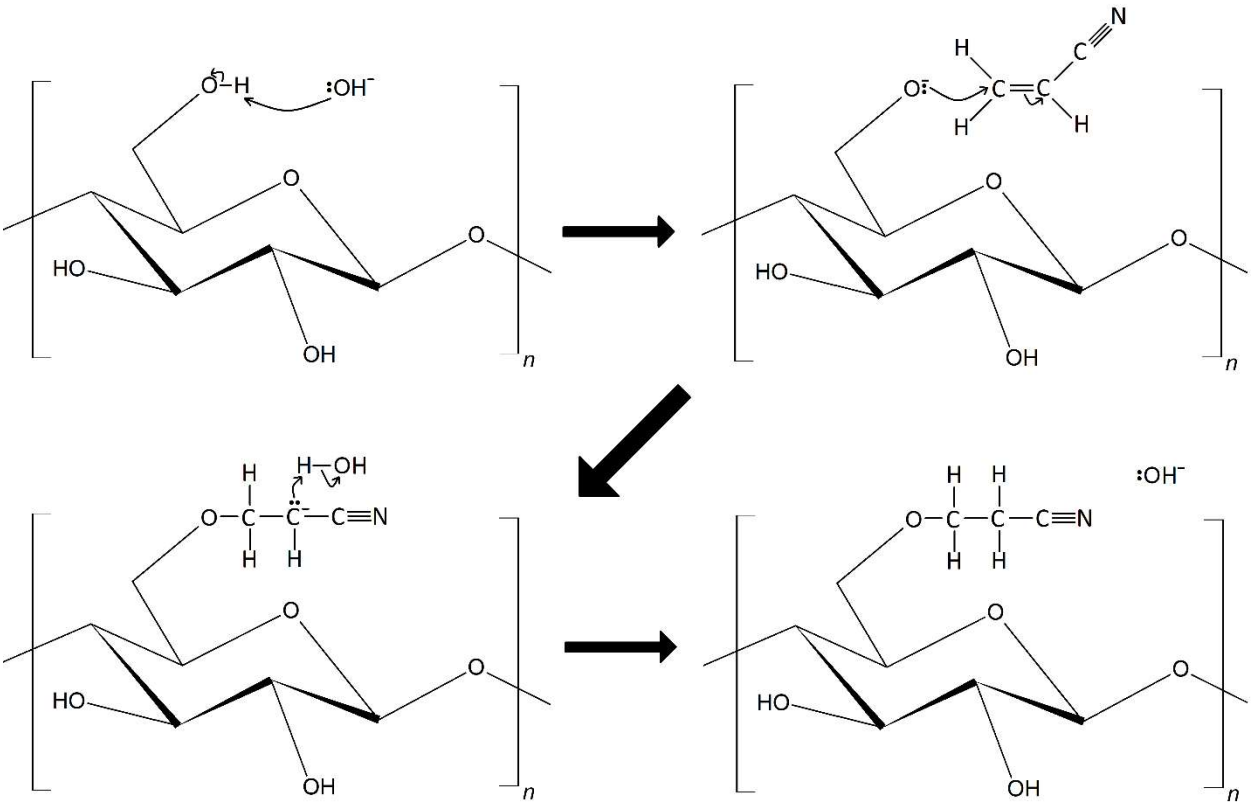

Figure 13 - Mechanism of cyanoethyl cellulose synthesis

As seen in the mechanism, the efficacy of the reaction will be dependent on the initiation step of deprotonation of the hydroxyl groups. In the synthesis method proposed by Kubota et al., the authors

slurried cellulose powder in a solution of acrylonitrile in which a small amount of concentrated sodium hydroxide solution was added [34]. To assist in the reaction, the cellulose was first atomized with a swelling agent, tetramethyl ammonium chloride, which acts to improve the surface area available for functionalization. The cyanoethyl cellulose was then functionalized to amidoxime functionalized cellulose via a reaction with hydroxylamine hydrochloride which had been neutralized to a pH value between 9 and 10 at elevated temperatures (80 °C), following the mechanism shown in Figure 14. The details for both reactions are discussed further in Chapter Four: Materials and Methods.

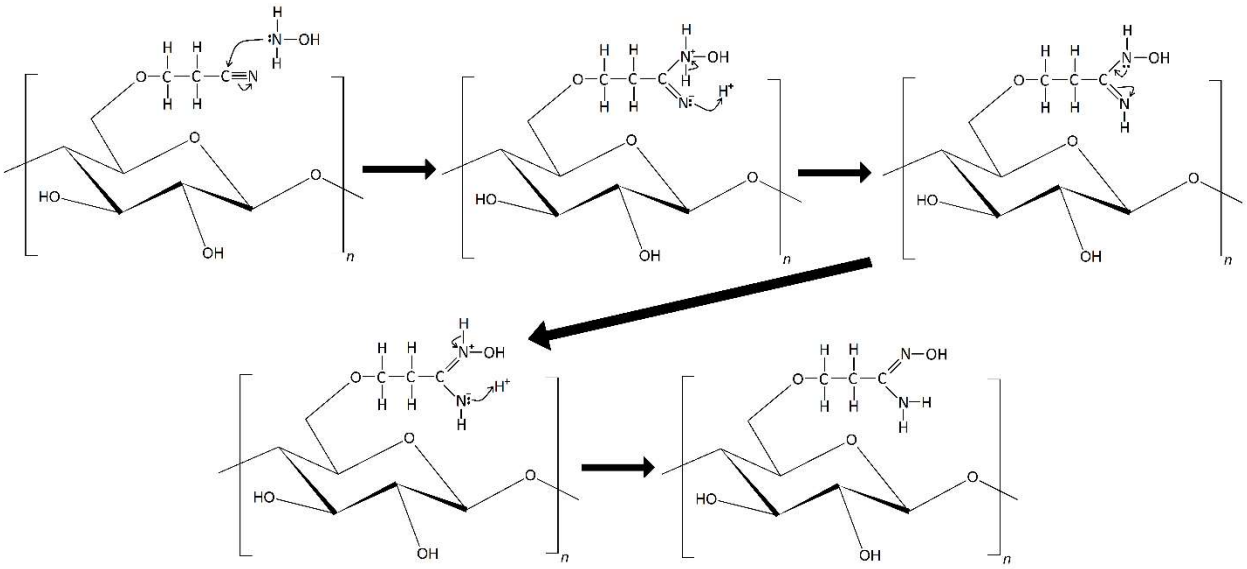

Figure 14 - Mechanism of amidoxime functionalized cellulose synthesis

It can be seen through the mechanism that the reaction will be dependent on the de-protonation of hydroxylamine hydrochloride shown in the first step of Figure 14. Therefore, it is expected that the reaction will require an alkaline environment to proceed which is consistent with conditions used by Kubota et al. However, at the elevated temperatures used, an alkaline solution will also promote the hydrolysis of nitrile groups to carboxylate. As a result, a slightly alkaline environment is desirable to limit the likelihood of hydrolysis occurring and to promote the conversion of cyano groups to amidoxime.

Another interesting result that was observed by Kubota et al. was that the adsorption capacity of the material towards copper was inversely related to the degree of substitution of the cyanoethyl cellulose used [34]. This is the opposite of what would be expected, as increased quantities of functional groups would typically result in an increased number of binding sites and thus, adsorption capacity. In their explanation the authors hypothesized that unreacted nitrile groups hindered the bonding of metal ions with the amidoxime groups. However, they did not conduct FTIR analysis which would have shown if nitrile groups were still present in the material and as a result, the true cause of the capacity reduction in their study is not fully understood.

Using a slightly modified synthesis methodology, Saliba et al. examined the suitability of amidoxime functionalized cellulose for adsorbing copper and chromium ions [36]. They observed that the bonding of both copper and chromium with amidoxime occurred at a 1:1 ratio which is contradictory with the results published by Kubota et al. which reported a value of 1:2 for copper, requiring two amidoxime groups to bond with a single copper ion. However, the difference may be explained by the authors using different concentrations of buffering solution during adsorption testing which can affect the complexation of metal ions. While Kubota et al. did not identify the concentration of buffer that they used, Saliba et al. used a buffer of 0.2 M potassium hydrogen phthalate which the authors identify as potentially playing a role in the binding complex with amidoxime. Indeed, in their hypothesized binding coordination, Saliba et al. proposed that one molecule of hydrogen phthalate and one amidoxime functionality bond with a single copper ion, in which the phthalate is occupying the coordination site that would normally be filled with another amidoxime, thus giving the 2:1 ratio that was observed by Kubota et al.

Work on functionalizing different cellulose based materials has continued, with many authors testing the adsorption properties of these materials [54] [94] [95] [96]. However, few authors identify the buffering solutions that are used, or the concentration of the buffering solutions. As identified above, and discussed in Chapter Six, the complexing agents that are present in the solution during adsorption can have dramatic

effects on the quantity of the metal that is ultimately adsorbed. Many authors identify the importance of the pH value in influencing the adsorption quantity, but few discuss the role of other dissolved species which could potentially help explain differences in experimental results and provide new insights into optimizing the adsorption capacity of materials.

While most methods for functionalizing cellulose were heterogenous, this can present problems when it comes to functionalization. Namely, ensuring that the surface of the cellulose powder has sufficient hydrophilicity to be wettable by the reagents and that all the reagents can be in the same phase. In the method proposed by Kubota et al. making a slurry of the cellulose powder in acrylonitrile not only presents a toxicity problem, but could theoretically lead to phase separation issues as well as the potential for a polymerization side-reaction due to the contact of acrylonitrile with a highly concentrated base [97].

As an alternative, advances in the dissolution of cellulose have allowed cellulose to be dissolved in an aqueous solution comprising of sodium hydroxide as well as other stabilizing agents such as urea [98]. Dissolving cellulose in a solution can allow phase interface issues to be removed, theoretically increasing the quantity of hydroxyl sites that are accessible for functionalization, ultimately resulting in a higher amidoxime surface concentration. Although they did not intend to use the amidoxime functionalized cellulose as an adsorbent, Li et al. developed a homogenous method for functionalizing cellulose, for use in nanoparticle stabilization [35].

By dissolving cellulose in a sodium hydroxide/urea solution for the cyanoethylation reaction, all three reagents necessary for the reaction are within the same phase and are readily available: cellulose, sodium hydroxide for deprotonation of the hydroxyl group, and acrylonitrile for the functionalization. As a result, the authors were able to obtain high degrees of substitution, with up to 2.39 of the 3 available hydroxyl groups being converted to cyanoethyl. However, the methodology for purifying the functionalized

cellulose after the reaction was complex, requiring a combination of dialysis and freeze drying to obtain the final solid product.

The authors chose to conduct amidoximation homogenously, requiring the use of dimethylformamide for cyanoethyl cellulose samples that had a high degree of functionalization. This required the same complex purification procedure as for the first reaction which together required approximately two weeks of experimental time to conduct the entire process. Additionally, the authors were looking to optimize the final product for an application in stabilizing gold nanoparticles, which required slight solubility in water. As a result, the final amidoxime functionalized cellulose samples were found to have a solubility of > 50 mg mL^{-1} due to the high degree of functionalization with amidoxime. While not exceptionally high, this level of solubility would be detrimental for applications in adsorption processes as there will be a limit on the cyclability of the material due to not only functional group degradation but also mass loss.

3.3 Utilization of cellulose beads

As a logical extension of powder-based adsorbents, the preparation and functionalization of cellulose beads would facilitate greater applicability, particularly in industrial applications where an adsorption column is used. Cellulose based materials have previously been synthesized through a method of chemically modifying cellulose, creating derivatives such as viscose or cellulose ethers which are easy to solubilize [99]. The solubilized derivative is then formed through addition to a coagulation bath which will re-convert the derivative to cellulose, hence the common name of “regenerated cellulose” [100]. Upon coagulation, the cellulose product can be formed into the desired shape, with many current applications utilizing a spinning process to produce cellulosic fibers such as rayon [100]. Further, the same principles can be used to generate cellulose beads which can have variable physical properties depending on the concentration of cellulose in the feed solution.

However, problems have emerged in the process of producing the cellulose derivative, viscose, namely, the toxicity of carbon disulfide which has been found to be highly detrimental to the health of workers that are exposed to it and these issues have been known since at least 1954 [101]. Therefore, it is desirable to find methods for solubilizing cellulose that does not require the process of derivatizing and then regenerating the material. Indeed, many authors have proposed different solvents for directly solubilizing cellulose such as LiCl/N,N-dimethylacetamide and dimethyl sulfoxide/ammonium fluoride, amongst others [102] [103]. However, these solvents often present the problem of being toxic, expensive, or both. As a result, recent research has been done on finding solvent systems that are both cost effective and non-toxic with sodium hydroxide solutions emerging as a promising candidate [99].

Currently, the production of cellulosic fiber using sodium hydroxide to dissolve the cellulose is problematic due to the low solubility of cellulose in these systems (< 10 wt.%) and the tendency of the system to form gels [99]. While these represent significant problems for the production of rayon fibers, for the production of porous cellulose materials such as beads, these properties are not detrimental as the low cellulose concentration results in greater porosity in the product and the formation of gels can allow for control over the solution viscosity. Furthermore, the use of an alkaline solvent system can allow for easy coagulation with strong mineral acids as the coagulating agent. These acids, such as nitric acid, have been found to produce beads that have specific surface areas in excess of 450 $m^2 g^{-1}$ [104]. In addition to the surface area observed, this can be beneficial due to the speed of acid-base reactions which allow the formation of a distinct “skin” on the surface of the bead which can improve the shape uniformity of the beads.

After formation, functionalization of cellulose beads can proceed through the same reaction pathways as for cellulose powder and an extensive review of the different functional groups that have been added to cellulose beads has been compiled by Gericke et al [105]. From their review, it is evident that cellulose beads are viewed as promising for a variety of applications. Beads have been functionalized to purify

proteins, purify blood cells, behave as an ion exchange medium, and chelate metal ions, with 60 unique functional groups identified in the review. The functional groups identified include a wide variety of oxygen, nitrogen, and sulfur functionalities, but did not identify amidoxime as a group that has previously been studied. Therefore, the application of amidoxime to cellulose beads is a natural extension of the work performed on functionalizing cellulose powders.

3.4 Influence of complexing agents on adsorption performance

The presence of organic ligands in aqueous streams can have a significant influence on the adsorption characteristics for many metals. The interaction between ligands, metal ions, and adsorbent surfaces has been documented from at least 1978 when Davis et al. examined the role of dissolved humic acids facilitating the adsorption of copper ions onto iron oxide particles [106]. Although the influence of dissolved ligands has been known, many authors examining adsorption performance have disregarded the role of ligands and have implicitly included them in their experiments using pH buffering solutions. Indeed, as previously discussed, the difference in copper adsorption in the experiments conducted by Saliba et al. and Kubota et al. may be explained by dissolved ligands occupying the metal ion's coordination sites [34] [36]. However, not all ligands may be beneficial for adsorption since they introduce additional chelation sites which compete with the functional groups on the adsorbent for the metal ions. Therefore, the influence of complexing agents is likely highly specific to both the dissolved ligand and the metals being adsorbed, potentially allowing a way to further enhance the selectivity towards a single metal.

In a study performed by Tseng et al., the authors examined the role of three complexing agents, ethylenediaminetetraacetic acid, citric acid, and tartaric acid, on the adsorption of copper onto chitosan [107]. They observed that at low bulk metal concentrations, all the ligands were found to have an enhancing influence, approximately doubling the adsorption capacity when the bulk concentration of copper was only 0.25 mM. However, as the bulk concentration increased, the benefit was found to largely

disappear, and the non-ligand solution plateaued at approximately the same adsorption capacity as the solutions that contained ligands. Therefore, the influence of a complexing agent is largely an equilibrium phenomenon and controlling the concentrations of both the ligands and metal ions is likely of great importance when optimizing the adsorption behaviour. This idea is further emphasized by the behaviour of the citrate ligand which demonstrated a drop in the adsorption capacity at high metal ion concentrations.

The importance of ligand concentrations is further emphasized by the work done by Tobin et al. wherein they observed several anionic ligands had strongly negative influences on the adsorption capacity of a biomass adsorbent [108]. This was particularly pronounced with ethylenediaminetetraacetic acid (EDTA) and uranyl ions where the addition of EDTA above a 2:1 EDTA to uranyl ion molar ratio resulted in no adsorption taking place, compared with an adsorption capacity of ~180 mg g^{-1} without EDTA present. The anion of common salts such as sulfate, SO_4^{2-}, and chloride, Cl^-, were also found to reduce the adsorption capacity, albeit at much higher concentration ratios than EDTA. Therefore, when testing for adsorbent performance, controlling the ionic strength of the solution will undoubtedly influence the capacity and this is often disregarded by many authors as it is common to use only a metal salt dissolved in deionized water as the adsorption solution. As a result, since there is no background electrolyte, it is impossible to change the concentration of the metal ion without also changing the concentration of the anionic ligand, potentially leading to erroneous results.

These trends have also been observed in more recent papers, Escudero et al. examined the adsorption of copper and nickel on a biomass adsorbent with and without EDTA and found a dramatic reduction in capacity when EDTA was present [109]. Furthermore, similar results were observed by Liu et al. when testing the adsorption of lead on modified mesoporous silica [110].

Ultimately, for most of the studies of the influence of ligands on adsorption, capacity has been found to decrease because of binding competition from the dissolved ligand. However, Tseng et al. observed that under certain conditions the capacity can be enhanced [107]. Therefore, enhancing the adsorption capacity requires a ligand that not only forms a strong bond with the dissolved metal ion, but one in which the metal-ligand complex has a greater affinity to the functional groups on the surface of the adsorbent than the free metal itself. Finding such a ligand-metal pair would likely be highly specific and as a result, represents a potential pathway towards tailoring selective adsorption processes.

3.5 Adsorption isotherms

Adsorption isotherms are critical for understanding the relationship between the adsorbate and the adsorbent and are necessary for designing solutions that can be applied in industry. Adsorption isotherms describe the equilibrium relationship between the concentration of a species in the bulk phase, liquid or gas, and the concentration that is immobilized on the surface of the adsorbent. Due to the multitude of factors that can influence the adsorption capacity of a material, isotherms are generated at a constant temperature and pH and are particularly useful for industries such as hydrometallurgy where the pH is controlled to enhance metal separation. By knowing the equilibrium relationship, engineers can design adsorption columns that will have a predictable capacity for any given outlet concentration. Furthermore, the shape and structure of an isotherm can give insights into the nature of the bonding interaction, whether the bonding is monolayer or multilayer, or the relative favourability of the interaction.

The development of adsorption models has been extensively studied in literature and over a dozen different types have been reported [111]. However, only two of these are primarily used in studies due to the fundamental behaviour that they describe, namely, the Langmuir and Freundlich isotherm models.

3.5.1 Langmuir isotherm model

The Langmuir isotherm model was developed in 1916 by Irving Langmuir and this contribution resulted in a Nobel prize in 1932 [112]. The model takes the form shown in equation (1) below where the concentration of adsorbate on the surface (q_e, mg g^{-1}) at equilibrium is a function of the concentration in the bulk solution (C_e), and the shape of the isotherm is controlled by two constants, K_L and q_m.

$$q_e = \frac{C_e K_L q_m}{(1 + C_e K_L)} \qquad (1)$$

The model is based upon a dynamic equilibrium being established on the surface of the adsorbent where the rate of an adsorbate molecule desorbing from the surface is equal to the rate at which adsorbate molecules bond with the surface. For an aqueous system and when the activity of the adsorbate can be approximated by the concentration, the rate expression for adsorption and desorption can be written as shown below.

$$r_{ad} = k_{ad}\,[C_A][S]$$

$$r_{de} = k_{de}\,[A_{ad}]$$

where k_{ad} and k_{de} are the rate constants for adsorption and desorption, respectively, $[C_A]$ is the concentration of adsorbate in the fluid phase, $[S]$ is the abundance of available bonding sites, and $[A_{ad}]$ is the concentration of bound adsorbate on the surface of the adsorbent. By equating the two rates, the ratio of k_{ad} and k_{de} can be represented as the combined constant K_L which describes the favourability of bonding due to the kinetics. Furthermore, since the rate of adsorption is dependent on the availability of bonding sites, this will decrease as more adsorbate is brought into contact with the surface. To account for this, the total quantity of sites can be split into those that are free, *S*, and those that are occupied, A_{ad}. From the substitution and rearrangement, the constant q_m represents the number of bonding sites available for the adsorbate.

To further understand the strength of bonding, many authors report the separation factor, R_L, which tells whether the adsorption is irreversible (R_L = 0), favourable (0 < R_L < 1), linear (R_L = 1), or unfavourable (R_L > 1) [113]. The separation factor is calculated via equation (2), which is dependent on the Langmuir constant, K_L, as well as the initial adsorbate concentration, C_o.

$$R_L = \frac{1}{1 + K_L C_o} \quad (2)$$

Due to the dependence on the initial adsorbate concentration, the separation factor will not be constant throughout the isotherm. However, it is generally used to determine how the adsorbent will behave at low concentrations where unfavourable adsorption will result in little to no adsorbate removal.

Even with its widespread use, the Langmuir model has assumptions that can limit its applicability. Since the model is derived for the kinetics of adsorption, the rate equation shown above makes the assumption that each site has the same bonding energetics which may not be true in many cases as the absorbate can influence the energy levels of nearby bonding sites. Furthermore, the derivation assumes that each bonding site can only interact with a single adsorbate such that only a monolayer can be formed. For chelating adsorption this is often the case as adsorption is driven by the interaction between a functional group and a metal ion. However, if precipitation is present in the system the Langmuir isotherm will fail to accurately predict the capacity as metal-metal interactions are not accounted for in the model.

3.5.2 Freundlich isotherm model

As an alternative to the Langmuir model, the Freundlich model is an empirical model that was found to fit multilayer adsorption systems well [114]. Although it is widely considered to be purely empirical, studies have worked on a theoretical derivation of the model and have found success when accounting for surface heterogeneity and its influence on adsorption energies [115] [116]. Therefore, in situations where more than one mechanism of adsorption is present, for example, multiple different functional groups, the

Freundlich model may be more applicable. The model follows equation (3) shown below where K_F and $\frac{1}{n}$ are constants that relate the bulk equilibrium concentration to the concentration adsorbed.

$$q_e = K_F C_e^{\frac{1}{n}} \quad (3)$$

In contrast with the Langmuir model, the Freundlich model does not exhibit a maximum value since it assumes that adsorption will always be possible given a sufficiently strong driving force. In this way the model can describe multilayer adsorption and the heterogeneity that arises in those situations. In a study on ion-exchange mechanisms in soil, Sposito found that the Freundlich isotherm correlated well when considering adsorption to be a combination of unique bonding groups, each with their own adsorption energetics [117]. Through this approach, each class of adsorption site was modelled with a Langmuir fit and the combined effect aligned with a Freundlich model. Therefore, the Freundlich model has been found to have a theoretical basis in situations where multiple types of adsorption site are present.

3.5.3 Linear and non-linear model fitting

Due to limitations in computational capability historically, non-linear models such as Langmuir or Freundlich are often converted into a linear form which can easily be plotted and fitted by hand. Even today, adsorption isotherms are commonly fit through linearization and solving for the two constants using the slope and intercept. Linearized forms of both Langmuir and Freundlich are shown below and it is important to note that different authors choose different linearization models and in the case of the Langmuir isotherm, more than four linearization models have been documented each with different sources of statistical error [118].

Linear forms of the Langmuir isotherm:

(Hanes-Woolf) $$\frac{C_e}{q_e} = \frac{1}{q_m K_L} + \frac{C_e}{q_m} \quad (4)$$

(Lineweaver-Burke) $$\frac{1}{q_e} = \frac{1}{q_m K_L}\frac{1}{C_e} + \frac{1}{q_m} \quad (5)$$

(Eadie-Hofstee) $$q_e = q_m - \frac{1}{K_L}\left(\frac{q_e}{C_e}\right) \quad (6)$$

(Scatchard) $$\frac{q_e}{C_e} = K_L q_m - K_L q_e \quad (7)$$

Linear form of the Freundlich isotherm:

$$\ln q_e = \ln K_F + \frac{1}{n}\ln C_e \quad (8)$$

For many of the linearized Langmuir equations, the dependent and independent axis of the resulting plots are not truly independent of one another. For example, in the Hanes-Woolf form, when $\frac{C_e}{q_e}$ is plotted as a function of C_e there is an inherent bias towards a linear trend, this can result in good correlation coefficients even when the data does not truly follow a Langmuir trend. As a result, there is an increasing expectation that non-linear regression methods such as a least-sum-of-squares should be used to avoid the tendency to report a good degree of correlation even when a model is not appropriate for the system [119].

3.6 Research gaps and opportunities

After reviewing the relevant literature, several research gaps are apparent. For the recovery of vanadium, the use of amidoxime functionalized cellulose has not been previously explored but based on the performance of amidoxime in seawater experiments, performance indications are promising. Furthermore, the synthesis methodology for functionalizing cellulose with amidoxime may be improved by conducting the cyanoethylation reaction in an alkaline aqueous medium. This would facilitate the conversion of cellulose I to cellulose II, enhancing hydroxyl availability, while also catalyzing the addition of cyanoethyl groups. From an applications perspective, this would also reduce inherent hazards in the process, namely, neat acrylonitrile which is highly toxic. Lastly, the role of dissolved complexing agents has been identified as important but is often overlooked. By identifying complexing agents that have beneficial interactions with both vanadium and amidoxime, the adsorption capacity can be enhanced, leading to a more effective material, particularly if the phenomenon is beneficial at very low metal ion concentrations.

Chapter Four: Materials and Methods

4.1 Experimental methods

4.1.1 Cellulose cyanoethylation and amidoximation

Homogenous reaction from literature

Homogenous cyanoethylation of cellulose was done through a homogeneous reaction as proposed by Li et al. [35]. A solution of urea, sodium hydroxide, and water was prepared with 12 wt.% urea and 7 wt.% NaOH. The solution was placed within an ice bath and the temperature was maintained between 5 °C and 10 °C. Under vigorous mixing, 50 g L^{-1} of cellulose powder was added slowly to the solution to allow for dissolution without agglomeration. Following dissolution, the solution was highly viscous, and a mechanical stirrer was necessary to maintain mixing.

Next, acrylonitrile was added dropwise to the solution to obtain a concentration of 2 M. Due to the occurrence of phase separation between acrylonitrile and water, slow addition was necessary to ensure rapid dissolution of acrylonitrile into the aqueous phase with a solubility of 50 mg mL^{-1} [120]. The rate of addition was controlled such that a phase of acrylonitrile did not become apparent on the surface of the solution. Following the complete addition of acrylonitrile to the solution, the solution was left to react for a given time, typically eight hours.

Afterwards, the reaction solution was removed from the ice bath and neutralized via the addition of acetic acid until the pH of the solution reached a value of 7. The solution was then transferred into dialysis tubing with a molecular weight cut-off of 3,500 and the filled tubes were placed within an 11 L dialysis bath, giving a dialysis volume ratio of 27.5. Dialysis was performed for 72 hrs with the dialysis water being replaced every 12 hrs, giving a total dialysis volume ratio of 165.

Following dialysis, the solid precipitate obtained was removed from the tubing and transferred to a beaker where it was slurried with water. The slurry mixture was then filtered with a vacuum filter to produce a white solid material. The solid material was subsequently transferred to a petri dish and placed within a vacuum oven to be left overnight at 50 °C. The resulting material was then dissolved in dimethylformamide and mixed with a prepared solution of 10 wt.% hydroxylamine hydrochloride neutralized in 5:1 ethanol to water to perform amidoximation. The reaction was performed at 75 °C for 8 hours and following the reaction, the solution was dialysed in the same manner as described above.

Heterogeneous reaction from literature

An alternative method was also investigated from literature for heterogeneously functionalizing cellulose [34]. In those trials, 3 g of cellulose powder was slurried with 72 mL of acrylonitrile under vigorous mixing. After agglomerations of cellulose powder had sufficiently dispersed, 2 mL of 36 wt.% sodium hydroxide solution was added. The resulting mixture reacted for 2 hrs without any temperature control. The slurry was then filtered with a vacuum filter and the residual was placed within a vacuum oven to dry overnight at 50 °C. The cyanoethyl cellulose was then reacted with a 10 wt.% solution of hydroxylamine hydrochloride neutralized to pH 7. The reaction took place at 75 °C and was conducted over 4 hrs.

Due to equipment limitations, modifications of the original process described in literature were necessary. Namely, there was no access to an atomizer and as a result, tetramethyl ammonium chloride could not be applied as a swelling agent. Furthermore, a freeze dryer was substituted for a vacuum oven during solid drying and purification which may have affected the physical properties of the final sample due to the different mechanisms of drying applied by both. Namely, evaporative drying is more likely to facilitate particle agglomeration whereas freeze drying will typically result in a more powdered product.

Novel reaction procedure

A reaction procedure was developed that incorporated ideas from both the heterogenous and homogenous procedures described in literature. The development of the procedure is described in Chapter 5 with the following conditions being found as the best performing. A solution of sodium hydroxide was prepared with a concentration of 100 g L^{-1}. For a 400 mL solution, 40 g of sodium hydroxide was dissolved, and the solution was heated on a hot plate to 35 °C under vigorous stirring. After the temperature was stable, 25 g of cellulose powder was slowly added to the solution at a rate that prevented agglomeration. After the cellulose powder was well dispersed within the beaker, 80 g of acrylonitrile was added dropwise to the solution so that the acrylonitrile to glucose monomer molar ratio was 10:1. Similar to the method noted previously, the rate of acrylonitrile addition was partially controlled by ensuring a separate phase of acrylonitrile did not become apparent. However, the addition of acrylonitrile was also controlled to maintain the reaction temperature at 35 °C as rapid addition resulted in an exothermic reaction. Altogether, addition of the complete mass of acrylonitrile typically required 15 min.

The reaction took place over two hours and the temperature was maintained throughout the experiment. Following the reaction, the slurry solution was filtered with a nitrogen filter press to separate the residual solution from the suspended cellulose particles. The recovered solid was continuously washed with deionized water and filtered until the filtrate had produced a pH reading of 7. The resulting solids were then transferred to a petri dish and dried on a hot plate at 40 °C overnight in a fume hood.

Amidoximation of cyanoethyl cellulose was performed through a heterogeneous reaction with hydroxylamine. Following the reaction optimization as outlined in Chapter 5, the reaction was performed at 75 °C with a pH value of 8 for 2 hrs. In more detail, 100 g of hydroxylamine hydrochloride was dissolved in 500 mL of RO water. The pH of the solution was then adjusted with 10 M NaOH to reach a value of 8

which was measured with a pH meter. The beaker was then covered with aluminium foil and placed on a combined magnetic stirrer and programmable hot plate, where the solution was heated to 75°C. Once the solution reached the desired temperature, 25 g of cyanoethyl cellulose was slowly added to the solution such that no cellulose aggregation was evident, and the cellulose powder was well dispersed within the slurry. After addition of the cellulose, the beaker was re-covered and was left to react for two hours.

Following the reaction, the slurry was quenched in a water bath and was briefly allowed to settle. The supernatant in the beaker was removed and the remaining mixture of solution and cellulose was filtered via nitrogen filter press as described previously. The solid sample was repeatedly rinsed with deionized water and was ultimately placed on a hot plate at 40 °C to dry overnight.

After drying, the cellulose sample was ground and sieved through a size 60 mesh to achieve size uniformity in the product. The sample was consecutively ground with a pestle and mortar and sieved until 15 g powder was recovered for subsequent adsorption testing.

4.1.2 Batch adsorption testing

Adsorption testing was performed by dispersing the adsorbent material in a synthetic metal solution, contained within a small, 25 mL or 50 mL, Erlenmeyer flask. The Erlenmeyer flask was then placed on a mechanical shaker where it was agitated for 24 hrs.

Two methods were used to evaluate the effect of pH on metal adsorption. In the first method, adsorption testing involved the addition of buffers to the synthetic metal solutions to maintain the desired pH value by counteracting the effects of metal hydrolysis upon their addition. Reverse osmosis (RO) water was utilized for all adsorption experiments and in the case of early experiments, two buffering agents were utilized: acetic acid to buffer within the pH range of 4 to 5 and citric acid to buffer within the pH range of 5 to 6, both with a molarity of 0.3 M. Two different concentrations of metal ions (a high value of 2,000 mg

L^{-1} and a low value of 500 mg L^{-1}) were prepared separately for individual metals by adding corresponding metal sulfates to the buffer solutions. In the second method, no pH buffer was added (except in the case where a complexing agent was desired), and the pH of the solution was corrected to the desired value following addition of the metal salt. Additionally, a background electrolyte of sodium sulfate at a concentration of 0.25 M was included to more accurately simulate a metal leach solution from a sulfuric acid leaching operation.

The pH was adjusted with either 10 M sodium hydroxide or 5 M sulfuric acid. A high concentration of acid / alkali was used so that the volumetric requirement was minimal, thus reducing the effect of dilution. A desired volume of the resulting solution was then transferred to an Erlenmeyer flask via a graduated syringe. Due to the capability of agitating multiple flasks on the shaker co-currently, nine adsorption trials were typically performed at the same time. Once all the flasks had been filled with the required volume of solution, a mass of adsorbent was weighed out on an analytical balance and added to the flask. The flask was then stoppered to prevent evaporative losses.

After adsorption, the solution was filtered using a nitrogen filter press with Whatman® Grade 40 ashless filters that had a pore size of 8 µm to remove any metal salt particles that did not dissolve. The filtrate solution was then prepared for analysis by inductively coupled plasma optical emission spectroscopy (ICP-OES) in accordance to the procedure outlined in section 4.2.2 ICP-OES analysis to determine the dissolved metal content. The loaded adsorbent was sparingly rinsed with RO water to remove the residual solution and was dried on a hot plate overnight.

Polymetallic selectivity testing

Selectivity testing was performed in a similar procedure to the single metal methodology. The primary difference between the procedures is the maximum dissolved metal content. While the single metal

adsorption experiments typically employed a dissolved metal content of 2,000 mg L^{-1}, polymetallic testing limited each metal to a concentration of 500 mg L^{-1}.

Four metals were tested: copper, nickel, chromium, and vanadium, and synthetic solutions were prepared by dissolving their respective sulfate salts in RO water with a 0.25 M sodium sulfate background electrolyte. The pH was adjusted with either 10 M sodium hydroxide or 5 M sulfuric acid and a desired mass of adsorbent was added to the solution. The mixture was agitated for 24 hours on a mechanical shaker and the resulting residual solution was removed and filtered in preparation for ICP-OES testing.

4.1.3 Cellulose bead synthesis

To further apply the developed adsorbent to an industrial application, cellulose beads were developed that could then be functionalized for use in an adsorption column. Functionalization of the cellulose beads largely followed the methodology developed above for functionalizing cellulose powder albeit with slight modifications. For both synthesis and adsorption testing, pumping was done with a VWR variable medium flow mini-pump with 1/16" tubing. Flow rates were determined by volume transfer to a graduated cylinder over a timed interval. These flow rates were then calibrated to the digitally displayed power level and were re-evaluated at the beginning of each day when the pump was needed.

In order to dissolve cellulose, a 300 mL solution of water, urea, and sodium hydroxide was prepared at a mass ratio of 81:12:7. The solution was placed within an ice bath and was cooled to a temperature between 5 °C and 10 °C. Next, 15 g of cellulose fibers were added to the mixture which was subject to vigorous mechanical stirring. The cellulose completely dissolved within 15 minutes and the solution was maintained between 5 °C and 10 °C. Utilizing a volume displacement pump, the dissolved cellulose solution was pumped through tubing which had a syringe needle fastened to the end. The droplets of dissolved cellulose were dropped into a 1.5 L, 1 M sulfuric acid bath which was gently agitated. The syringe

needle was maintained at a relatively constant height above the water level and throughout the experiment the height of the needle was adjusted to correct for the rising level of the bath.

After all the solution had been dripped into the bath, the beads were left to cure overnight. After curing, the beads were removed from the sulfuric acid and were rinsed thoroughly with RO water and were stored in deionized water for a minimum of 24 hours in preparation for functionalization.

Cellulose bead functionalization

Bead functionalization was performed under similar reaction conditions as described above for the functionalization of cellulose powder. However, slight modifications to the conditions were necessary, primarily to maintain the bead structure. To accomplish this, the concentration of sodium hydroxide during the addition of acrylonitrile was reduced by half to 50 g L^{-1}. At this concentration, the beads did not dissolve when reacted at 35 °C for 2 hours. To reduce the probability of error in adsorption column testing, a 1 kg batch of beads was synthesized. A 1 L solution containing 50 g of NaOH was prepared and 1 kg of beads was slowly added under slight agitation from a magnetic stir bar. Next, 130 mL of acrylonitrile was added dropwise to the solution to obtain a concentration of approximately 2 M. However, due to the entrained water within the cellulose beads, the true concentration was less than the target value. As in the procedure for cellulose powder, the rate of acrylonitrile addition was controlled such that no acrylonitrile phase was observed, indicating that the acrylonitrile was successfully dissolving into the solution.

Following the addition of cyanoethyl groups to the cellulose beads, the beads were reacted with hydroxylamine in a similar method to that of cellulose powder. A reagent solution was prepared with 200 g of hydroxylamine hydrochloride dissolved in 1 L of RO water and the pH of the solution was adjusted to a value of 8. The solution was heated on a programmable hot plate to a temperature of 75 °C, 1 kg of cyanoethyl functionalized cellulose beads was then added. As opposed to the functionalization of the

cellulose powder, the mass of beads added is a combination of both cellulose and entrained water within the beads. As a result, the true concentration of hydroxylamine is diluted, approximately by the mass of beads, as ~90% of the beads mass is water.

After reacting for 2 hours, the solution was quenched in a water bath and the beads were washed with deionized water. Washing was repeated 5 times and afterwards the beads were transferred to a bottle of reverse osmosis water for storage.

4.1.4 Adsorption column testing

To analyze the performance of the functionalized cellulose beads, a laboratory scale adsorption column was designed and built. The dimensions of the column are shown below in Figure 15 and give a total bed volume of approximately 100 mL. The fixtures on both ends were 3D printed with polycarbonate and sealed with nitrile O-rings. The end fixtures are not shown in the figure which included a nozzle for connecting to external tubing and a stainless-steel mesh to eliminate the potential of bead loss through fluidization.

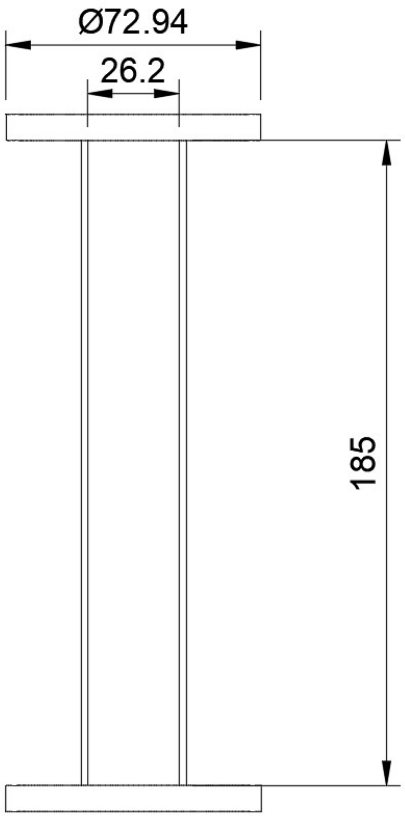

Figure 15 - Adsorption column dimensions. All measurements in mm. Capping fixtures on both ends are not shown.

For adsorption trials, a 1 L solution of 2,000 mg L^{-1} vanadium at pH 4.5 with an acetic acid concentration of 0.5 M was used. The effluent samples were collected in a 35.7 mL vial and the time interval between each sample was measured to estimate the flow rate over time. The targeted flow rate was 2.6 mL min^{-1} and over the three adsorption trials, the pumping flow rate was found to be 2.57 mL min^{-1} with a standard deviation of 0.16 mL min^{-1}. At this speed, the superficial flow velocity within the column was approximately 4.8 mm min^{-1} or 0.08 mm s^{-1}.

4.2 Analytical methods

4.2.1 pH control and measurement

The pH measurements were performed with a Fisherbrand™ accumet™ XL 200 pH/Conductivity Benchtop meter which was paired with a Fisherbrand™ accuTupH™ Rugged Bulb pH electrode. The pH probe was calibrated using a three-point calibration curve at 4.01, 7.00, and 10.01 with buffers supplied by Oakton that were prepared in accordance to NIST standards. The probe was recalibrated using the same pH buffer solutions every two weeks, or in the case of a longer lapse in experiments, immediately before the experiment was performed. The reported accuracy of the pH probe and meter is ± 0.03.

4.2.2 ICP-OES analysis

Inductively coupled plasma optical emission spectroscopy was performed with an iCAP 7000 Series ICP Spectrometer. In order to meet the desired operating concentration window of the ICP instrument (less than 100 mg L^{-1}), all residual samples required dilution due to the high concentration of the initial stock solution, 500 mg L^{-1} to 3,000 mg L^{-1}. A 2 wt.% nitric acid solution was prepared from 70% nitric acid and deionized water, which was used to dilute residual samples to achieve a target metal concentration below 60 mg L^{-1}.

For samples obtained from experiments using a synthetic solution concentration of 2,000 mg L^{-1}, 0.4 mL of the residual solution was pipetted into a 20 mL volumetric flask which was then filled with 2 wt.% nitric acid. This resulted in a 50 times dilution, and thus a maximum metal concentration of approximately 40 mg L^{-1}. Similarly, for samples obtained from experiments using a synthetic solution concentration of 500 mg L^{-1}, 2 mL of the residual solution was pipetted into a 20 mL volumetric flask which was then filled with 2 wt.% nitric acid, resulting in a 10 times dilution and a maximum metal concentration of approximately 50 mg L^{-1}.

Calibration standards were prepared for pure vanadium as well as polymetallic solutions through dilution of purchased ICP standard solutions which had the following concentrations for each metal: 996 ± 5 mg L^{-1} for vanadium, 1000 ± 4 mg L^{-1} for chromium, 1006 ± 5 mg L^{-1} for nickel, and 1001 ± 2 mg L^{-1} for copper. The prepared standards were made at concentrations of 1, 5, 25, and 50 mg L^{-1} to minimize the risk of extrapolation. Dilutions were performed with a 50 mL volumetric flask and used 2 wt.% nitric acid as a diluent.

For all metals analyzed: copper, nickel, vanadium, and chromium, emission wavelengths were identified that did not result in any spectra overlap. Typically, a principal wavelength was used for each metal and the wavelengths are identified in Table 5 below, but multiple wavelengths for each metal were often measured to characterize variance and identify the suitability of a wavelength.

Table 5 - Primary wavelengths examined for ICP analysis for different elements

Element	Wavelength (nm)
Nickel	361.939
Vanadium	311.071
Chromium	284.325
Copper	219.958

Following the determination of the metal concentrations, the quantity of adsorbed metal was calculated through a mass balance on the system. In other words, the quantity of vanadium adsorbed was inferred through the difference of the vanadium in the stock solution and the vanadium in the filtrate solution after adsorption which is represented through equation (9) below.

$$q_e = \frac{(C_o - C_e)\, V_{Sol}}{m_{ad}} \qquad (9)$$

where q_e is the quantity of adsorbed metal per unit mass of adsorbent (mg g^{-1}), C_o is the concentration of metal in the stock solution (mg L^{-1}), C_e is the concentration of metal in the residual solution (mg L^{-1}), V_{Sol} is the volume of metal solution (L), and m_{ad} is the mass of adsorbent added in the trial (g).

4.2.3 Elemental analysis (CHN)

Elemental analysis was conducted at the department of chemistry in the University of Calgary. The experiments were performed by Mr. Jian Jun Li, an analytical laboratory technician, on a PE2400 CHN Analyzer with a combustion temperature of 800 °C. All samples were run in duplicates and the reported results are the average of the two with the calculated 95% confidence interval.

Using the measured nitrogen content, the degree of substitution for both cyanoethylation and amidoximation can be calculated. Using the mass balance of the cyanoethylation reaction, the degree of substitution can be calculated. The degree of substitution (*D.S.*$_1$) is defined as the average number of hydroxyl groups converted to cyanoethyl groups per cellulose monomer. Since a cellulose monomer contains 3 hydroxyl groups, the degree of substitution will have an upper bound of 3, which would signify complete substitution. The rearranged mass balance is shown below in equation (10) .

$$D.S._1 = \frac{M_{Cel} \times w_N}{M_N - w_N \times M_{ACN}} \qquad (10)$$

where M_{Cel} is the molecular weight of a cellulose monomer (162.16 g mol^{-1}), M_N is the molecular weight of nitrogen (14.01 g mol^{-1}), and M_{ACN} is the molecular weight of acrylonitrile (53.05 g mol^{-1}), and w_N is the mass fraction of nitrogen within the sample.

Similarly, the degree of substitution (*D.S.*$_2$) can be calculated for the conversion of cyanoethyl groups to amidoxime shown in equation (11). Since $D.S._2$ represents the conversion of cyanoethyl groups, its upper limit is bounded by $D.S._1$.

$$D.S._2 = \frac{(M_{Cel} + M_{ACN} \times D.S._1)(w_{N_2} - w_{N_1})}{M_N - (w_{N_2} \times M_{HA})} \quad (11)$$

where M_{HA} is the molecular weight of hydroxylamine (33.03 g mol^{-1}), w_{N_2} is the nitrogen mass fraction following conversion to amidoxime, and w_{N_1} is the nitrogen mass fraction after cyanoethylation. For both calculations, the degree of substitution is expressed as functional groups substituted per mole of monomer. Additionally, it is assumed that no side reactions are taking place, therefore, the calculated degrees of substitutions are primarily used to gauge the extent of reaction and do not carry analytical certainty.

4.2.4 Statistical analysis

As part of data testing and analysis, statistical experiments were formed on certain sets of data to establish the repeatability and significance of both the testing result as well as the methodology. Most commonly, a simple *t*-test was performed when changes to methodologies were done to assess whether the effect of the change was significant or not. Additionally, an initial 2^3 level full factorial set of experiments were performed to assess the impact of reaction time and pH on the amidoximation reaction, as well as the effect of the concentration of acetate on adsorption during batch adsorption experiments. The results of the factorial test were then analyzed through analysis of variance (ANOVA) to determine the effect of each of the explored factors and to identify whether the results were statistically significant.

As part of the statistical analysis of the 2^3 level full factorial experiments, the effect of each of the parameters was calculated to assess its contribution and to see if there are any interactions between the tested parameters. The effect of each parameter can be calculated by the following equation,

$$\text{Effect} = \frac{\text{Contrast}}{n \times 2^{k-1}} \quad (12)$$

where *n* is the number of trials for each parameter, *k* is the number of factors, and contrast is the summation of results that include the parameter being tested minus the summation of results that do not include the parameter being tested.

The contrast for each parameter is determined by identifying a positive or negative condition for each of the factors and adding or subtracting the summed capacities under those conditions. For example, the contrast for effect A is shown below where the conditions *a*, *ab*, *ac*, and *abc* are positive conditions as opposed to *(1)*, *b*, *c*, and *bc* which are negative conditions.

$$\text{Effect}_{\text{A}} = \frac{(a + ab + ac + abc - (1) - b - c - bc)}{n \times 2^{k-1}} \qquad \textit{(13)}$$

t-test

As another analysis tool, *t* testing was performed on some results to check for statistical significance and to get an understanding of the variance associated with the developed testing procedures. Due to the small sample sizes, often 2-3 repeats, a *Z* test was determined to be not suitable since 30 samples are often recommended to establish a representative approximation of the population. A *t* test is more suitable because it uses the variance of the sample as opposed to the standard deviation of the population, which corrects for the small sample size.

For a given set of data, the sample variance can be calculated as follows.

$$s = \sqrt{\frac{\sum_{i=1}^{N}(x_i - \bar{x})^2}{N - 1}} \qquad \textit{(14)}$$

From this, a confidence interval around a sample mean can be established.

$$\bar{x} \pm t \frac{s}{\sqrt{n}} \qquad \textit{(15)}$$

The value of *t* was determined depending on the confidence level, α, as well as the degrees of freedom for the sample, $N-1$. For example, with a confidence level of 95% and two degrees of freedom (total of three replicates), the *t* value will be 4.3027 [121].

ANOVA

Analysis of variance (ANOVA) is a statistical method that examines the variance between experimental groups to determine whether the means of the groups are statistically different or can be explained by random experimental error [121]. For a one-way ANOVA test, the total variation can be split into two sub-categories, the variation amongst the group (SSA) and the variation within a group (SSW). By examining these two, if the variances of the two sub-categories are similar, it is likely that they both represent the variance of the population and thus, there is no difference between them. However, if the variances are statistically different, it suggests that they are measuring the variances of two separate populations and that the tested treatment successfully altered the properties of the treated population. The variations are calculated as follows:

$$\mathrm{SSA} = \sum_{j=1}^{c} n_j \left(\bar{X}_j - \bar{\bar{X}}\right)^2 \qquad (16)$$

where, c is the number of groups being compared, n_j is the number of observations within a group, $\bar{X}_j$ is the mean observation within group j, and $\bar{\bar{X}}$ is the overall mean.

$$\mathrm{SSW} = \sum_{j=1}^{c} \sum_{i=1}^{n_j} \left(X_{ij} - \bar{X}_j\right)^2 \qquad (17)$$

where, X_{ij} is the *i*th measured value within group j.

The degrees of freedom for each sum of squares can be determined by the quantity of observable data points within each measurement. For the sum of squares amongst groups (SSA) the degrees of freedom is determined by the number of groups being compared, represented by c, minus one. While for the sum of squares within groups the degrees of freedom are found by the difference between the total number of data points and the number of groups.

$$\mathrm{DoF\ (SSA)} = c - 1$$
$$\mathrm{DoF\ (SSW)} = n - c$$

From this, the degree of freedom corrected sum of squares can be calculated to give the mean square amongst (MSA) and the mean square within (MSW) which is shown below.

$$\mathrm{MSA} = \frac{\mathrm{SSA}}{c - 1}$$
$$\mathrm{MSW} = \frac{\mathrm{SSW}}{n - c}$$

The ratio of the two values can then be used to calculate the *f* value which is then used in an *f*-test to determine the significance of the difference in variation.

$$f = \frac{\mathrm{MSA}}{\mathrm{MSW}}$$

The critical *f* value will depend on both, the degrees of freedom for the numerator and the denominator, as well as the confidence interval that is required, which in this report is 95% unless otherwise stated. For example, if the MSW has 16 degrees of freedom and the MSA has one degree of freedom, the critical *f* value will be 4.49.

ANOVA testing can also be expanded to test within factorial designs, where multiple factors as well as potential interactions between them are examined. In contrast with a one-way ANOVA test, for testing factorial designs, the sum of squares total (SST) is split into several different subcategories, one for each of the factors being examined as well as for the interactions between the tested factors as opposed to

forming two groups, the sum of squares within a group (SSW) and the sum of squares amongst the groups (SSA). For factorial experiments, this is visualized by Figure 16 shown below.

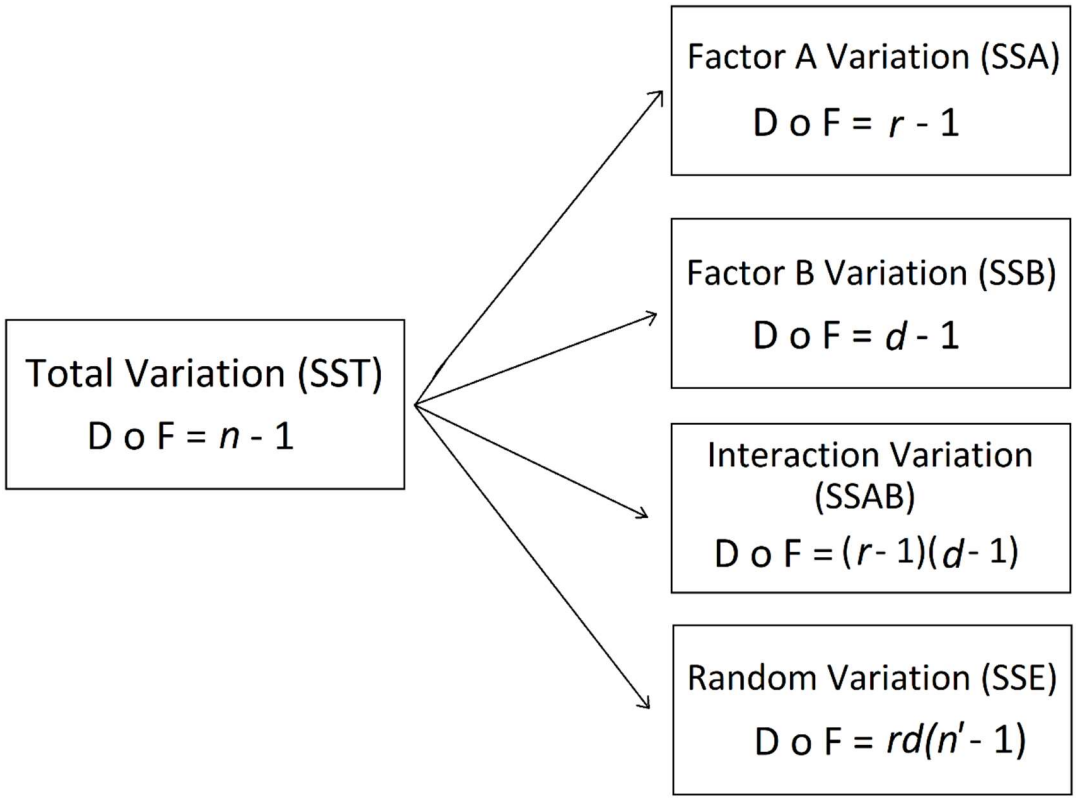

Figure 16 - Variation breakdown for a 2 factorial experimental design with n' replicates where r and d are the number of levels for each respective factor.

In the case where three factors are considered, each with two levels, the SST is split into eight blocks. The blocks are SSA, SSB, SSC, SSAB, SSAC, SSBC, SSACB, and SSE. Where SSX represents the sum of squares for factor X, SSXY represents the sum of squares for the interaction between factors X and Y, and SSE represents the sum of squares for the random error.

The sum of squares are calculated similarly to those in a one-way ANOVA test but slight modifications are made as shown below,

$$\mathrm{SSA} = edn' \sum_{j=1}^{r} \left(\bar{X}_j - \bar{\bar{X}}\right)^2 \qquad (18)$$

where, *r* is the number of levels of factor A, *d* is the number of levels of factor B, *e* is the number of levels of factor C, and n' in the number of replications for each testing condition (assuming equal amounts of replicates for each testing condition). This can be similarly calculated for the interaction sum of squares as shown below.

$$\text{SSAB} = e\, n' \sum_{j=1}^{d} \sum_{i=1}^{r} \left(X_{ij} - \bar{X}_j - \bar{X}_i + \bar{\bar{X}}\right)^2 \qquad (19)$$

Finally, the SSE can be calculated as shown below.

$$\text{SSE} = \sum_{j=1}^{d} \sum_{i=1}^{r} \sum_{k=1}^{e} \sum_{f=1}^{n'} \left(X_{jikf} - \bar{X}_{ijk}\right)^2 \qquad (20)$$

Similar to a one-way ANOVA, the sum of squares are divided by their respective degrees of freedom to yield the mean squares.

$$\text{MSA} = \frac{\text{SSA}}{r-1}$$

$$\text{MSB} = \frac{\text{SSB}}{d-1}$$

$$\text{MSC} = \frac{\text{SSC}}{e-1}$$

$$\text{MSAB} = \frac{\text{SSAB}}{(r-1)\,(d-1)}$$

$$\text{MSAC} = \frac{\text{SSAC}}{(r-1)\,(e-1)}$$

$$\text{MSBC} = \frac{\text{SSBC}}{(d-1)\,(e-1)}$$

$$\text{MSABC} = \frac{\text{SSABC}}{(r-1)\,(d-1)\,(e-1)}$$

$$\text{MSE} = \frac{\text{SSE}}{rde(n'-1)}$$

To examine the significant of each factor or interaction, the mean square of the factor is divided by that of the error and compared with a critical *f* value. If the ratio exceeds the critical *f* value, it can be said that there is sufficient evidence to state that the factor being tested alters the result in a way that cannot be examined by random error. Due to the computational complexity of ANOVA testing when multiple factors are considered, the analysis is principally performed by statistical software and in the analysis performed in this report, MINITAB was used.

Error analysis

To fully understand the magnitude of introduced errors, a propagation of errors calculation was performed for the methodology of batch adsorption testing and subsequent ICP analysis. As discussed previously, the loading of a solid adsorbent can be calculated via equation (9), where the difference in the metal concentration between the residual and stock solutions are measured.

In adsorption experiments, three operations are performed that may introduce error into the system; measurement of the vanadium concentration, measurement of the volume of solution that was added to the flask, and measurement of the mass of adsorbent that was added to the flask. Together, the error for the calculated adsorption loading can be determined through equation (21) shown below where the influence of each source is proportional to the derivative of the final value as a function of the source.

$$s = \sqrt{\left(\frac{\mathrm{d}f}{\mathrm{d}\Delta[Van]}\right)^2 \left(s_{\Delta[Van]}\right)^2 + \left(\frac{\mathrm{d}f}{\mathrm{d}V_{Sol}}\right)^2 \left(s_{V_{Sol}}\right)^2 + \left(\frac{\mathrm{d}f}{\mathrm{d}m_{ad}}\right)^2 \left(s_{m_{ad}}\right)^2} \qquad (21)$$

where $[Van]$ is the concentration of vanadium $(\mathrm{mg\ L^{-1}})$, V_{Sol} is the volume of pipetted solution (L), and m_{ad} is the mass of adsorbent added (g). The error for the mass of the adsorbent, $s_{m_{ad}}$, was determined based on the accuracy of the mass balance used, which was found to be ± 0.0005 g. Similarly, the error from volume measurement was 1% when a pipette was utilized or ± 0.4 mL when a graduated cylinder

was used [122]. The variance of the concentration measurement was calculated from the repeats performed by the ICP instrument and was typically found to be under 0.2 mg L^{-1}. Together, these represented an error of 1.6 mg g^{-1} for batch adsorption which is less than 1% for the majority of experimental trials.

4.2.5 Fitting Adsorption Isotherms

Several batch adsorption experiments were performed at varying volumes of vanadium solution as well as mass of adsorbent to generate an adsorption isotherm. Adsorption isotherms describe the relationship between the surface concentration of metal adsorbed to the concentration of metal ions within the bulk solution and are typically fitted to the Langmuir or the Freundlich model.

The Langmuir model describes monolayer adsorption and is derived from the kinetic equilibrium between the surface and the bulk phases. The model is typically expressed through equation (1) shown again below, where there are two constants that need to be determined to describe the system, K_L and q_m.

$$q_e = \frac{C_e K_L q_m}{(1 + C_e K_L)}$$

where q_e is the loading of adsorbate on the adsorbent (mg g^{-1}), C_e is the equilibrium concentration of the metal ion within the bulk solution (mg L^{-1}), K_L is the Langmuir isotherm constant (L mg^{-1}), and q_m is the maximum quantity of adsorbed metal (mg g^{-1}).

Conversely, the Freundlich isotherm describes multilayer adsorption which may occur when precipitation is removing dissolved metal species from the aqueous phase. The Freundlich isotherm can be expressed by equation (3) shown again below, and similar to the Langmuir isotherm, two constants must be solved in order to describe the system, K_F and the exponent $\frac{1}{n}$.

$$q_e = K_F C_e^{\frac{1}{n}}$$

where q_e is the loading of adsorbate on the adsorbent (mg g^{-1}), K_F the Freundlich constant which correlates to the adsorption capacity (L mg^{-1}), C_e is the equilibrium concentration of the metal ion within the bulk solution (mg L^{-1}), and n is the adsorption intensity.

For chelating adsorption processes, the dependence on surface functional groups means that the Langmuir isotherm is often the most suitable since it describes monolayer adsorption. As a result, when an adsorption isotherm appears to be Freundlich in nature, it is likely that the dissolved metal is unstable in the solution and is undergoing precipitation, so that the dissolved concentration will decrease independently of the surface functionalization. This is most prominently seen at high solution concentrations, where a Freundlich fit shows a gradual increase in adsorption capacity as the bulk concentration increases whereas a Langmuir fit will plateau once all the surface functional groups have been saturated.

To fit each model, a non-linear regression was performed through a sum of least squares analysis. For each data point, the difference between the predicted value and the measured value is calculated and squared. Together, all these values are summed and act as an indicator to the quality of the parameters in accurately describing the observed data. During regression, the two constants were varied through Excel's built-in solver function to minimize the magnitude of the sum of squares, thus giving optimized parameters. The relevant equation for the algorithm is shown below as equation (22).

$$\text{Sum of Squares} = \sum_{i=1}^{N} (q_{Measured} - q_{Predicted})^2 \qquad (22)$$

4.3 Materials

Chemicals

Chemicals used, the manufacturer, and their purity are listed below.

Sodium hydroxide (VWR, > 97%), urea (Sigma-Aldrich, > 99.5%), Sodium sulfate anhydrous (VWR, > 99%), Hydroxylamine hydrochloride (Alfa Aesar, > 99%), Citric acid (VWR, > 99.5%), Glacial acetic acid (Sigma-Aldrich, > 99.7%), sulfuric acid (Sigma-Aldrich, 95 – 97%).

Four metal ions were examined for determining adsorbent selectivity: copper, nickel, chromium, and vanadium. Both copper and nickel were dissolved from metal sulfate salt hydrates and have a valency of two, $CuSO_4 \cdot xH_2O$ (Sigma-Aldrich, > 99%) and $NiSO_4 \cdot xH_2O$ (Alfa Aesar, > 98%), respectively. Similarly, chromium (III) was obtained through the dissolution of chromium sulfate, $Cr_2(SO_4)_3 \cdot xH_2O$ (Sigma-Aldrich, > 99%) , and vanadium (IV) was obtained through the dissolution of vanadium oxysulfate, $VOSO_4 \cdot xH_2O$ (NOAH Technologies Corporation, > 99.5%).

Dialysis was performed with SnakeSkin™ dialysis tubing with a molecular weight cut-off of 3.5 kDA provided by Thermo Scientific.

Chapter Five: Synthesis of an Amidoxime functionalized Cellulose powder for adsorption

5.1 Identifying literature methodology issues and opportunities

As discussed in Chapter Three, cyanoethylation and subsequent amidoximation has previously been performed on cellulose fibers. Two predominant methods are available in literature, heterogenous functionalization by slurrying cellulose or homogenous functionalization through dissolving cellulose. Both methods were replicated and the apparent issues corresponding to each were identified. Ultimately, the methods were either complex due to the difficulty in separating the reaction products as was the case with homogenous functionalization methods (section 5.1.1) or required pre-treatment with a swelling agent to achieve sufficient functionalization when the reactions are conducted heterogeneously (section 5.1.2). Hence, to address the issues, a new hybrid methodology was developed which overcomes some of these shortcomings and is discussed in section 5.2.

5.1.1 Amidoxime functionalization through homogenous reactions – Crystallinity issues

Homogenous functionalization was performed according to the methods described by Li et al. albeit without a freeze dryer [35]. In place of a freeze dryer, a vacuum oven was used to separate the residual water from the solid functionalized cellulose sample. A vacuum oven was chosen since it would accelerate water evaporation while maintaining a low temperature, minimizing the risk of damaging the cellulose samples. The resulting product was highly crystalline and hard as shown in Figure 17.

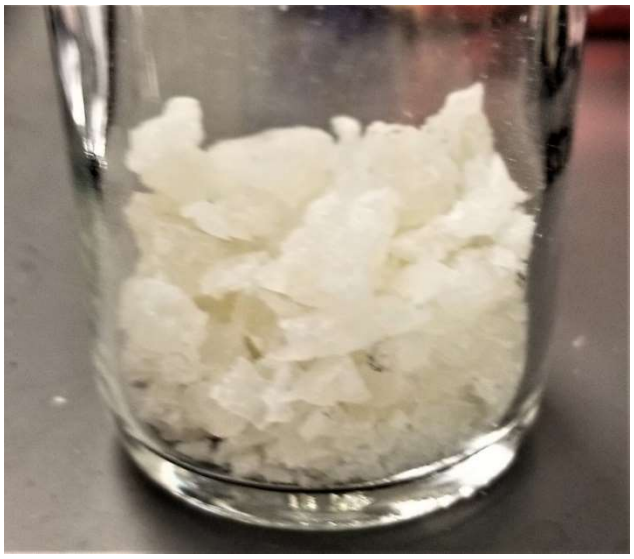

Figure 17 - Appearance of homogenously functionalized cyanoethyl cellulose after drying in a vacuum oven.

Once the cyanoethyl cellulose had been dried and collected, it was further functionalized to form amidoxime functionalized cellulose. The crystalline cellulose sample was dissolved in dimethylformamide due to its insolubility in a non-alkaline aqueous solution. The reaction to amidoxime was performed through addition of hydroxylamine hydrochloride at elevated temperatures (75 °C). The solution of hydroxylamine hydrochloride (10 wt.%), which was neutralized on a mole to mole basis with sodium hydroxide, was dissolved in a solution of 83 v.% ethanol and 13 v.% water.

Upon neutralization, the hydroxylamine solution developed a white precipitate that had the appearance of a salt, which was not reported in literature. This was believed to be sodium chloride precipitates due to the salt's low solubility, 0.65 g per kg of ethanol, even with 17 mL of water being included in the system [123]. While theoretically the solution of ethanol and water would be able to dissolve 6.17 g NaCl per 100 ml, it is likely that the interactions between the solvents as well as the presence of hydroxylamine reduce the availability of the solvents such that the true solubility is not as high as the theoretical value.

Regardless, the hydroxylamine solution (including the precipitate) was added dropwise to the dissolved cellulose and was reacted at 75 °C for 8 hours under vigorous stirring. After 4 hours of reaction time, a

noticeable colour change was observed in the solution, from an off yellow transparent colour to a blue-grey tinge which strengthened for the remainder of the reaction.

The resulting solution was transferred to dialysis tubing and dialyzed for 3 days. The solution was then transferred to a beaker and placed in a vacuum oven at 50 °C for 2 days to evaporate the residual water. The resulting solid was again crystalline, but smaller crystals were formed when compared with the solid following cyanoethylation. The solids are shown in Figure 18 below.

Figure 18 - Appearance of homogenously functionalized amidoximated cellulose after drying

Samples of both cyanoethyl cellulose and amidoxime functionalized cellulose were sent for elemental analysis to determine their nitrogen content. The nitrogen content was then used as a proxy for determining the extent of both reactions, as these reactions were the only way that nitrogen could be chemically added to the cellulose. The results from elemental analysis are shown in Table 6 below.

Table 6 - Elemental analysis of homogenously functionalized cellulose

	Cyanoethylation		Amidoximation	
	Target (wt.%) [35]	Actual (wt.%)	Target (wt.%) [35]	Actual (wt.%)
C	52	51.60 ± 0.01	43	44.05 ± 0.13
H	7	5.75 ± 0.15	7.3	6.32 ± 0.07
N	8.6	9.09 ± 0.02	14.3	11.69 ± 0.04

From the elemental analysis results, it is likely that the reactions proceeded successfully as significant amounts of nitrogen were added to the samples. Additionally, FTIR was attempted on the samples to identify the nature of the nitrogen bonding. However, due to the crystallinity of the samples, manual size reduction was not possible and the resulting reflectance spectra was noisy due to the inability to achieve a smooth powder surface. Therefore, it is unknown whether the nitrogen is truly bonded as cyanoethyl or amidoxime for each respective sample.

To analyze the adsorption capability of the amidoxime functionalized sample, an adsorption test was performed for removing nickel (Ni) from a solution of nickel sulfate using acetate as a buffer at pH 5 ± 0.25. The adsorbent was only able to adsorb 3.7 mg g^{-1}. This is much lower than the theoretical adsorption capacity based on the nitrogen content, assuming that nitrogen exists as the amidoxime functional group. Using equation (10) and equation (11) from Chapter 4, the degree of substitution for both reactions can be calculated. The degree of substitution for the first reaction would be 1.6 while the second would be lower at 0.66. This would result in an amidoxime concentration of approximately 2.6×10^{-3} mol amidoxime per g of adsorbent. This converts to a maximum theoretical adsorption capacity of 75 mg g^{-1} if two amidoxime functional sites are required to bond with one nickel ion. Therefore, the adsorption loading of the sample was lower than the expected by a factor of 20 which shows adsorption limitations not due to a lack of available functional sites.

The clear discrepancy between the quantity of theoretical bonding sites and the available bonding sites indicate that there is potentially limited surface area so that not all the nitrogen functional groups are accessible for adsorption. Since the adsorbent functionalization was performed homogenously, functionalization will occur while the cellulose molecule is dissolved and upon precipitation, those functional groups can effectively be hidden within the center of the particle. This hypothesis was reinforced through visual observations in which the adsorption was seen to change to a dark green-black colour on the surface of the material but there was no colour change evident beyond the surface layer.

As a result, the homogeneous method was determined to be unsuitable for synthesizing an effective adsorbent material. While the degree of functionalization was high, the complexity of the process combined with the lack of effective surface area, lead to poor adsorbent performance. Therefore, another synthesis pathway was investigated to address the observed shortcomings while still achieving a moderate to high degree of functionalization.

5.1.2 Cyanoethylation through heterogenous reactions

To address the issues outlined above, a method for functionalizing cellulose in a heterogenous reaction was examined. The method utilized by Kubota and Shigehisa slurries cellulose powder into acrylonitrile while adding a small amount (approximately 4 wt.%) of concentrated sodium hydroxide solution (36 wt.%) to catalyze the reaction [34]. However, in their method, the authors utilize an atomizer to add a swelling agent, tetramethyl ammonium chloride, to the cellulose to promote an increase in the effective surface area. Unfortunately, an atomizer was not available for this project, so the procedure was followed absent the pre-treatment step.

For the reaction, 3 g of cellulose was slurried in 72 mL of acrylonitrile. The cellulose was found to disperse well within the organic medium and no agglomeration was observed. However, upon addition of the 2 mL of 36 wt.% sodium hydroxide, phase separation was evident, and the density differences caused the

sodium hydroxide solution to quickly settle to the bottom of the beaker, even under vigorous stirring. At the end of the two-hour reaction time, it was observed that some of the cellulose had agglomerated.

After separating the cellulose and acrylonitrile, the cellulose was repeatedly washed with DI water and the residual wash solution was found to be highly alkaline, pH > 14, for the first few washing cycles. Therefore, it is feasible that the sodium hydroxide concentrate absorbed into the cellulose during the reaction which would have caused both the agglomeration at the end of the reaction as well as the elevated pH while washing the sample.

The lack of phase interfacing is further evident in the nitrogen content of the resulting sample which was only 2.5 wt.%. Similarly, as explored by Saliba et al. [36] who followed this method, the degree of functionalization is dependent on atomizing a swelling agent onto the cellulose fibers prior to functionalization. Saliba et al. found that with the addition of the swelling agent, the nitrogen content of the sample after cyanoethylation was increased by almost a factor of three, rising from 3.59% to 9.84% [36]. Therefore, to use pure acrylonitrile as the reaction medium the addition of a swelling agent during pre-treatment is needed.

Furthermore, after the experiment was completed several practical problems with the method were identified. Pure acrylonitrile is problematic to work with due to its relatively high vapour pressure of 11 kPa at 20 °C and the health risk through inhalation [124] [125]. As a result, it would be beneficial from a safety perspective to dissolve the acrylonitrile in water, where the interactions between the water and acrylonitrile may reduce the volatility of the acrylonitrile. At the same time, having water as the slurring medium reduces the total amount of acrylonitrile since only the amount required for the reaction needs to be added.

Ultimately, the heterogenous functionalization method proposed by Kubota and Shigehisa was not desirable for a few reasons. The most significant was the lack of an atomizer to apply a swelling agent to

the cellulose, which was identified as crucial for functionalization. Further, neat acrylonitrile is inherently toxic and volatile which complicates its use. Therefore, a new methodology was necessary to overcome these detriments.

5.2 Development and optimization of a new aqueous-based heterogenous methodology for cellulose functionalization

A novel functionalization procedure was developed that used a heterogenous reaction in an aqueous solution. By dissolving acrylonitrile into the water solvent, the health hazards of acrylonitrile can be minimized due to lower concentrations and volatility. Additionally, by exposing the cellulose to an aqueous sodium hydroxide solution, it was hypothesized that the sodium hydroxide would act as a swelling agent, increasing the effective surface area and degree of functionalization without the need for a complicated pre-treatment step.

5.2.1 Addition of cyanoethyl groups

As previously mentioned, the ability to swell cellulose was imperative to achieving a high degree of functionalization as this allows more functionalization sites to be accessible by the bulk solution. Sodium hydroxide solutions have been identified as potential methods to both swell and dissolve cellulose as researchers have explored alternative methods for processing cellulose fibers [126]. Given the mechanism of the cyanoethylation reaction, the de-protonation of the hydroxide functional groups on cellulose is required to activate them as shown in the reaction schematic below (Figure 19). This allows for dual functionality when using a sodium hydroxide solution, the solution can facilitate swelling of the cellulose while at the same time catalyzing the cyanoethylation reaction.

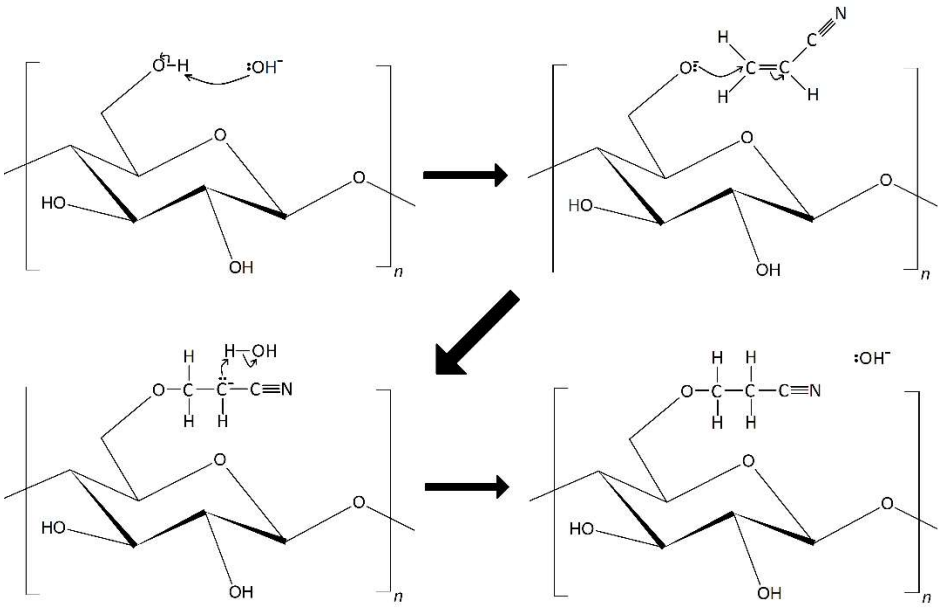

Figure 19 - Mechanism of cyanoethylation of cellulose catalyzed with sodium hydroxide shown on a glucose subunit. Bonds not drawn to scale.

In combination with the literature outlined in Chapter 3, both the concentration of sodium hydroxide and the reaction time for cyanoethylation were identified for further study. When conducted heterogeneously, the availability of functionalization sites can be limited due to the pore network of the cellulose powder. As a result, sodium hydroxide can play a role in improving the accessibility of reaction sites through swelling and mercerizing the cellulose. Similarly, due to potential mass transfer limitations, the reaction time may be critical depending on the kinetics of both the reaction as well as reagent diffusion. Therefore, both of these parameters were examined in further detail.

When conducted at room temperature and with a sodium hydroxide concentration of 25 g L^{-1}, only a small variation in the nitrogen content as a function of reaction time was observed as seen in Figure 20a. When the reaction was conducted over 2 hours, the nitrogen content of cyanoethyl cellulose was 2.1% whereas when the reaction was conducted over 6 hours the nitrogen content was 2.5%. This shows that the reaction was rapid, with most of the reaction occurring within the first 2 hours.

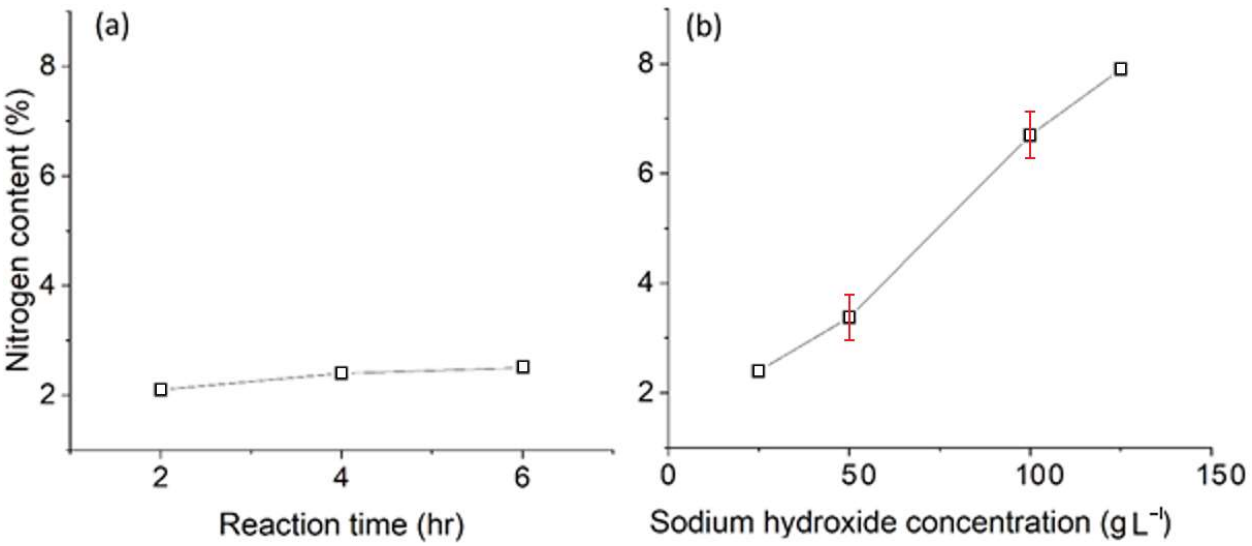

Figure 20 – (a) Nitrogen content as a function of cyanoethylation reaction time. Reaction performed at room temperature with a sodium hydroxide concentration of 25 g L^{-1}. (b) Nitrogen content as function of sodium hydroxide concentration within the slurry solution during cyanoethylation. Reaction performed at room temperature with a reaction time of 4 hours.

Conversely, the resulting nitrogen content was found to have a strong, positive correlation with the sodium hydroxide concentration seen in Figure 20b. The influence on the nitrogen content can be attributed to the two properties mentioned previously, the tendency for cellulose to swell under sodium hydroxide as well as causing the deprotonation of hydroxyl groups on the cellulose surface, catalyzing the cyanoethylation reaction. The large jump in nitrogen content observed between 50 and 100 g L^{-1} can be explained through the swelling phenomena, also referred to as mercerization. During mercerization, the cellulose structure changes from cellulose I to cellulose II as described in section 3.1, increasing the quantity of available hydroxyl sites for functionalization which results in a higher conversion to cyanoethyl groups. Similar to crystalline phase changes exhibited by metals, the transition from cellulose I to cellulose II occurs at a critical concentration of NaOH, dependent on the solution temperature as well as the cellulose source, varying from 1 wt.% NaOH at -17 °C to 11 wt.% NaOH at 25 °C [127]. Therefore, for this cellulose sample, conducted at ~22 °C, it is likely that mercerization has occurred between 50 and 100 g L^{-1}. Furthermore, at higher concentrations of sodium hydroxide the tendency for cellulose to solubilize will increase, leading to the potential onset of homogenous reaction conditions which largely removes the limitation of hydroxyl group availability.

This was visually supported as the slurry underwent a change in viscosity, from low to high, when the reaction was conducted at room temperature with sodium hydroxide concentrations at 100 g L^{-1} and above. The variation in viscosity shows that the system changed from a heterogenous slurry to a homogenous solution, signifying the dissolution of cellulose. The change in viscosity also corresponded to an increase in the optical transparency of the system which supports cellulose dissolution.

The results for cyanoethylation were comparable to those previously reported in literature. The experimental trials in this work found a maximum nitrogen content of 7.9% which is similar, albeit slightly lower, than the maximum reported by Saliba et al. who obtained a nitrogen content of 10.1% [36]. As described in Chapter 3, Saliba et al. used tetramethyl-ammonium chloride as a swelling agent which needed to be atomized onto the cellulose fibers as a pre-treatment to cyanoethylation. This additional step is complex and would be problematic when attempting to scale up production if the material were to be used in an industrial application. As a result, by only immersing the cellulose powder in a sodium hydroxide slurry, comparable levels of functionalization could be achieved, which makes the proposed process promising for scale up.

Following the cyanoethylation trials, a larger batch sample was synthesized with the reaction conditions of 100 g L^{-1} NaOH, a reaction time of 2 hours, and with a targeted temperature of room temperature (22 °C). However, in a post-examination of the reaction, it was determined that due to the large batch size and the exothermic reaction from dissolving sodium hydroxide, that the reaction slurry was unable to cool down to room temperature (22 °C). As a result, the elevated temperature decreased the solubility of cellulose and the linked swelling effects, leading to a lower than expected nitrogen content, 5.5% as opposed to 6.7% observed at room temperature. Furthermore, in subsequent reactions to form amidoxime, it was observed that when sodium hydroxide concentrations were sufficiently high to solubilize cellulose, the physical properties of the resulting adsorbent were unfavourable (high apparent crystallinity) which is described in greater detail below. Therefore, it was concluded that under conditions

that allow for the dissolution of cellulose, the resulting material following amidoximation was undesirable and these conditions were not investigated further in this work.

In agreement with this hypothesis, the cyanoethylation reaction temperature was examined for a sodium hydroxide concentration of 100 g L^{-1} and it was determined that a solution temperature of 35 °C was necessary to prevent cellulose dissolution. For experiments conducted at 25 °C and 30 °C, the characteristic change in viscosity was observed and the resulting material following amidoximation was found to be crystalline with a hardness that made size reduction with a pestle and mortar difficult (Figure 21). Conversely, at a temperature of 40 °C, the addition of acrylonitrile to the solution resulted in the rapid, exothermic hydrolysis of acrylonitrile causing the temperature to spike. Therefore, for synthesizing the final adsorbent material, cyanoethylation was conducted at 35 °C with a sodium hydroxide concentration of 100 g L^{-1} for a total of 2 hours.

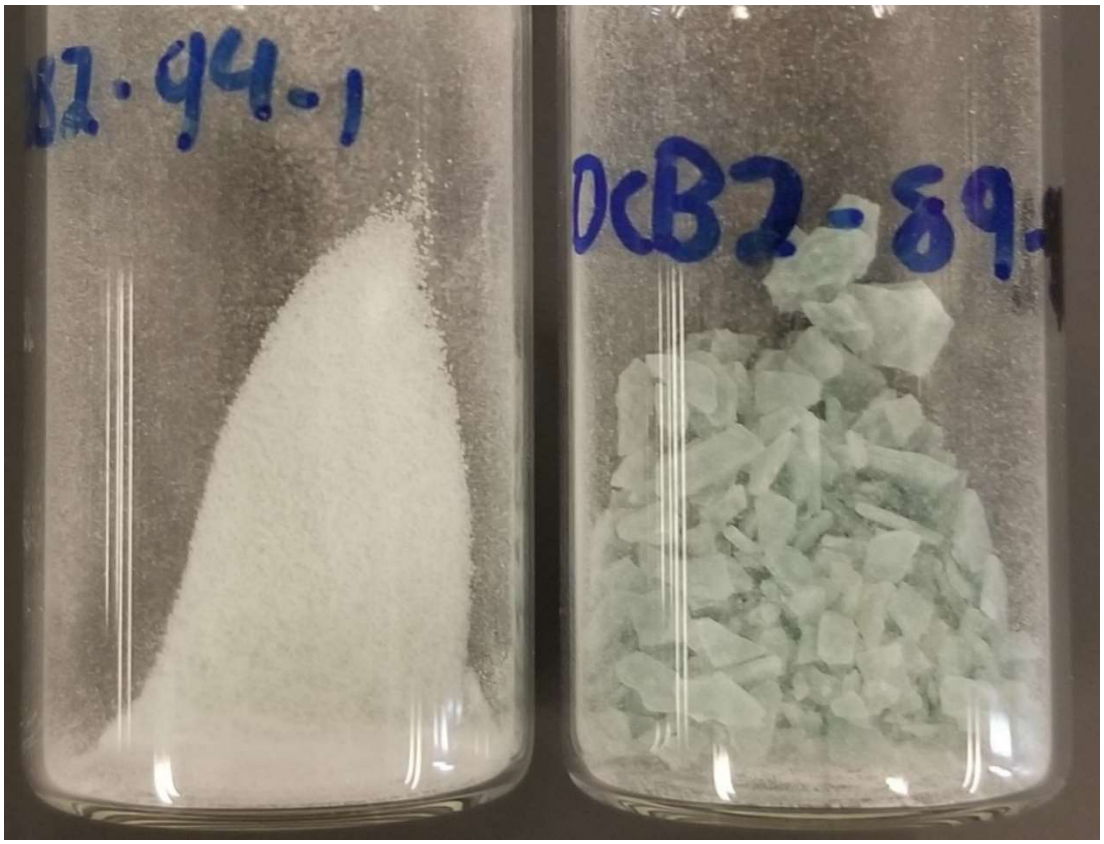

Figure 21 - Resulting functionalized cellulose following amidoximation when different cyanoethylation temperature samples were used as feedstock. Left sample underwent cyanoethylation at 35 °C while the right sample was at 30 °C, both with 100 g L^{-1} NaOH. Blue tinge is attributable to amidoxime functionalities.

The FTIR spectra and CHN analysis for the resulting final batch are shown below in Figure 22 and Table 7, respectively. The FTIR spectra shows the presence of nitrile groups due to the emergence of a characteristic peak at 2,250 cm^{-1} [36]. The sample also had a nitrogen content of 5.3% which is expected due to running the reaction at 35 °C. In agreement with the observed temperature dependence, the batch sample had a powdery appearance following both cyanoethylation and amidoximation, with the amidoximated sample shown in the left-hand panel of Figure 21.

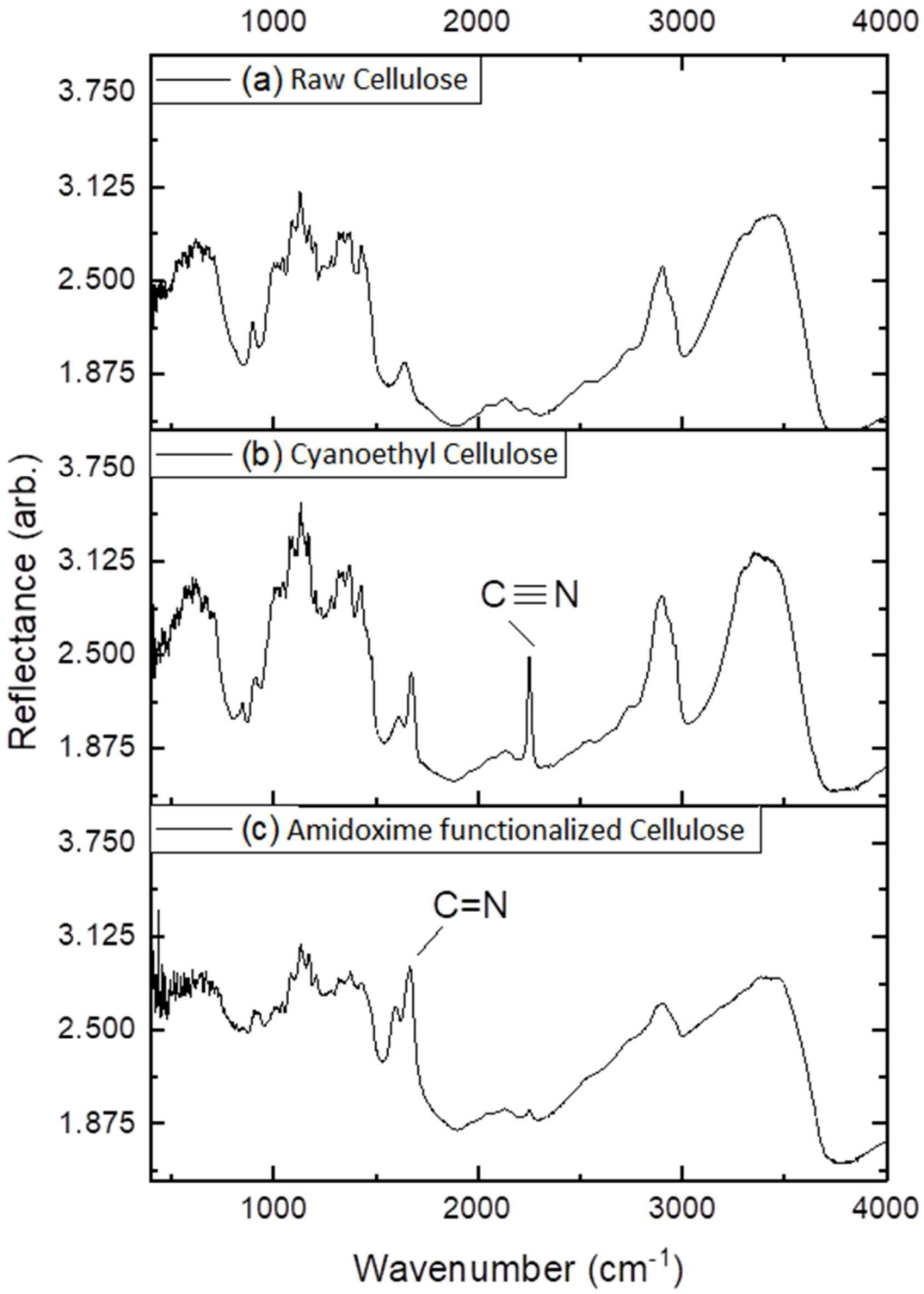

Figure 22 - FTIR spectra of cellulose samples. (a) Raw cellulose. (b) Cyanoethyl cellulose. (c) Amidoxime functionalized cellulose

Table 7 – CHN (Carbon, hydrogen, and nitrogen) analysis of the batch functionalized cellulose sample. Variation is from measurement during elemental analysis. Replicates were not performed due to the sample being a single batch.

Sample	CHN (wt.%)	
Raw Cellulose	Nitrogen	0.02 ± 0.01
	Carbon	43.08 ± 0.04
	Hydrogen	6.29 ± 0.16
Cyanoethyl cellulose	Nitrogen	5.33 ± 0.02
	Carbon	48.28 ± 0.08
	Hydrogen	6.11 ± 0.04
Amidoxime functionalized Cellulose	Nitrogen	7.65
	Carbon	42.46
	Hydrogen	6.56

Ultimately, identifying the optimal conditions for cyanoethylation to form an adsorbent material was found to be complex and could not be identified with nitrogen content as the sole indicator. Further work will need to be done to balance the desire for a high degree of functionalization while maintaining favourable physical properties in the resulting material.

5.2.2 Conversion of cyanoethyl groups to amidoxime

Conversion of nitrile functionalities to amidoxime has been explored previously in the literature and is discussed in detail in Chapter 3 [34] [35]. However, due to the changes from literature for cyanoethylation as discussed in section 5.2.1, experiments were conducted on the amidoximation reaction parameters to determine the impact on the resulting functionalization and the materials usability as an adsorbent.

Development of a 2^3 factorial design experiment to examine reaction parameters

To examine the factors for both amidoximation and subsequent adsorption, a 2^3 factorial design experiment was conducted which examined the role of pH and reaction time for the amidoximation reaction, and also studied the role of acetate concentration when the adsorbent is used in adsorption experiments. As discussed in Chapter 3, the pH of the amidoximation reaction can have an influence by controlling both the de-protonation of hydroxylamine hydrochloride and the rate of nitrile hydrolysis.

Since the reaction was performed heterogeneously, the reaction time may play a large role if the pore network of the cellulose particles is not conducive to reagent diffusion and in such a case, more reaction time will be required. Therefore, both of these factors were considered for the factorial design. In all amidoximation reactions, the temperature was kept constant at 75 °C.

Furthermore, acetic acid was found to enhance the adsorption capacity of vanadium in preliminary work, which is discussed in Chapter 6, and the influence of acetic acid concentration was also investigated in the factorial design. Additionally, in the factorial design experiment the vanadium adsorption capacity was used as the responding variable. By measuring the adsorption capacity of the material as opposed to other characteristics such as elemental composition, a better indication of the resulting performance of the material can be obtained. This is reinforced by experimental trials on the cyanoethylation reaction which found that some samples produced a high nitrogen content (degree of functionality) but resulted in low adsorption performance due to detrimental physical properties. In this trial, eight experimental conditions were performed for adsorption capacity, as shown in the test matrix (Figure 23) below. The vertices are labeled with the “high” value while the “low” values correspond to 0.1 M, pH 7, and 8 hours, for factors a, b, and c, respectively.

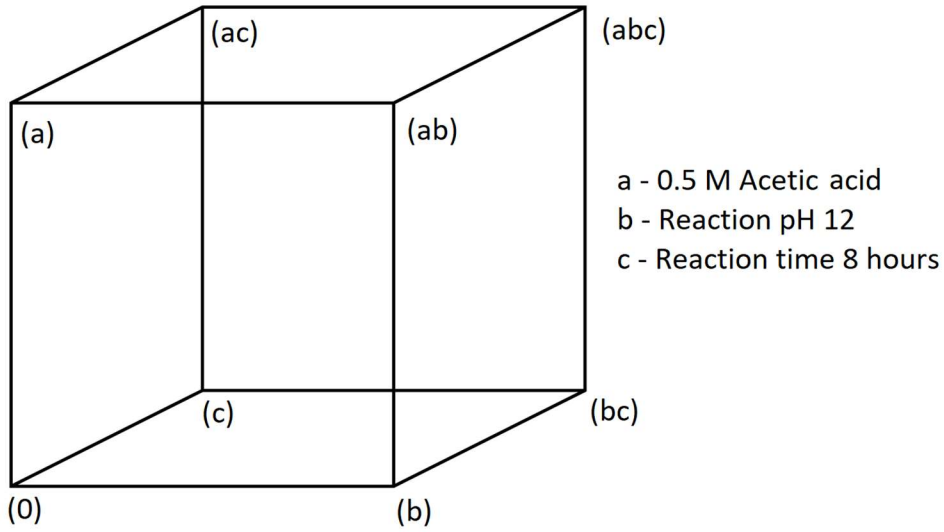

Figure 23 - 2^3 factorial testing conditions expressed as high and low values for each factor. Lower values for (a) is 0.1 M, (b) is pH 7, (c) is 1 hour.

For the amidoximation reaction, four conditions were examined, a high and a low value for both pH and time. For the pH trials, amidoximation was conducted at either pH 7 or pH 12. While for the reaction time, the reaction lasted for either 1 hour or 8 hours. All other reaction conditions remained the same and in accordance with previous testing procedures. Additionally, all the reactions used the same cyanoethyl cellulose, which was prepared in a sufficiently large batch, 20 g, to reduce the probability of error arising from the cyanoethylation reaction.

Following the functionalized cellulose synthesis, the four conditions were then tested for vanadium adsorption in vanadium solutions containing either 0.1 M or 0.5 M acetate at a pH value of 4.25 ± 0.25, a background electrolyte concentration of 0.25 M Na_2SO_4 and 2,000 mg L^{-1} vanadium. Each of the conditions were replicated twice, giving three data points for each of the eight conditions. For examining the effect of each parameter, the high and low results are contrasted as described in Section 4.2.4. Figure 24 shows the resulting adsorption capacities for each of the vertices of the testing matrix.

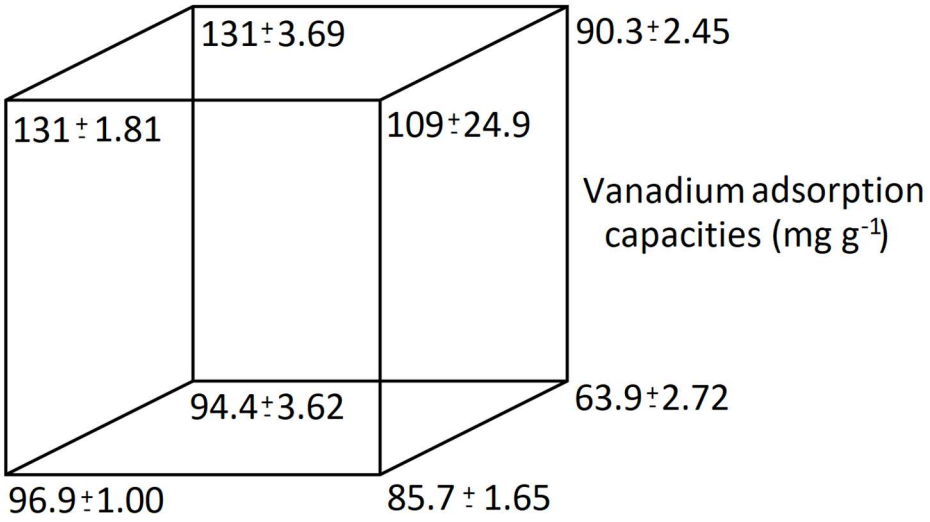

Figure 24 - Resulting adsorption capacities for the factorial testing matrix. Vertices correspond to the ones shown in Figure 23

The upper plane of the cube has higher values than the lower plane, showing that a higher acetic acid concentration may be beneficial for enhancing the adsorption of vanadium. Similarly, the left-hand plane has greater adsorption values than the right-hand plane, suggesting that a reaction pH of 12 is detrimental to the functional groups on the surface. These observations were quantified and the effect of each of the parameters was calculated as shown in chapter 4, and the results are shown in Table 8 below. In the table, (A) represents increasing the acetate concentration from 0.1 M to 0.5 M, (B) represents increasing the reaction pH from a value of 7 to a value of 12, and (C) represents increasing the reaction time from 1 hour to 8 hours.

Table 8 - Calculated effects for the three different factors and their interactions.

Factor	Effect (mg g^{-1})
A	30.0
B	-26.2
C	-10.5
AB	-5.3
AC	1.7
BC	-9.6
ABC	0.0

For maximizing adsorption loading, the results show that increasing the acetate concentration in the vanadium solution from 0.1 M to 0.5 M has the largest beneficial effect, raising the average adsorption loading by 30 mg g^{-1}. On the other hand, increasing the reaction pH from 7 to 12 was found to have the largest detrimental influence, dropping the adsorption loading of the adsorbent by an average of 26.2 mg g^{-1}.

To analyze the statistical significance of the results, analysis of variance (ANOVA) was performed on the data. Since each factor was analyzed at two levels, high and low, each has a single degree of freedom. From this, and with a confidence interval of 95%, an *f* value of 4.49 is needed to justify the statistical significance of a factor. The ANOVA table is shown in Table 9 below and from it, it can be seen that all three of the primary factors are significant with the acetate concentration and reaction pH having the largest *f* values.

Table 9 - ANOVA results for the factorial experiments

Analysis of Variance

Source	DF	Adj SS	Adj MS	F-Value	P-Value
Time	1	657.9	657.91	48.57	0.000
pH	1	4116.9	4116.92	303.96	0.000
Concentration	1	5403.0	5402.98	398.91	0.000
Time*pH	1	553.3	553.29	40.85	0.000
Time*Concentration	1	16.5	16.50	1.22	0.286
pH*Concentration	1	169.1	169.06	12.48	0.003
Time*pH*Concentration	1	0.0	0.00	0.00	0.994
Error	16	216.7	13.54		
Total	23	11133.4			

Furthermore, the interaction between reaction time and pH was also found to be significant. This is potentially explained through the hydrolysis of nitrile groups which has been discussed earlier in this chapter. With an elevated pH and temperature, the hydrolysis of nitrile groups becomes much more favourable, as it is a standard chemical synthesis to hydrolyze nitrile groups to carboxylates under alkaline conditions and reflux. Therefore, it would be likely that under the reaction conditions performed, many of the nitrile groups would hydrolyze to carboxylate, reducing the quantity of amidoxime groups that are available for vanadium bonding. The time and pH are likely confounding due to this side reaction taking place and increasing the length of time under these conditions increases the probability of nitrogen functional groups being replaced by oxygen functional groups.

Therefore, from this experimental trial it was observed that the concentration of acetate in the adsorption solution has a statistically significant effect on the vanadium adsorption capacity for this adsorbent which is discussed further in the following chapter. Additionally, conducting the amidoximation reaction under highly alkaline conditions is not favourable, likely due to the hydrolysis of the cyanoethyl groups as discussed previously. Similarly, the reaction was found to proceed rapidly, and a longer reaction time was determined to be detrimental to the adsorption performance of the material.

Determining the influence of factors on amidoximation

From the insights gained in the factorial study, the pH and to a lesser extent, the reaction time, were determined to be consequential for the resulting adsorption loading. Furthermore, previous studies in literature have found that the reaction temperature plays a role in success of functionalization [34]. This is thought to be due to the reaction being limited by equilibrium constraints as opposed to kinetics. Amidoximation was performed under a range of conditions, and the resulting nitrogen contents are shown in Figure 25.

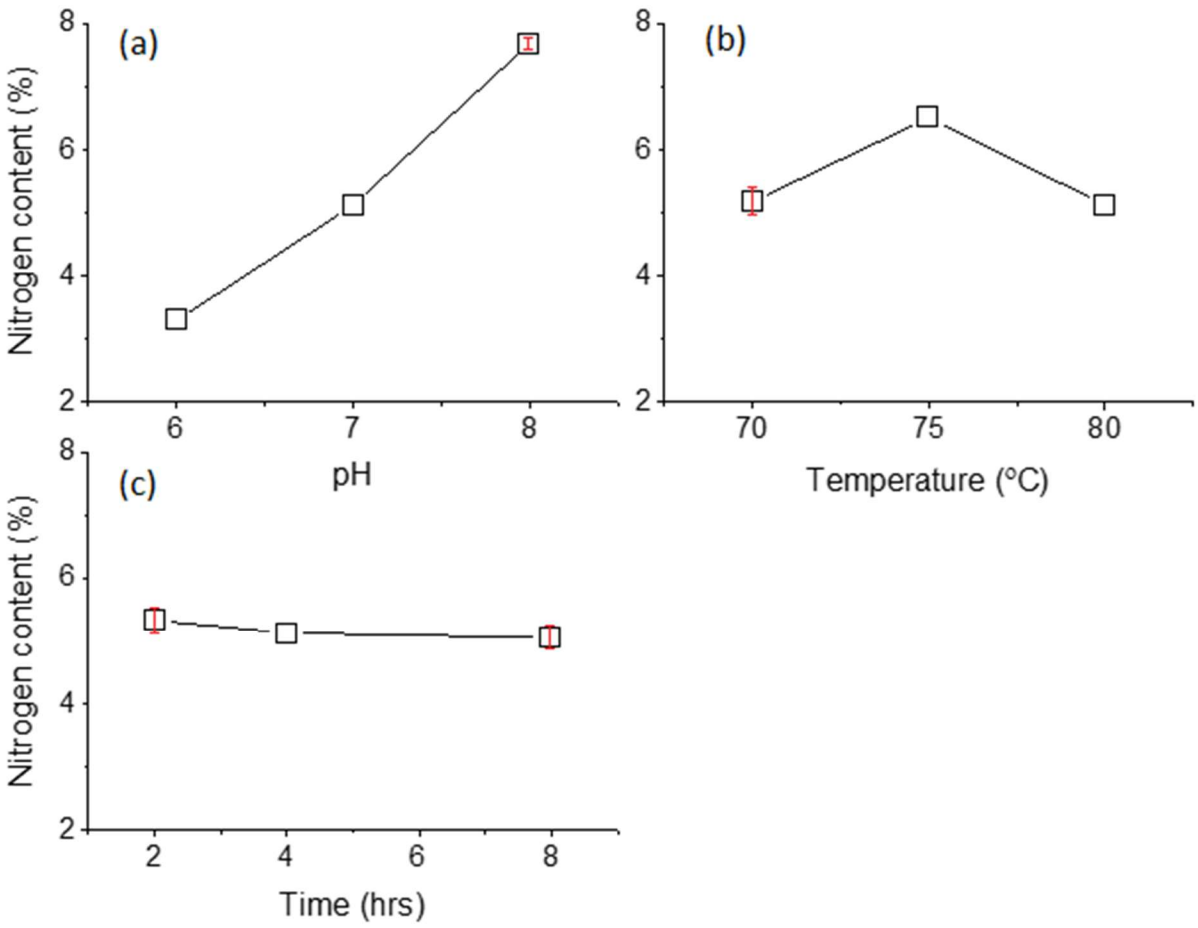

Figure 25 - Nitrogen content for different amidoxime synthesis conditions. (a) Nitrogen content as function of pH while maintaining a temperature of 80 °C and a reaction time of 4 hours. (b) Nitrogen content as a function of temperature while maintaining a pH of 7 and a reaction time of 4 hours. (c) Nitrogen content as a function of time while maintaining a temperature of 80 °C and a pH of 7.

The nitrogen content was found to have a strong dependence on the pH of the reaction as seen in Figure 25a, which is consistent with previous studies [35] and the mechanism in Figure 14. This agrees with the hypothesis that the de-protonation of hydroxylamine hydrochloride is necessary for the reaction to proceed. Since the cyanoethyl cellulose used as the feedstock already contained 3.2% nitrogen, at pH 6 very little nitrogen is added showing that the conversion of cyano groups to amidoxime was unsuccessful. Conversely, at pH 8 the sample achieved a nitrogen content more than twice that of pH 6. Due to the importance of de-protonating hydroxylamine hydrochloride, it is expected that the reaction would be highly sensitive in this region. The pKa of hydroxylamine hydrochloride is 6.03 and at pH 8, 99% of the

species will be in the de-protonated form. This is contrasted with pH 6, where only half of the hydroxylamine will be in the de-protonated form. Since it is thought that the reaction is equilibrium controlled, the change in effective reagent concentration will result in the equilibrium shifting to favour more products which is seen in the nitrogen content. However, as shown in the factorial experiment, raising the pH even higher (12) is detrimental due to the hydrolysis of nitrile groups which is substantial at elevated temperatures [128].

Interestingly, the nitrogen content was maximum, 6.5%, at 75 °C and dropped to 5.2% when the reaction was performed at 80 °C (Figure 25b). This could be explained through the occurrence of a secondary reaction in which two adjacent amidoxime functional groups can cyclize to form a dioxime group. In this process, ammonia is released which could account for the decrease in nitrogen content observed [129] [130] [131]. The temperature dependence of the dioxime formation has also been observed previously, suggesting an equilibrium-controlled reaction [93]. This would help explain the high sensitivity to temperature (Figure 25b).

Similar to cyanoethylation, there were no statistically significant changes in the nitrogen content with respect to time which suggests that the reaction kinetics are rapid and there is no limitation due to diffusion into the particle pores (Figure 25c).

Based on the results of both the cyanoethylation and amidoximation investigations, a 50 g batch of adsorbent was prepared for analyzing the adsorption performance. The batch from cyanoethylation was described in the previous section and the elemental results following amidoximation are given in Table 7. Using equation (11), the degree of substitution for amidoximation was calculated to be 0.32, showing that approximately 40% of cyanoethyl groups were converted to amidoxime. Therefore, further work to optimize the reaction parameters is necessary to ensure that nitrile groups are effectively converted to amidoxime. From the FTIR spectra shown in

Figure 22c, the peaks due to nitrile groups disappear following the amidoximation reaction which shows that the groups are being chemically converted. Since the elemental analysis suggests that not all the groups are being converted to amidoxime, it is likely that they are undergoing a side-reaction, potentially hydrolyzing even at the relatively neutral pH of 8.

Ultimately, the alternative reaction procedure produced an acceptably functionalized adsorbent material while being substantially simpler than those previously discussed in literature. The elimination of a pre-treatment atomization step could facilitate scale-up, while not conducting the reaction homogenously allows for reduced energy consumption by removing chilling and the mixing of the high viscosity cellulose solution. By slurrying the cellulose in a sodium hydroxide solution, two benefits are observed, enhancing the quantity of surface sites available due to swelling/mercerizing the material, and improving the reaction due to the de-protonation of hydroxyl groups on the cellulose surface. However, both reactions require further development to optimize the degree of functionalization while limiting the tendency to form crystalline structures which reduce the surface area available for adsorption.

Chapter Six: Utilization of amidoxime functionalized cellulose for vanadium adsorption

During the synthesis procedure discussed in Chapter 5, adsorption experiments were used to provide another quantification method for how effective the synthesis methodology was. As discussed in Chapter 3, the influence of co-ions on adsorption has fallen out of focus in the literature and often studies are conducted with no background electrolyte to control ionic strength or are conducted in the presence of buffers but no discussion is dedicated to analyzing their potential influence [34] [36]. Older studies have identified that anionic ligands can play a substantial role in altering adsorption, often decreasing the adsorption performance since the dissolved ligand will compete with the surface functional groups for the metal ions [106] [107] [108] [109]. However, it is possible for a complexing ligand to enhance adsorption, if the resulting ligand-metal complex interacts favourably with the surface functional groups [107]. Due to how specific such an interaction would be, a ligand – surface functional group pairing could be highly selective towards a particular ion, which would be beneficial for processes such as hydrometallurgy that look to selectively enrich certain elements for further processing.

This chapter will discuss the experiments that identified acetic acid as a beneficial complexing agent for vanadium on amidoxime functionalized cellulose, as well as further experiments to quantify the phenomena over a range of pH values and metal ion concentrations.

6.1 Identification of acetate-vanadium complexes

As part of an initial trial to determine the efficacy of the synthesis parameters and the amidoxime functional group, the amidoxime functionalized cellulose was tested for adsorbing metals other than vanadium to gain an idea of the potential selectivity. Initially, a qualitative adsorption test was performed for copper (Cu(II)), chromium (Cr(III)), iron (Fe(III)), and vanadium (V(IV)), all performed at pH 5 with an acetic acid buffer. Following the test, all the adsorbent samples exhibited colour changes. However, the

adsorbent that had been exposed to vanadium showed remarkable colour change, altering from an initial white colour to a dark brown/black. Therefore, to quantify the amount of vanadium that had been adsorbed, the residual solution was analyzed with ICP.

The ICP results showed that the vanadium loading was 150 mg g^{-1}, a substantial increase when compared with initial testing. To assess whether the result was an anomaly, three repeats of the adsorption test were performed, and loading was determined to be 148.9 ± 0.82 mg g^{-1}. This confirmed that the presence of acetate had an enhancing effect for vanadium adsorption onto the adsorbent.

Interestingly, to assess whether the age of the complex solution influenced adsorption, a two-week-old solution was used in a subsequent experiment. No precipitation was evident in the two-week-old sample, but the opacity of the solution was less than that of a fresh sample. The three trials yielded an adsorption loading of 86.3 ± 1.05 mg g^{-1}, which suggests that there is a time dependence on the stock solution for adsorption performance. The time dependence is likely caused by the degradation of the vanadium acetate complex, potentially due to the oxidation of the complex over time. This is reinforced through visual observations of the solution, first changing from light blue to dark green when the vanadium acetate complex is formed, followed by the dark green complex solution slowly becoming lighter and more transparent over time. Figure 26 illustrates the changes in the solution colour over time, showing the emergence of a complex over 20 minutes.

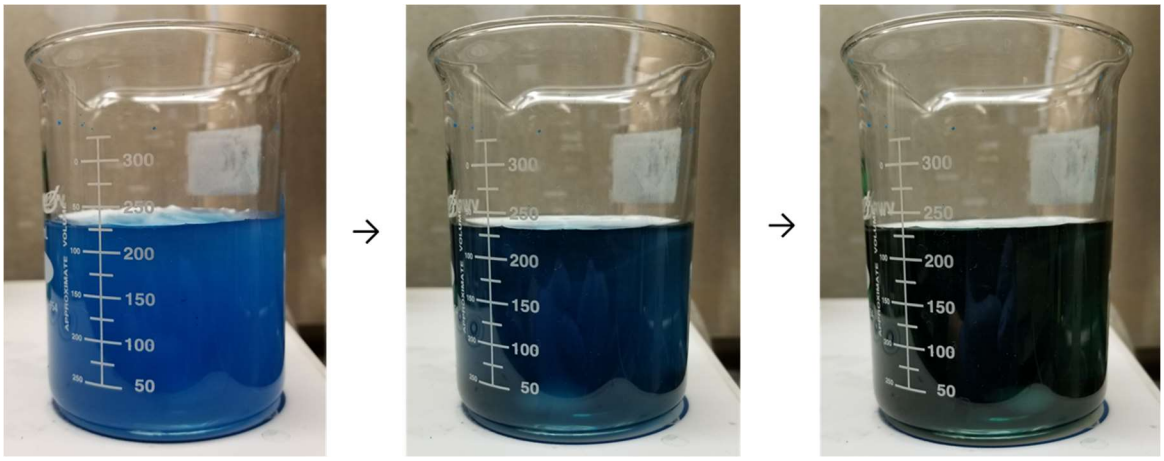

Figure 26 - Vanadium acetate complex formation as a function of time. Shown at times: 0 minutes, 8 minutes, and 19 minutes. V^{4+} concentration of 2,000 mg L^{-1} at pH 4.5 with an acetic acid concentration of 0.5 M.

The acetic acid adsorption performance is strongly contrasted with the adsorption performance at pH 6, where a citric acid buffer was used. For the citric acid solution, the adsorption loading was found to be only 10.6 mg g^{-1}, an order of magnitude lower than acetic acid. Considering the typical pH behaviour for chelating materials as discussed in Chapter 2 (Figure 4), it is expected that the adsorption loading would increase or at least stay the same at pH 6 as opposed to pH 5. Both citric acid and acetic acid are carboxylic acids and could theoretically be forming vanadium carboxylate complexes. However, the lack of adsorption enhancement suggests that the chemical structure of the complexing agent is important, potentially to facilitate the formation of polymetallic aqueous complexes in which the complexing agent acts as a bridge between several metallic ions. Similar polynuclear vanadium acetate complexes have been observed for trivalent vanadium (V^{3+}) so it is likely that tetravalent vanadium (V^{4+}) could form structurally similar complexes [132]. This idea is supported by the dependence on adsorption solution pH which is discussed further in section 6.4.

6.2 Influence of synthesis parameters on adsorption

Following the synthesis of amidoxime functionalized cellulose as outlined in the previous chapter, the adsorbent was used to investigate the interaction between amidoxime and aqueous vanadium species through a series of adsorption trials. As mentioned in the previous Chapter, the nitrogen content may not be representative of the adsorption performance of the material. As a result, all the synthesized samples were also tested for vanadium adsorption capacities with the results shown in Figure 27.

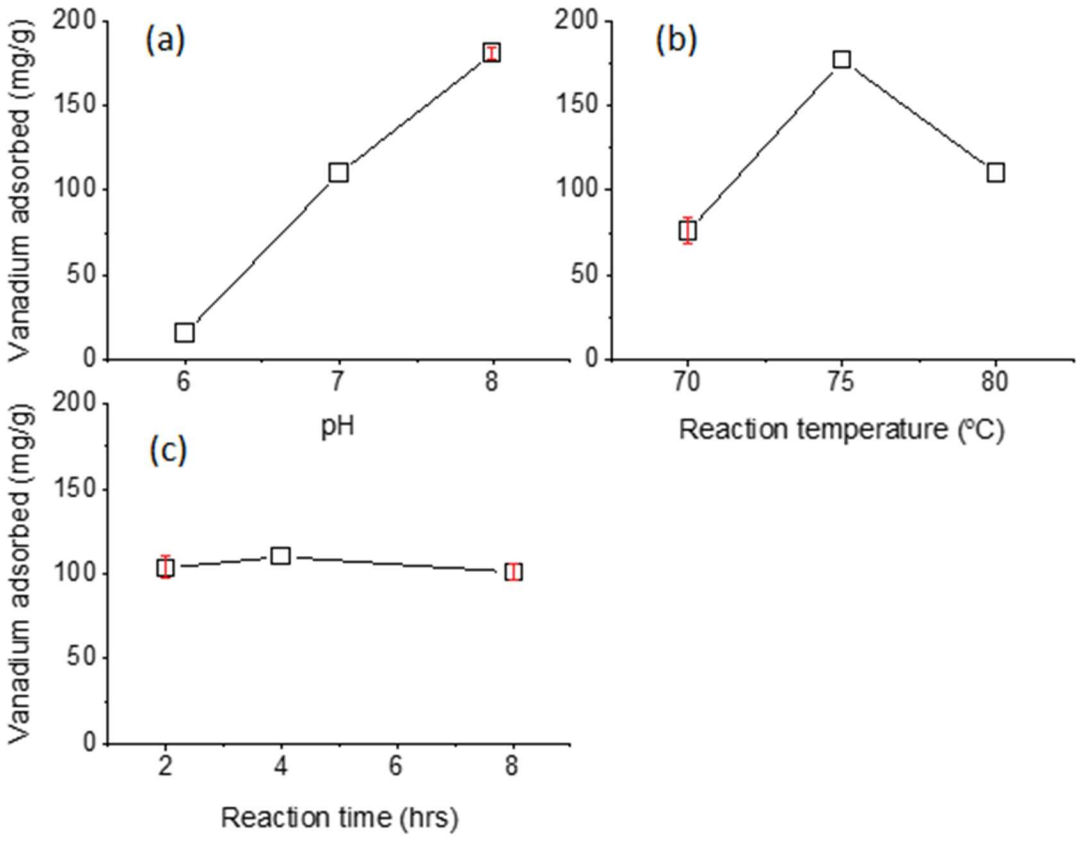

Figure 27 - V^{4+} adsorption quantities (pH 4.5, $[Van]_O$ = 2,000 mg L^{-1}, [Acetate] = 0.5 M, $[Na_2SO_4]$ = 0.25 M) for different amidoxime synthesis conditions.(a) Adsorbed quantity as function of pH while maintaining a temperature of 80 °C and a reaction time of 4 hours. (b) Adsorbed quantity as a function of temperature while maintaining a pH of 7 ± 0.03 and a reaction time of 4 hours. (c) Adsorbed quantity as a function of time while maintaining a temperature of 80 °C and a pH of 7 ± 0.03.

When comparing the nitrogen content (Figure 25) with the vanadium adsorption capacities shown in Figure 27, it is clear that there is a strong positive correlation between the two. Since the adsorption experiments were conducted in the presence of acetic acid, the associated nitrogen functionality interacts positively with the acetate-vanadium complex, shown by the elevated adsorption loadings.

The highest V^{4+} adsorption loading was observed for functionalized cellulose synthesized at pH 8 ± 0.03 (Figure 27a). Specifically, a 10-fold increase in the adsorption loading was observed at pH 8 as compared to pH 6. Although the nitrogen content only differs by a factor of 3, this 10-fold increase in the adsorption loading can be attributed to nitrile groups not being converted to amidoxime at pH 6. This result indicates that nitrile groups do not have a strong affinity to the vanadium complexes and amidoxime functionality is necessary for binding.

From Figure 27b, the reaction temperature corresponding to the maximum adsorption loading for vanadium was found to be 75 °C. This temperature has been found to be an optimal temperature for forming amidoxime groups previously in literature, which again supports the adsorption dependence on amidoxime groups [34]. The decrease in adsorption capacity at 80 °C can be explained by the formation of cyclic dioxime groups discussed in section 3.2 and section 5.5.2. The conversion to dioxime results in the loss of a bonding site since the two bidentate amidoxime groups combine to form a single tridentate functional group.

When plotting the adsorption loading as a function of the nitrogen content a linear correlation is seen as shown in Figure 28. However, the intercept of zero adsorption appears to occur at an elevated nitrogen content. This suggests that some of the nitrogen groups may not be involved in the adsorption of vanadium.

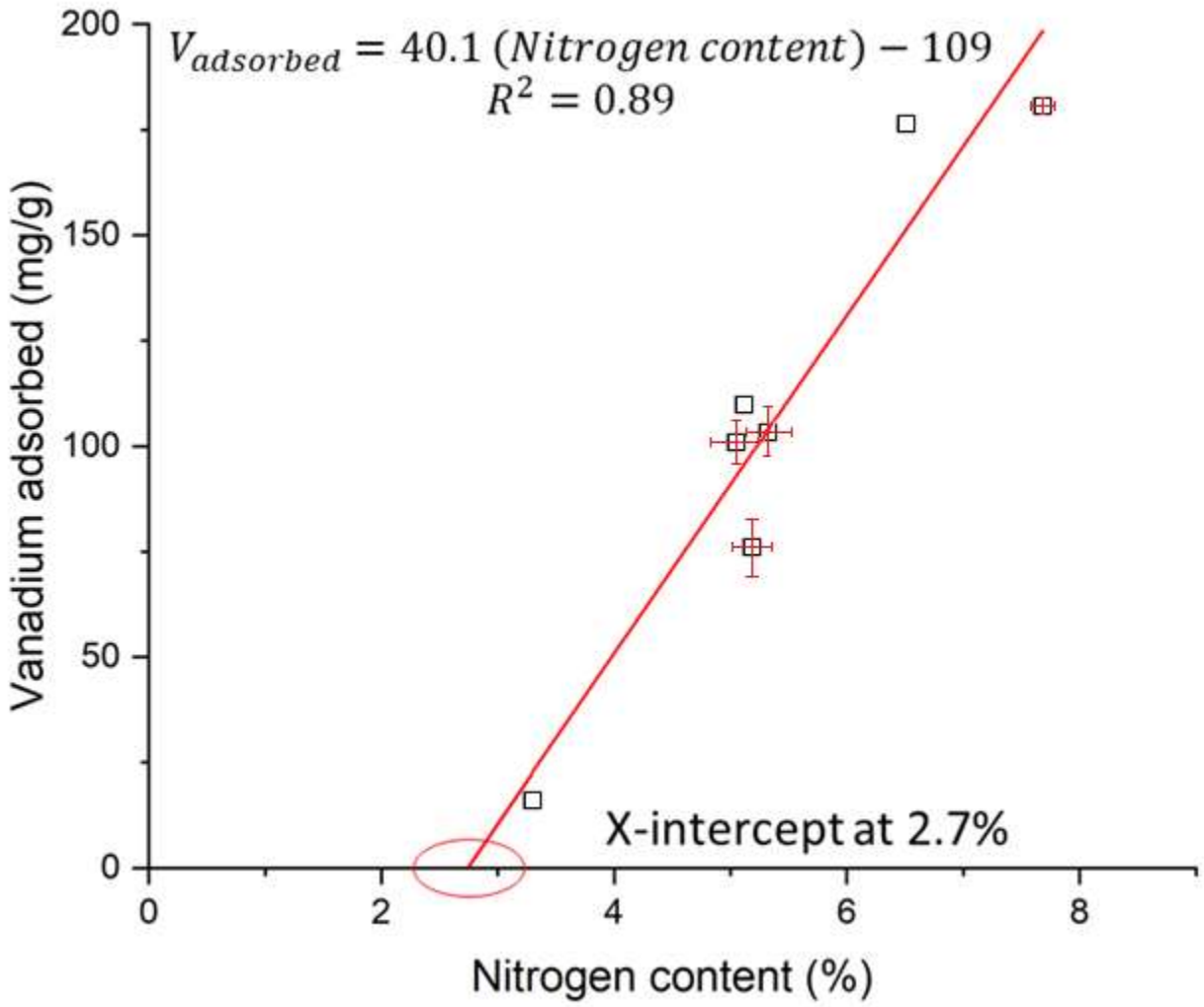

Figure 28 Adsorbent loading of vanadium as a function of nitrogen content for amidoxime functionalized cellulose. The synthesis conditions and the associated nitrogen content are shown in Figure 25, while the adsorption performance is shown in Figure 27. Adsorption was carried out using a solution at pH 4.5, $[Van]_O$ = 2,000 mg L^{-1} as $VOSO_4$, [Acetate] = 0.5 M, $[Na_2SO_4]$ = 0.25 M, room temperature (22 °C).

This is likely attributable to nitrogen being present as different functional groups, such as the cyclic dioxime group discussed above, or residual nitrile groups, expected for the amidoximation reaction performed at pH 6. The efficacy of each of these functionalities is still debated in the literature and the results shown above indicate that certain nitrogen functionalities are active towards the acetate-vanadium complex while others are not. From the reaction conditions observed, it is likely that the nitrogen functionality is primarily in the form of amidoxime which is supported by the FTIR spectra shown in Figure 22. However, further characterization is required to confirm the functional structure of the

nitrogen, which is obscured by spectral overlap of carbon-elemental double bonds in FTIR (nitrogen and oxygen) and to determine which groups are desirable for maximizing adsorption. Furthermore, CHN analysis inherently has uncertainty since multiple elements are added during the reactions, namely oxygen during conversion to amidoxime. As a result, it is difficult to differentiate between a lower nitrogen content indicating lower conversion, or the addition of oxygen which acts to dilute the weight percent of nitrogen. Therefore, additional characterization is necessary to identify the quantity of functional groups in the sample.

6.3 Effect of Solution pH on Adsorption

Due to mechanism of chelation as discussed in Chapter 3, it was expected that the adsorption performance would depend strongly on the solution pH. A series of adsorption experiments were performed at a range of pH values between pH 2 ± 0.03 and 5 ± 0.03 to evaluate its influence which is seen in Figure 29.

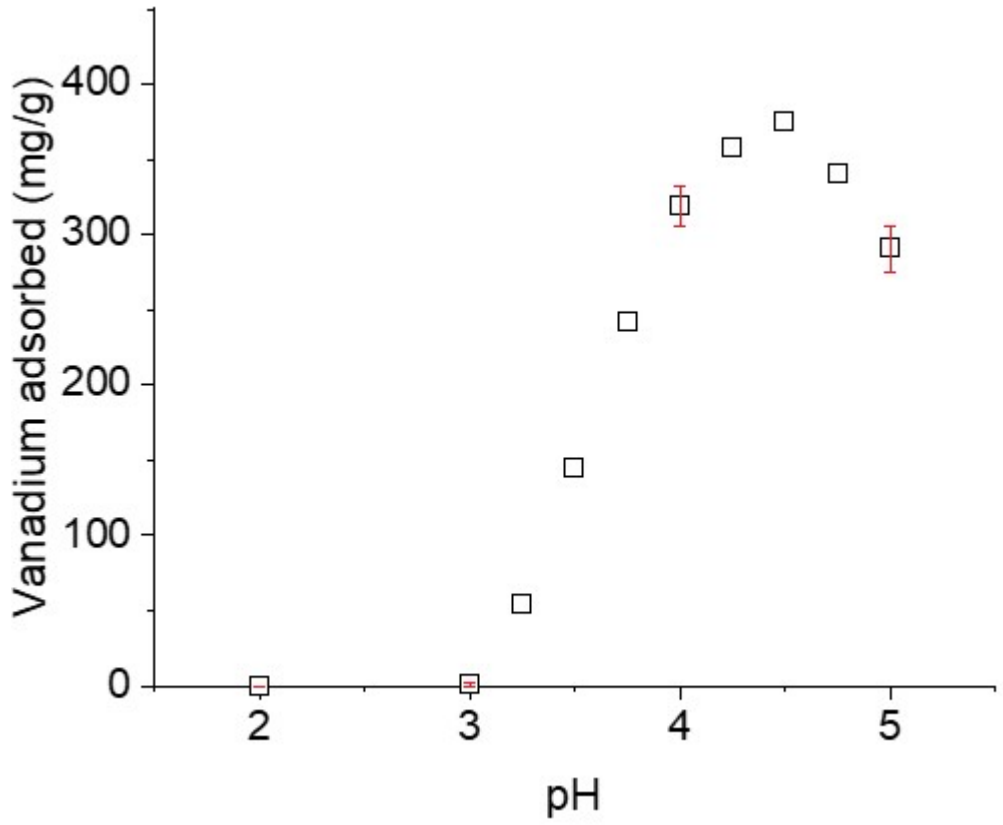

Figure 29 - pH dependence of V^{4+} adsorption with 0.5 M acetic acid and an initial vanadium concentration of 2,000 mg L^{-1}.

For experiments conducted at both pH 2 and 3, no statistically significant adsorption was observed (below detection limit, 1.6 mg g^{-1}). However, an increase in the adsorption loading was observed at higher pH values, with a maximum loading of 375 mg g^{-1} at pH 4.5. Between pH 4.5 and 5, a slight drop in the loading was observed which may be attributed to the vanadium complex becoming less favourable in the presence of increasing hydroxide ion concentrations and the speciation of vanadium changing to anionic. However, further study is needed to support this hypothesis. Above pH 5, the 2,000 mg L^{-1} solution was not stable over the 24-hour period needed for adsorption experiments and as a result, an accurate adsorption loading could not be determined.

The steep onset of adsorption above pH 3 (Figure 29) can be correlated to deprotonation of acetic acid (pKa = 4.76), supporting the theory that deprotonated acetate molecules complex with vanadium ions.

The adsorption onset at a pH well below the pKa of acetic acid can be explained by the high concentration of acetic acid. With an acetic acid concentration of 0.5 M and 2,000 mg L^{-1} vanadium, equimolar concentrations of vanadium and acetate ions would be achieved at pH 3.7, while a 2:1 acetate : vanadium ratio would exist at pH 4.0, assuming that the acetic acid/acetate equilibrium is not significantly shifted due to complexation. Therefore, the high sensitivity in this pH range is expected as acetate begins to be available at stoichiometric ratios to the vanadium ions.

Notably, the adsorption onset at pH 3 is close to pH 3.5 where the formation of the polynuclear vanadium complexes with acetate have been observed [132]. The proposed structures of these complexes are shown in Figure 30.

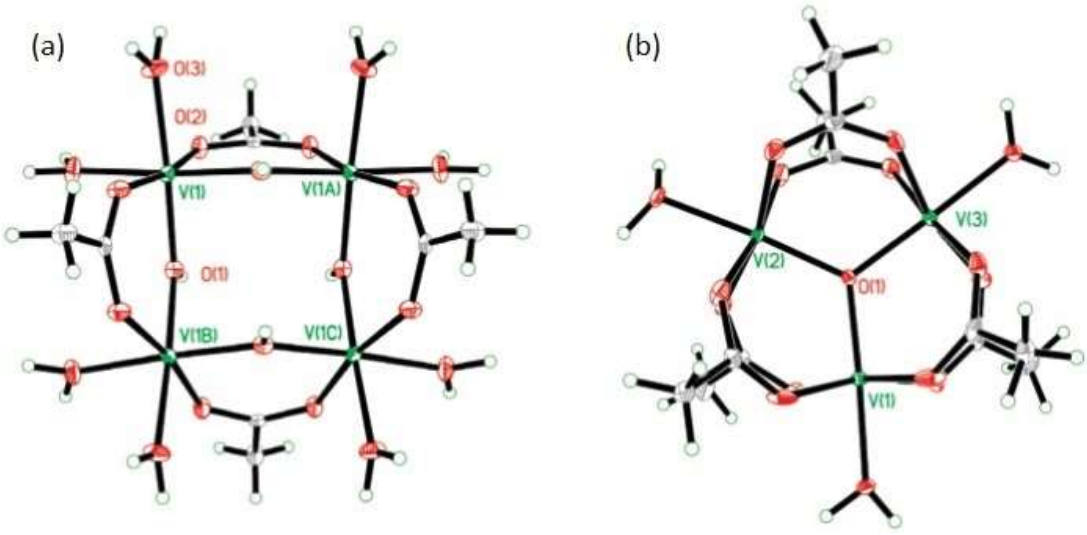

Figure 30 - Polynuclear V^{3+}- acetate complexes in an aqueous system. (a) $[V_4(\mu\text{-}OH)_4(\mu\text{-}OOCCH_3)_4\ (OH_2)_8]^{4+}$.(b) $[V_3(\mu 3\text{-}O)(\mu\text{-}OOCCH_3)_6(OH_2)_3]^{+}$ [132]

The formation of vanadium acetate complexes can explain the observation that the addition of acetate ions improves the solubility of vanadium above pH 4.25. Without acetate present, stock solutions with a vanadium concentration of 2,000 mg L^{-1} precipitated at pH values above 4.25 over 24 hours. However, with the addition of 0.25 M acetate, the stock solutions at the same vanadium concentration were found to be stable for 7 days at a pH of up to 6 without any precipitate evident. Thus, the adsorption effects of

the complexing agent are not due to an increased tendency to precipitate, but potentially due to the formation of polynuclear complexes in the solution bulk and/or at the interface. Furthermore, the solution colour change observed by Fry et al. aligns well with the colour changes observed in this work shown in Figure 26 [132]. This further supports the hypothesis that vanadium-acetate complexes are forming in the solution.

The promoting effect of acetate on V^{4+} adsorption can be explained by improving the ion exchange efficiency when binding with amidoxime groups present on the cellulose surface. In the absence of a complexing agent, V^{4+} is expected to be in the form of VO^{2+}, with a ratio of one vanadium atom for every two units of positive charge. However, the formation of polynuclear structures, as shown in Figure 30, can alter the charge ratio. Structure (a) has a ratio of one vanadium atom to one unit charge (1:1) whereas, structure (b) has a ratio of 3:1. Although the structures shown in Figure 30 exist for V^{3+}, it is likely that similar structures exist for V^{4+}. Thus, the complexation of vanadium with acetate enables chelation of more vanadium with amidoxime functional groups, while maintaining the charge balance of the system.

6.4 Vanadium adsorption isotherms with and without acetic acid

As with any adsorption study, the development of isotherms is critical for understanding the performance of the adsorbent material under a range of concentrations, and to gain insight into how the adsorbate is interacting with the surface. As discussed in section 3.5, two isotherm models are principally used for describing adsorption: the Freundlich and Langmuir isotherms. The key differences between the two relate to the interaction of the adsorbate with the surface of the adsorbent. The Langmuir model assumes that a monolayer will form and that once a site is occupied, another adsorbate molecule cannot interact with the surface. For aqueous adsorption conditions, this model describes chelating interactions between functional groups and dissolved ions since a functional group only constitutes a single bonding site. Conversely, the Freundlich model describes multilayer adsorption and would better describe metal

precipitation on the surface of the adsorbent since precipitation will not be limited by the availability of functional groups.

To further analyze the influence of acetate, equilibrium isotherms for V^{4+} were generated without acetate, as well as with 0.5 M acetate in solution at a pH of 4.5 which corresponded to the pH of maximum adsorption. The experimental adsorption isotherm data and the corresponding Langmuir and Freundlich isotherms (fitted by non-linear regression) are shown in Figure *31*. By varying the mass of adsorbent and the volume of V^{4+} solution added to the batch experiment, different residual equilibrium concentrations for V^{4+} could be achieved without diluting the stock solution.

To gain insight into adsorption mechanisms, the adsorption isotherms were fit with the Langmuir and Freundlich models (Figure *31* a and c). The corresponding residuals for the fitting method are shown in Figure *31* b and d.

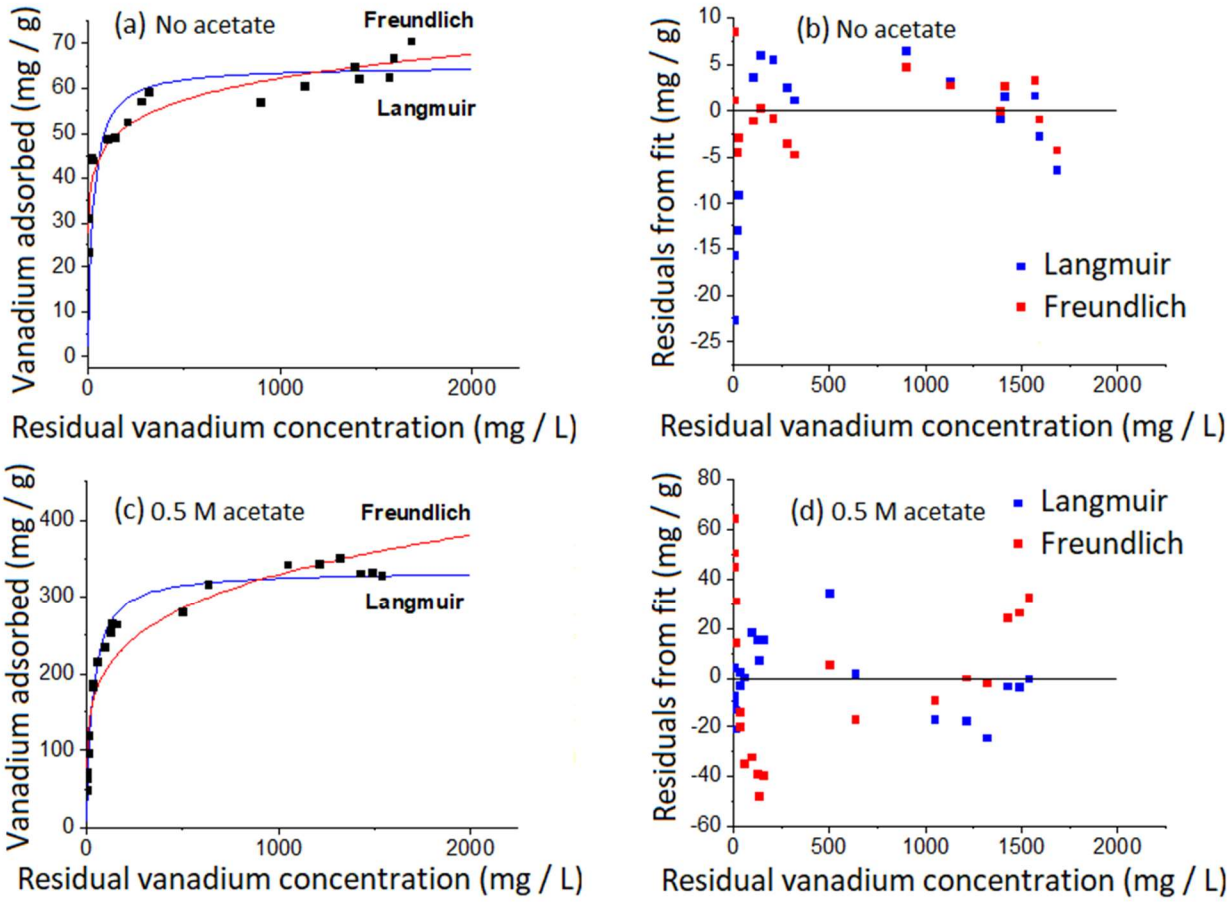

Figure 31 - *V^{4+} adsorption isotherms and resulting residuals for Langmuir and Freundlich models, without and with acetate. Panel (a) – V^{4+} isotherm without acetate. Panel (b) Residuals of model fitting for the isotherm without acetate. Panel (c) V^{4+} isotherm with 0.5 M acetate. Panel (d) Residuals of model fitting for the isotherm with 0.5 M acetate. The raw adsorption data was fit using non-linear regression utilizing the method of least sum of squares. Experiments were conducted at pH 4.5 and equilibrated over 24 hours.*

The adsorption isotherm without acetate is better fit by a Freundlich model when compared to a Langmuir model (Figure *31*a). The resulting Freundlich constant (K_f) is 27.6 while the inverse exponent ($1/n$) is 0.118. The better fit is particularly evident in the low concentration region where the Langmuir model underestimates the capacity by a factor of more than three, 8.3 mg g^{-1} predicted versus 31 mg g^{-1} measured (as also illustrated in the residuals, Figure *31*b). The better fit for the Freundlich isotherm suggests that adsorption is complemented by precipitation of V^{4+} at pH 4.5. Precipitation was observed in the background electrolyte, and without a complexing agent V^{4+} begins to precipitate at pH 4.3 at a concentration of 2,000 mg L^{-1} as discussed in the previous section. Therefore, as the residual equilibrium

concentration increases from 0.5 mg L^{-1} to 1,600 mg L^{-1}, it is expected that more V^{4+} compounds will precipitate and attach to the adsorbent surface, with multilayer adsorption following the Freundlich isotherm.

In contrast, the Langmuir model is a better fit for the isotherm obtained in the presence of acetate (Figure *31*c and d). This is particularly evident at low concentrations where the Freundlich model overestimates the capacity by upwards of 60 mg g^{-1}. From the Langmuir model, the fitted adsorption capacity, q_m, for V^{4+} was 332 mg g^{-1}, or 6.52 mmol g^{-1}, in the presence of acetate, and adsorption was found to be highly favorable with a separation factor, R_L, from equation (2) of 0.015. The Langmuir constant, K_L, obtained was 3.24 x 10^{-2} L mg^{-1}. The better fit with a Langmuir isotherm suggests monolayer bonding of V^{4+}, which is due to its strong chemical interactions with surface functional groups that can only accommodate a limited number of complexes. Therefore, acetate enables the specific site bonding of V^{4+} to amidoxime groups of the adsorbent rather than its precipitation under the conditions studied.

With acetate, the adsorption capacity of the amidoxime functionalized cellulose for V^{4+} (330 mg g^{-1}) is comparable to other vanadium adsorbents shown in Table 10 below. Chitosan based adsorbents perform well in comparison with other adsorbents, and this is attributable to the abundance of nitrogen functional groups within the biomaterial [133] [134] [135]. In comparison, with an absence of acetate, the adsorption capacity of the amidoxime functionalized cellulose prepared in this study is relatively low, 68 mg g^{-1}. This can be attributed to a relatively low degree of functionalization of the cellulose sample and further study is needed to increase the functionalization, which may result in substantial increases in the adsorption capacity. Similarly, applying acetate as a complexing agent for chitosan adsorbents may provide a step change increase in adsorption capacity.

Table 10 - Comparison between other vanadium adsorbents, both inorganic and organic

Adsorbent material	Vanadium loading (mg g^{-1})	Reference
Amidoxime functionalized cellulose (with acetate)	330	This study
Amidoxime functionalized cellulose (without acetate)	68	This study
Chitosan	425	[134]
Thio-functionalized nanochitosan	275	[133]
Chitosan film	251	[135]
Calcined Mg/Al hydrotalcite	225	[136]
Iron hydroxide	111	[137]
Magnetized natural zeolite-polypyrrole	65	[138]
$ZnCl_2$ activated carbon	24.9	[139]
Aluminum-Pillared Bentonite	24	[140]

6.5 Enhancement of vanadium selectivity through complexation with acetate

The selectivity of the adsorbent towards vanadium (V^{4+}) was compared with chromium (Cr^{3+}), nickel (Ni^{2+}), and copper (Cu^{2+}), through exposure to polymetallic solutions at pH 4. The initial solutions contained approximately 450 mg L^{-1} of each metal at different concentrations of acetate.

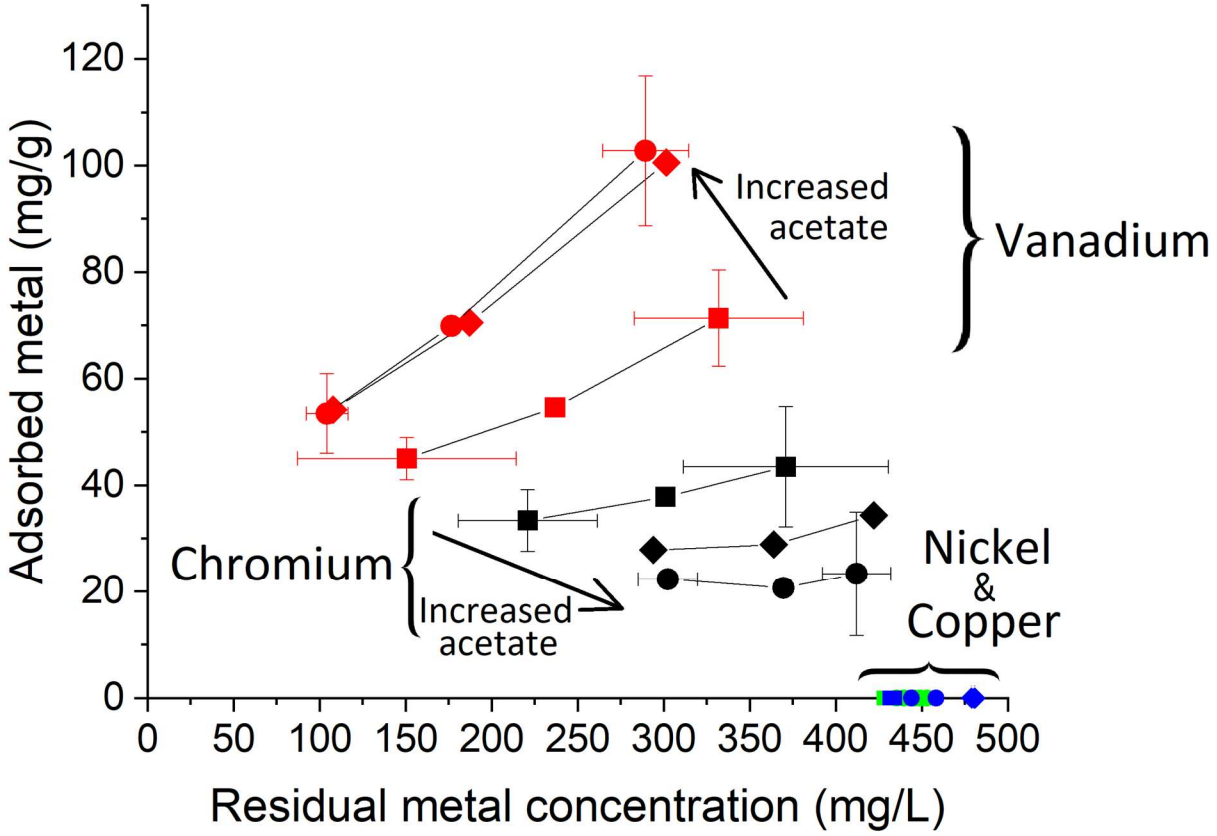

Figure 32 - Multi-metal adsorption test at varying acetate concentrations and a pH value of 4. Initial metal salt concentration = 450 mg L^{-1}, room temperature. □ – Acetate concentration = 0 M. ◊– Acetate concentration = 0.25 M. ○ - Acetate concentration = 0.5 M. Red – vanadium, black – chromium, green – copper, blue – nickel.

Without acetate, no detectable adsorption (< 1.6 mg g^{-1}) was observed for either Cu^{2+} or Ni^{2+}, while Cr^{3+} was less selectively adsorbed over V^{4+} under all conditions as shown in Figure 32. When in competition, the maximum observed adsorption capacity under the conditions studied for V^{4+} was around 102 ± 14 mg g^{-1} with 0.5 M acetate, whereas the maximum for Cr^{3+} is 43 ± 11 mg g^{-1} when no acetate was present.

Interestingly, the effect of acetate was different for chromium and vanadium. As seen from Figure 32, in contrast to V^{4+}, the capacity for Cr^{3+} decreased from 43 ± 11 mg g^{-1} when no acetate was present to 23 ± 11 mg g^{-1} in 0.5 M acetate. There was no effect of acetate on Ni^{2+} and Cu^{2+} adsorption when in competition with V^{4+} and Cr^{3+}, as there was no detectable adsorption with or without acetate present. By defining the selectivity between vanadium and chromium as shown in equation (23), the relative affinity of each metal to the adsorbent can be calculated.

$$S_{\frac{V^{4+}}{Cr^{3+}}} = \frac{\left(\frac{q_e}{C_e}\right)_{V^{4+}}}{\left(\frac{q_e}{C_e}\right)_{Cr^{3+}}} \qquad (23)$$

The largest improvement in the selectivity was seen at lower residual concentrations. Without any acetate present in the solution, the selectivity towards vanadium was 2.0 ± 0.5. When acetate was included in the system at 0.5 M, the selectivity increased to 7.0 ± 0.2. Similarly, when higher residual concentrations are examined, the selectivity without acetate is only 1.8 ± 0.4 which increased to 6.3 ± 0.5 when acetate was present.

The selectivity results further support the conclusion that formation of polynuclear complexes with acetate is responsible for the enhanced adsorption and selectivity towards V^{4+}. Although Cr^{3+} can form similar polynuclear complexes with acetate to vanadium [141], potential enhancement by acetate on Cr^{3+} adsorption is overshadowed by the competition with vanadium complexes. This suggests that the Cr^{3+} complexes do not have the same adsorption affinity to the adsorbent when compared with those of vanadium. However, a detailed coordination chemistry study is required to verify this explanation.

Ultimately, vanadium was found to be selectively adsorbed onto the surface of amidoxime functionalized cellulose. The largest separation was observed between vanadium and nickel or copper, wherein the selectivity was at least 150 as copper or nickel loading was below the detectable limit (1.6 mg g^{-1}) when

the residual concentration was 450 mg L^{-1}. Since the same was observed without acetic acid in the solution, vanadium and chromium preferentially interact with amidoxime when compared with nickel and copper, even when not in a complexed form. When acetic acid is present, vanadium was found to be more preferentially bound when compared to chromium, even though chromium is also capable of forming similar polynuclear complexes. The selectivity towards vanadium was found to be positively correlated to the acetic acid concentration with the highest degree of separation observed at an acetic acid concentration of 0.5 M.

6.6 Scale-up and adsorption column testing utilizing amidoxime functionalized cellulose beads

As a natural extension to the functionalization of cellulose powder, the functionalization of cellulose beads will allow for greater applications in adsorption columns where mechanical properties and considerations regarding liquid flow are of importance. As discussed in Chapter 3, cellulose beads have been utilized as an adsorbent material for a variety of applications including protein purification, RNA isolation, ion exchange, as well as heavy metal removal [105]. While all of these applications start with the same cellulose chemistry, the addition of different functional groups through several reaction methods allows the beads to be tailored to a specific usage. Therefore, it is hypothesized that the addition of amidoxime functional groups through the methods discussed in Chapter 5 will exhibit similar selectivity towards vanadium and thus, by functionalizing a porous bead, the material will be suitable for use in an adsorption column.

6.6.1 Cellulose bead synthesis

As discussed in Chapter 3, cellulose beads can be formed by dissolving cellulose in an appropriate solvent and then coagulating the material through dropwise addition to a coagulation medium. Since preliminary cellulose functionalization work was performed in a homogenous environment (section 5.1.1), the same solvent system, NaOH/urea, was utilized to dissolve cellulose under slightly chilled conditions, 5 – 10 °C.

A solution of 12 wt.% urea and 7 wt.% NaOH was prepared and 5 g of cellulose was dissolved for every 100 mL. This was then coagulated into a coagulation bath of variable concentrations of different mineral acids under minimal agitation. Table 11 shows the coagulants that result in bead formation. As expected, since the solubility of cellulose in the solution was dependent on the alkalinity, having a coagulant that is strongly acidic was found to be more likely to result in bead formation.

Table 11 - Bead formation with different coagulants

Coagulant	Bead formation
Water	No
0.5 M H_2SO_4	No
1 M H_2SO_4	Yes
2 M H_2SO_4	Yes
2 M HNO_3	Yes

To form a spherical bead, the quick formation of a skin layer is necessary to ensure that the cellulose remains within the droplet upon contact with the coagulant bath. With low proton concentrations such as with water or 0.5 M H_2SO_4, the formation of the skin layer was too slow, and the cellulose was able to disperse within the coagulant bath. Under these conditions, the cellulose formed films and did not exhibit any structural strength. Upon attempting to remove the cellulose films from the bath, the films would easily rip and were determined to be unsuitable for use as an adsorbent.

At sufficiently high acid concentrations, the formation of a skin layer provides structure to the bead and allows for the slow mixing of the acid and base within the bead. By limiting the diffusion through the skin,

a pore network is formed as the acid diffuses into the bead, neutralizing the base, and precipitating the dissolved cellulose. Unfortunately, due to technical limitations, the pore network of the beads could not be analyzed in detail as common methods such as nitrogen adsorption would require the beads to be dried, which would result in damage to the pore network and would not be representative of the hydrated pore structure.

6.6.2 Bead functionalization and batch adsorption testing

After formation, the beads were then washed and stored as described in section 4.1.5. In comparison with the functionalization of cellulose powder, the beads were found to dissolve in a solution of 100 g L^{-1} NaOH at both room temperature and 35°C, a favourable temperature for powder functionalization. As a result, the concentration of NaOH was decreased until no dissolution was evident while maintaining a solution temperature of 35°C. A concentration of 50 g L^{-1} NaOH was found to be suitable, and was used in the preparation of a 1 kg batch of cellulose beads. Since the cellulose had already undergone swelling/dissolution during the formation of the beads, the role of NaOH would be strictly catalytic in bead functionalization.

Amidoximation of the cellulose beads was performed with the same conditions as the cellulose powder. A reagent solution with a hydroxylamine concentration of 200 g L^{-1} was neutralized to pH 8 and was placed in a water bath that was heated to 75 °C. For every 1 kg of beads to be functionalized, 1 L of reagent solution was prepared. The beads were weighed and transferred to a sealed container and immersed within the heated water bath. Once both the beads and the reagent solution reached 75 °C, they were mixed together and reacted for 2 hours. Afterwards, the beads were separated from the reagent solution and dumped into a beaker of RO water to quenched them. The beads were rinsed multiple times and stored in RO water for use in adsorption experiments.

Subsequent adsorption experiments were performed on the beads using similar conditions to that of cellulose powder, 2000 mg L^{-1} vanadium solution and a pH value of 4.5. The beads were found to have an adsorption capacity of 37.2 ± 7.4 mg g^{-1} and while this appears to be substantially less than that for the functionalized powder, the mass of the beads is primarily water which dilutes the adsorption capacity per unit mass. To calculate the approximate mass of water within the cellulose beads, 10 g of beads were dried in a vacuum oven and after 24 hours at 60 °C, only 0.9 g of mass remained, suggesting that approximately 91% of the bead mass is comprised of water. When accounting for this, the adsorption capacity of the beads per gram of cellulose (413 ± 82 mg g^{-1}) was comparable to that of the cellulose powder (~375 mg g^{-1}) as expected.

6.6.3 Adsorption column performance

The adsorption performance of the functionalized cellulose beads was evaluated in an adsorption column, which is typically utilized for industrial applications. A laboratory scale column was constructed with the dimensions shown in Figure 15 with a total bed volume of 100 mL. For each adsorption trial, a 2,000 mg L^{-1} stock solution of vanadium at pH 4.5 was used because this was observed to give maximum adsorption capacity as previously described. Further, the solution contained a total acetic acid concentration of 0.5 M with a 0.25 M Na_2SO_4 background electrolyte.

The first time the column was tested, the column was slowly filled with beads and the mass of beads required to fill the column was 55.9 g. This mass of beads was then added in all subsequent experiments, irrespective of the height of the bed in the column. However, all three trials had a similar bed height, which suggests that the filling procedure was repeatable and that the bed porosity within the column was similar between trials.

Once the column was prepared, the feed solution was pumped through with a peristaltic pump at a flow rate of 2.57 mL min^{-1}. The average flow rate was checked by timing every 37 mL passing through the

column (corresponding to a sample), and slight corrections were made to the pumping speed as necessary. To minimize the variations in flow rate, the pump was allowed to run for at least 30 minutes before each experiment and once the pump had warmed up, the output flow rate was found to be relatively stable, with a standard deviation over all adsorption trials of 0.16 mL min^{-1}.

Since only 55.9 g of beads were able to fit in the column, it was assumed the remaining volume is attributable to pore space. The density of the cellulose beads was estimated by calculating the weighted average of the cellulose and entrained water density within the beads and resulted in an approximation of 1.045 g cm^{-3}. This corresponded to a bed porosity of approximately 0.46. Assuming that the beads are perfectly spherical, the equivalent diameter for fluid flow can be calculated through the following equation (Eq. (24)) [142].

$$D_{eq} = \frac{2}{3} D_p \frac{\epsilon}{1-\epsilon} \tag{24}$$

where D_p is the particle diameter, ϵ is the bed void fraction, and D_{eq} is the equivalent channel diameter to represent the void channels.

To determine the flow regime in the column, the Reynolds number can be calculated as follows (Eq. (25)):

$$\mathrm{Re} = \frac{\rho\, V_i\, D_{eq}}{\mu} = \frac{\rho \left(\frac{V_s}{\epsilon}\right)\left(\frac{2}{3} D_p \frac{\epsilon}{1-\epsilon}\right)}{\mu} = 0.196 \tag{25}$$

where V_i is the interstitial velocity, V_s is the superficial velocity, ρ is the fluid density, and μ is the fluid dynamic viscosity. Under these flow conditions, the flow regime is laminar since for a packed bed the Reynold's Number must exceed 10 in order to be considered transitionary [143].

It is also important to consider the possibility that the adsorption bed could fluidize as this may impact performance by allowing the beads to move, potentially forming channels or mixing the beads as they load with vanadium. To calculate the minimum velocity necessary for fluidization, a force balance can be performed on a bead. If the gravitational force on the bead exceeds the upwards force due to fluid drag, the column will be stable, otherwise the column will fluidize. The force balance is derived from the Ergun equation and is shown as equation (26) below [142].

$$\frac{150\,\mu\,V_C}{D_p^2}\,\frac{(1-\epsilon)}{\epsilon^3}+\frac{1.75\,\rho\,V_C^2}{D_p}\,\frac{1}{\epsilon^3}=\,g\,(\rho_p-\,\rho) \qquad (26)$$

where μ is the dynamic viscosity, D_p is the particle diameter, V_C is the critical velocity for fluidization, ρ is the fluid density, and ρ_p is the particle density.

Using a numeric solver to minimize the difference between the left- and right-hand sides, the critical velocity can be solved. In this situation, the critical velocity was found to be 2×10^{-3} m s^{-1}. This is much greater than the superficial velocity of the column, 8×10^{-5} m s^{-1}, and as a result, it is not expected that any fluidization will be present. Furthermore, as adsorption proceeds, the adsorption of vanadium onto the beads will result in a greater density that will decrease the likelihood of fluidization.

The resulting breakthrough curve for the column is shown in Figure 33 below. The curve does not show the ideal "S" curve which is typically expected for adsorption breakthrough. In contrast, the effluent concentration from the column begins to rise almost immediately following the filling of the column, with a small concentration of vanadium (3 ± 2 mg L^{-1}) present in the first effluent sample (37 mL). The effluent concentration then gradually increased approximately linearly for the entire duration of the experiment. This suggests that the mass transfer zone is longer than the length of the column, making it difficult to quantify the mass transfer and adsorption characteristics of the column from these experiments.

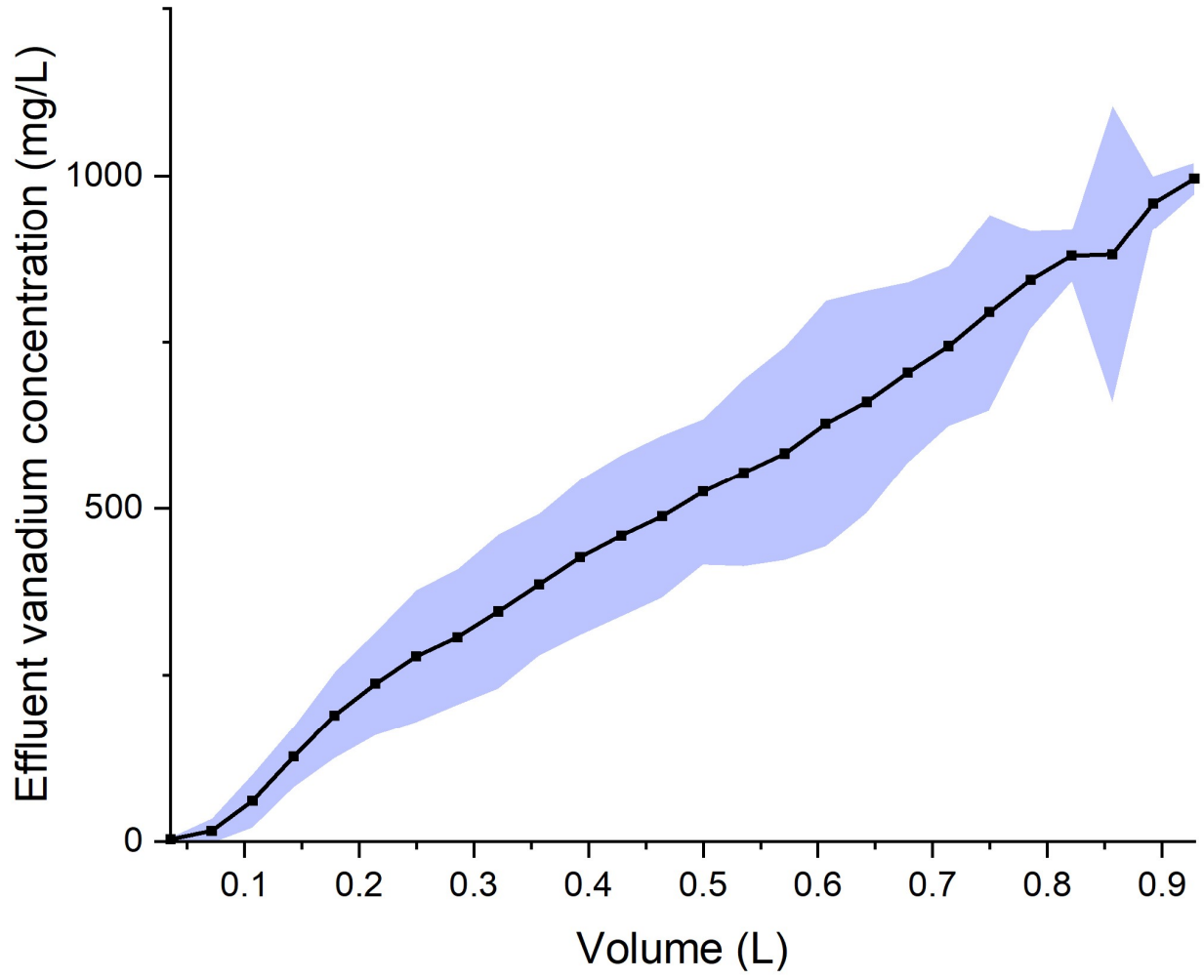

Figure 33 – Adsorption column breakthrough curve for amidoxime cellulose beads. Flow rate = 2.57 mL min^{-1} with 55.9 g of beads. Feed vanadium concentration = 2,000 mg L^{-1}. The shaded area shows a 95% confidence interval.

The long mass transfer zone may be attributable to suboptimal column design (e.g. channeling and bypass flow) or slow adsorption kinetics for the beads. From observing the colour change of the beads during adsorption, it was concluded that slow kinetics was likely to be the primary cause of the long mass transfer zone. In batch adsorption experiments, the surface of the beads was observed to rapidly turn black upon contact with the vanadium solution. A shell loaded on the outer surface of the beads was evident, and upon dissection of a loaded bead, this shell was noticeably harder than the initial beads. However, the physical properties of this layer were not further quantified. This layer may present significant resistance to mass transfer into the pore network of the bead and given that the majority of the surface area is

present within the pore space, this may limit the adsorption kinetics. At the conclusion of the adsorption column experiment, the effluent concentration only reached 1,000 mg L^{-1} (see Figure 40), half of the feed vanadium concentration. This suggests that the beads still have a significant portion of their adsorption capacity available, but the slow kinetics of adsorption and mass transport within the pore space is limiting the effectiveness of the column. As the vanadium loading increases, it is likely that swelling of the functionalized cellulose may reduce the pore space and further limit diffusion or potentially block pore channels. To increase the kinetic performance of the beads, modifications to the pore structure may be needed, however this is beyond the scope of this study.

In comparison with batch testing, the beads in the column were found to have loading with a similar order of magnitude, but the adsorption capacity observed in batch testing was higher due to the kinetic limitations. As shown in Figure 34, the adsorbent loading in the column increases linearly initially, but begins to plateau as vanadium begins to slip through in the effluent. At the end of the test, the column was loaded with approximately 23 mg g^{-1} which is approximately 60% of the capacity measured during batch testing. Due to the poor kinetics, to saturate the beads in the column would require a much higher volume passing through than used in these experiments.

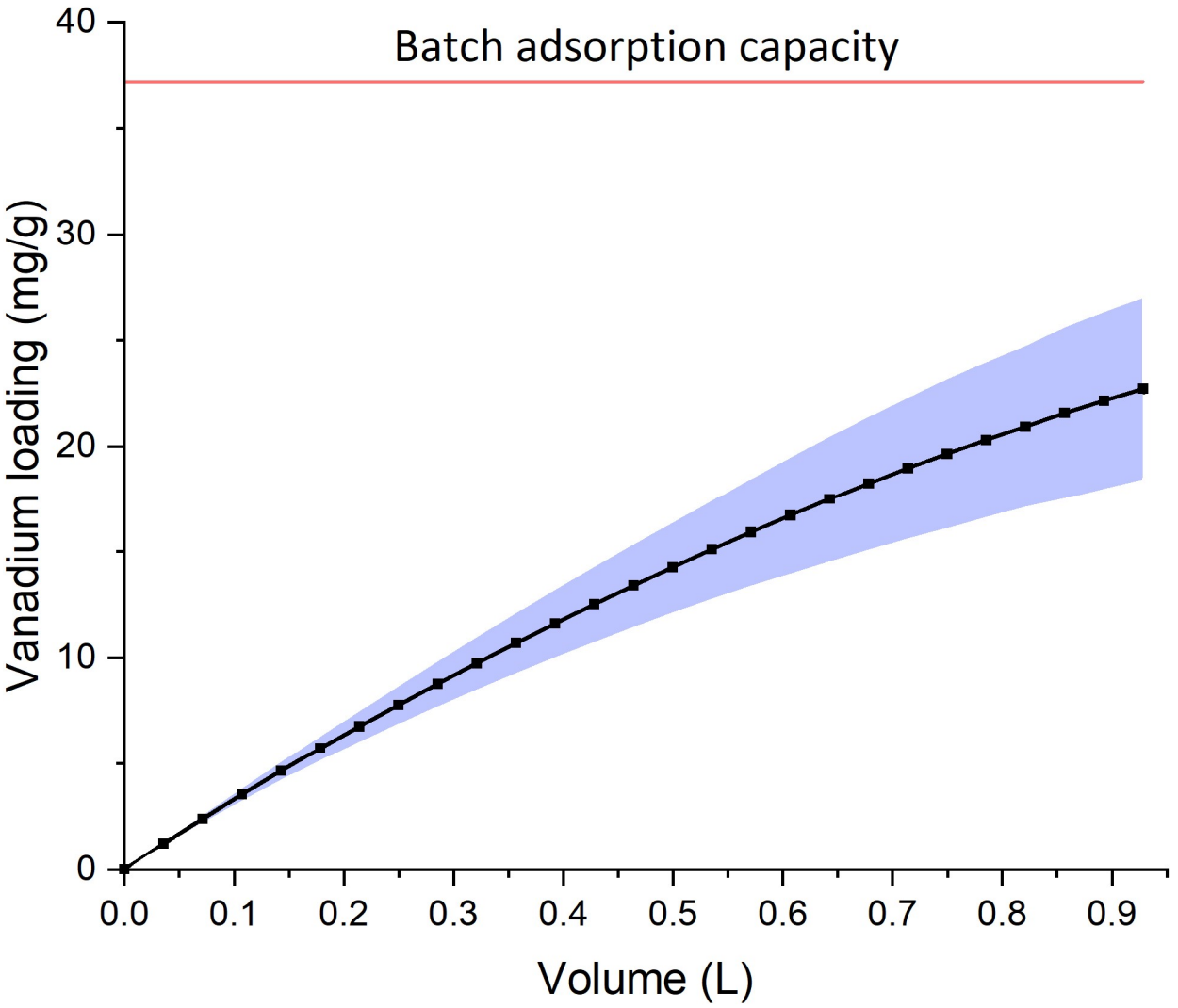

Figure 34 - Vanadium loading within the adsorption column. Calculated from the experimental data shown in Figure 33.

Following adsorption, the residual stock solution was drained, and 0.5 M sulfuric acid was pumped through the column to desorb the vanadium. The resulting effluent concentrations from desorption is shown in Figure 35. Initially, the vanadium effluent concentration was stable and centered around 3,500 mg L^{-1} for the first 175 mL, before an exponential decay was observed, reaching 120 mg L^{-1} after 750 mL had passed through the column. Interestingly, the stable initial concentration suggests that this is an inherent limit for the elution solution and this concentration was previously observed in preliminary desorption trials for the beads. By utilizing a different elution solution composition, by varying the concentration or the type of acid, it may be possible to increase the effluent concentration. By increasing

the concentration, less eluent would be required. This would be favourable for commercialization of the adsorption process, since the regeneration time would be reduced and recovery of vanadium from a higher concentration stream would be easier, as discussed in Chapter 2.

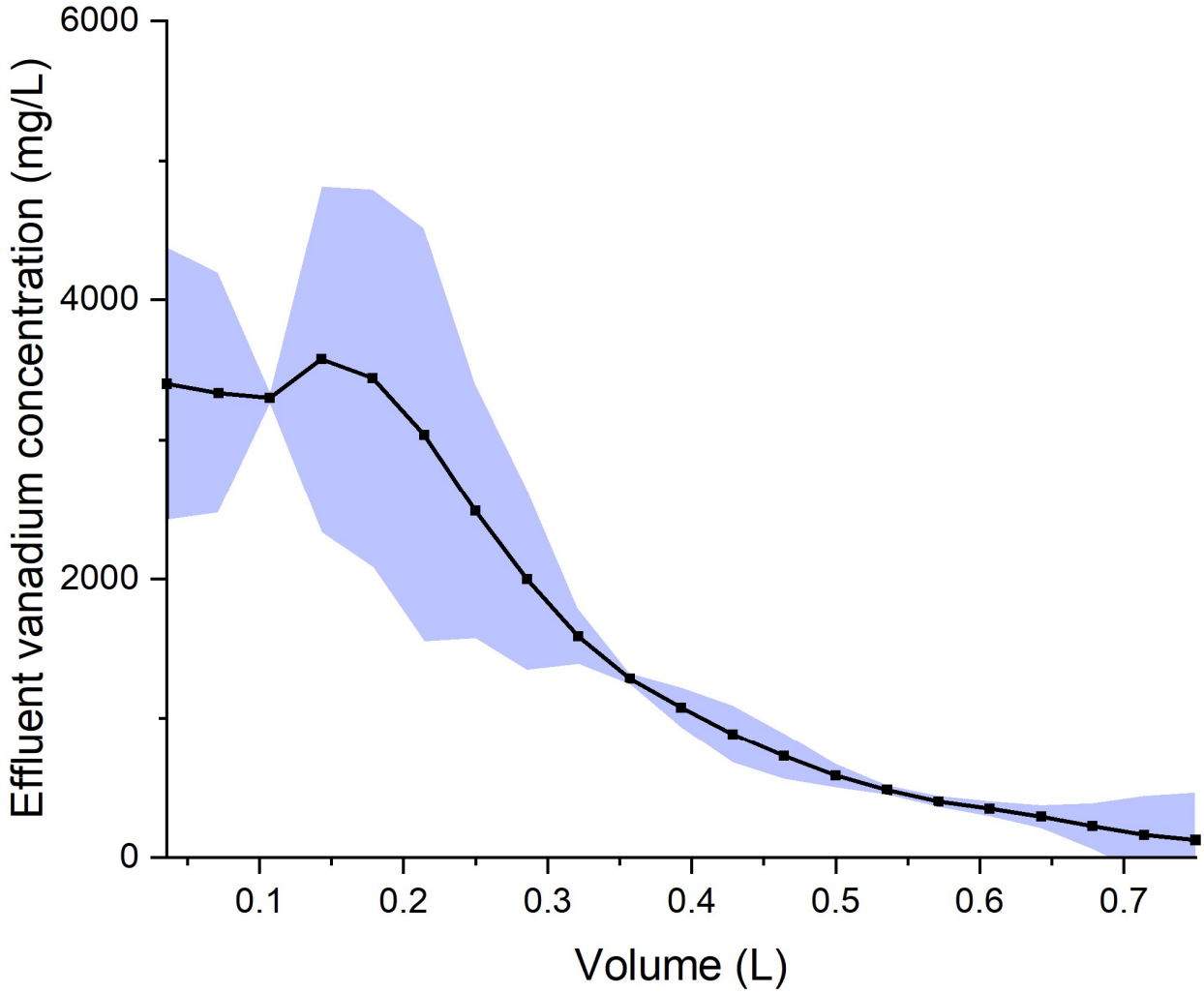

Figure 35 – Adsorption column effluent vanadium concentration from desorption with 0.5 M H_2SO_4. Desorption testing was conducted following adsorption shown in Figure 33 with a flow rate of 2.57 mL min^{-1}.

A substantial amount of variability in the effluent concentration was observed at the beginning of desorption, but the variability decreased after around 300 mL of regenerant solution had flowed through the column. This may be attributable to channeling within the column during desorption which was visually observed. Curiously, channeling was not visually evident (by bead colour changes) during adsorption but was prominent in desorption as shown in Figure 36. A desorption channel was evident in

each of the replicate experiments, but upon examination of the column following the experiments it was not clear what was causing flow to preferentially flow on one side of the column. However, since adsorption and desorption experiments were conducted on sequential days, the loaded beads had to sit in the column for approximately 12 hours without any fluid support. Therefore, the weight of the beads may have compressed the beads at the bottom of the column or rearranged them such that channels formed in the beginning of desorption. It is feasible that upon 0.5 M H_2SO_4 flowing through the column that these channels would rearrange by the end of the experiment, removing evidence of them. However, further study is needed to understand the cause.

Figure 36 - Channeling within the column during desorption as seen in middle panel. Light region in the center of the column shows the pathing of sulfuric acid leading to vanadium desorption. Left panel shows bead without any vanadium adsorbed. Right panel shows vanadium loaded beads.

Although further optimizations of bead properties are possible, the amidoxime functionalized cellulose beads synthesized in this work show promise for applications in vanadium extraction, purification, and concentration. In converting the functionalized medium from a powder to a bead, the adsorbent can be

utilized in an adsorption column due to the mechanical properties of the bead. While the kinetics of adsorption need to be improved, the capacity of the beads was high at 37.2 ± 7.4 mg g^{-1}, which when corrected for the water content had a capacity of 413 ± 82 mg g^{-1} cellulose. Further optimization of the bead synthesis and functionalization procedure is possible, as there are many factors such as cellulose loading, coagulant concentration, reagent concentrations, and others, which could affect the adsorption performance.

Chapter Seven: Conclusions and Future Work

In this work, amidoxime functionalized cellulose was investigated for its potential use as an adsorbent material for the selective recovery of vanadium. The use of cellulose presents a greener alternative to traditional hydrometallurgical methods such as solvent extraction that utilizes organic solvents and toxic extractants. Although many green alternatives are being developed in a variety of fields, ultimately, the adoption within industry is dependent on the usability and economics of their deployment. Even if a novel solution presents attractive performance, adoption can still be inhibited if the methods to fabricate the material are complex or time consuming. The cyanoethylation method outlined in this work addresses these concerns by eliminating the need for pre-treating cellulose with a swelling agent and by removing dialysis as a purification step which generated substantial amounts of waste. Additionally, the use of acetic acid as a complexing agent allowed for greatly enhanced vanadium adsorption performance, increasing the vanadium adsorption capacity from 68 mg g^{-1} to 330 mg g^{-1}, while at the same time being both renewable and biodegradable. The selectivity towards vanadium over chromium also increased as a result of acetic acid, increasing from 2.0 ± 0.5 to 7.0 ± 0.2 with an acetic acid concentration of 0.5 M. When in competition with vanadium, both copper and nickel exhibited no detectable adsorption (< 1.6 mg g^{-1}) on the adsorbent which demonstrates its potential for separating these metals. Together, the simpler functionalization pathway combined with enhanced adsorption performance results in an attractive material, and the results from this work may be extended to other metal species where the formation of complexes could improve their separation.

7.1 Functionalization insights

Conducting cyanoethylation heterogeneously has many advantages, in particular the ease of separation, and also achieving favourable physical properties without the need for freeze drying. By slurrying the cellulose heterogeneously in an aqueous system, separation can be easily achieved through filtration as opposed to a homogenous reaction where dialysis is necessary to recover the functionalized cellulose. Dialysis not only adds significant time to the process but results in the generation of a large amount of wastewater which needs to be treated. For the homogenous process outlined in literature, a dialysis volume ratio of 165 was used, meaning 165 mL of waste is generated for every 1 mL of reaction solution. Considering that only 5 wt.% of cellulose was solubilized in the reaction solution, vast quantities of waste would be necessary to produce a meaningful amount of functionalized cellulose. A heterogenous reaction eliminates this wastewater, while at the same time cellulose can be swelled using an aqueous system by dissolved sodium hydroxide which also catalyzes the cyanoethylation reaction. Furthermore, the homogenous reaction produced crystals, with minimal surface area and poor adsorption performance. When conducted heterogeneously, varying the reaction temperature and sodium hydroxide concentration allowed for greater control of the physical properties of the product. A reaction temperature of 35 °C with a sodium hydroxide concentration of 100 g L^{-1} was found to be favourable for the cellulose powder which resulted in a nitrogen content of 5.3%.

Although a higher nitrogen content was achievable, over functionalization was found to detrimentally impact the physical properties of the material following amidoximation due to the tendency to form a crystalline material similar to that observed with the homogenous reaction. From visual observations of the cyanoethylation reaction, a temporary change in the slurry viscosity from low to high, showing dissolution, correlated with higher nitrogen content. This was also found to correlate with increased crystallinity following amidoximation. Therefore, reaction conditions were examined that reduced the

likelihood of dissolution while as the same time maintaining the advantages outlined above. This was achieved through slightly increasing the temperature of the solution as cellulose is less soluble at higher temperatures with crystalline material apparent at 25 °C and 30 °C but not at 35 °C. Due to the observed sensitivity to the reaction temperature, accurate temperature regulation was found to be important and abnormalities in preliminary experiments were attributed to a lack of temperature control.

Although more work needs to be done to optimize the reaction conditions for cyanoethylation, the modified functionalization methodology presented in this work provides a promising alternative that is a simpler process which should be easier to scale-up while at the same time achieving comparable degrees of functionalization.

7.2 Adsorption performance and complexing

Through the inclusion of acetic acid in the adsorption solution, vanadium adsorption was improved, in terms of both selectivity and capacity. Vanadium capacity was found to positively correlate with the nitrogen content of the material (before the onset of crystallinity as discussed above), suggesting that adsorption occurs at the amidoxime functional groups, as opposed to carboxylate groups that may have been formed through the hydrolysis of cyano or amidoxime groups. The adsorption capacity was found to increase by a factor of more than 4 when 0.5 M acetic acid was added to the system, increasing from 68 mg g^{-1} to 330 mg g^{-1} at pH 4.5. This strongly supports the hypothesis that vanadium is forming polynuclear complexes when exposed to acetic acid and that these complexes are subsequently interacting with the adsorbent surface. This is further supported by the variation in adsorption capacity as a function of pH, which showed a maximum at 4.5, close to the pKa of acetic acid. The enhancement of adsorption starting above pH 3 can be explained by the high concentration of acetic acid present in the solution, with equal moles of acetate and vanadium available at pH 3.7 facilitating complex formation below the pKa of acetic acid. This suggests that acetic acid may still enhance the adsorption performance

at concentrations lower than 0.5 M which would improve the economic feasibility of the process since acetate is believed to be in stoichiometric excess.

Amidoxime was confirmed to be selective towards vanadium and this selectivity was further enhanced in the presence of acetic acid. With and without acetic acid, the adsorbent was found to be selective to vanadium and chromium over the divalent cations nickel and copper. With 0.5 M acetic acid, the selectivity between vanadium and chromium was enhanced with the selectivity increasing from 2.0 ± 0.5 to 7.0 ± 0.2 when the residual vanadium concentration was 100 mg L^{-1}. The selectivity also showed enhancement when residual concentrations were higher (325 mg L^{-1}), increasing from 1.8 ± 0.4 to 6.3 ± 0.5. With and without acetate, the adsorbent showed a high degree of selectivity to both copper and nickel which was calculated to be at least 150 from the detectability limit for adsorption experiments. By enhancing selectivity, the usability of the material for recovering vanadium is improved, not only for hydrometallurgical processes, but also potentially as a method for the treatment of wastewater.

The same adsorption characteristics were observed when cellulose beads were functionalized and used in an adsorption column, which supports their further applicability in scaled-up applications. However, further scale-up needs more optimization, particularly with respect to mass transfer limitations and overall kinetics.

7.3 Future work

Extensions of the results described in this work may be applicable to a variety of fields and applications. By functionalizing cellulose in an aqueous media the complexity of the process has been reduced. However, the feed cellulose used in this study had been purified and does not contain the contaminants that would normally be present in natural biomass. Therefore, further study will need to be done on natural raw cellulose to ensure the robustness of the process. Similarly, adsorption testing was done with synthetic metal solutions and the use of field samples may present complications. Ultimately, if

subsequent testing on field samples supports the conclusions outlined in this work, there may be a wide variety of applications for this material ranging from wastewater treatment to hydrometallurgical processing, potentially for a range of metal ions.

As discussed in Chapter Five, the optimization of the methodology for functionalizing the cellulose powder was limited and further work should be done to identify the conditions that lead to the highest degree of functionalization while maintaining the physical properties of the material. As was observed at a sodium hydroxide concentration of 100 g L^{-1}, the system is very sensitive to temperature and careful optimization is required for maximizing the adsorption capacity. Finding the combination of conditions that allows for the swelling of the cellulose surface but not a complete change of the structure would be beneficial for reducing the crystallinity of the product while improving the accessibility of functional groups for cyanoethylation. Varying the sodium hydroxide concentration as well as the temperature were identified as ways to control this, but further study of the kinetics of the phase transitions are needed. The kinetics of cyanoethylation were only tested under low sodium hydroxide concentrations (25 g L^{-1}), therefore, the kinetic behaviour of the system under high concentrations still needs to be studied. By understanding the kinetics under more severe conditions may allow for the reaction to be halted before a detrimental change occurs while maintaining the benefits of using a higher concentration of sodium hydroxide at room temperature.

When functionalizing cellulose beads, the conditions developed for the cellulose powder were found to be too severe for the beads and a sodium hydroxide concentration of 100 g L^{-1} was found to destroy the pore structure and subsequently, a lower concentration of 50 g L^{-1} was used. However, little optimization was done for the beads and further work needs to be done to understand the importance of the sodium hydroxide concentration for the bead synthesis process. The nitrogen content of the beads could not be assessed through CHN analysis due to their physical properties, namely their high water content and that they dried to hard spheres, so further adsorption experiments are necessary to quantify their

performance. While the sodium hydroxide concentration was found to be important for the cellulose powder, through the process of synthesizing beads, the material would have already undergone the transition to cellulose II during dissolution and subsequent coagulation. Therefore, the influence of sodium hydroxide would likely be limited to the catalytic effects which may be maximized at much lower concentrations.

Further study of the mechanisms behind the adsorption enhancement are also necessary to potentially expand applications beyond vanadium to other metals. The interaction between different surface functionalities and/or different metal ions in the presence of acetic acid is unknown. If different functional group and metal ion pairings are found to complex favourably with acetic acid, the applications will naturally expand and may present an opportunity to tailor the selectivity of a process depending on the desired parameters. This can be advantageous in the processing of rare-earth elements where achieving selectivity between many chemically similar elements is challenging. Developing an additive that enhances the separation steps would allow for fewer stages, leading to improved economic feasibility and a smaller plant footprint. Understanding the mechanism will also be vital for predicting how the system will behave when exposed to field leachate samples, particularly with regards to dissolved organics which may influence the formation of complexes.

Altogether, the results discussed in this work present a promising solution for enhancing the adsorption of vanadium for applications in wastewater treatment and hydrometallurgical processing. However, further studies are needed to ensure the robustness of the process under real conditions, in the presence of contaminants that might affect the adsorption process. If the robustness can be demonstrated, these processes may be extended to other metal groups, particularly the rare-earth family where current processing pathways cause heavy environmental pollution due to the difficulty of selectivity separating the elements from one another. More generally, the functionalization method developed provides the groundwork for a simplified pathway that is more conducive to scale-up, facilitating the application of

functionalized cellulose to wastewater treatment processes. This is further emphasized when combined with the application of cellulose beads which provide an effective medium for adsorption and can be utilized in an adsorption column. Ultimately, the results outlined in this work offer a starting point from which further work can be undertaken, both in terms of cellulose functionalization and the utilization of complexing agents to enhance adsorption.

References

[1] J. D. Birkett, "A brief illustrated history of desalination: From the bible to 1940," *Desalination,* vol. 50, pp. 17-52, 1984.

[2] Government of Ontario, "Rules for treating industrial wastewater," 9 May 2019. [Online]. Available: https://www.ontario.ca/page/rules-treating-industrial-wastewater. [Accessed 21 March 2020].

[3] M. A. Barakat, "New trends in removing heavy metals from industrial wastewater," *Arabian Journal of Chemistry,* vol. 4, no. 4, pp. 361-377, 2011.

[4] J. G. Dean, F. L. Bosqui and K. H. Lanouette, "Removing heavy metals from waste water," *Environmental Science and Technology,* vol. 6, no. 6, pp. 518-522, 1972.

[5] F. Fu and Q. Wang, "Removal of heavy metal ions from wastewaters: A review," *Journal of Environmental Management,* vol. 92, no. 3, pp. 407-418, 2011.

[6] J. Guilbaud, A. Massé, Y. Andrs, F. Combe and P. Jaouen, "Laundry water recycling in ship by direct nanofiltration with tubular membranes," *Resources, Conservation and Recycling,* vol. 55, no. 2, pp. 148-154, 2010.

[7] E. T. Igunnu and G. Z. Chen, "Produced water treatment technologies," *International Journal of Low-Carbon Technologies,* vol. 9, no. 3, pp. 157-177, 2014.

[8] C. Peng, Y. Liu, J. Bi, H. Xu and A. S. Ahmed, "Recovery of copper and water from copper-electroplating wastewater by the combination process of electrolysis and electrodialysis," *Journal of Hazardous Materials,* vol. 189, no. 3, pp. 814-820, 2011.

[9] S. Edition and A. C. Reardon, "Metallurgy for the Non-Metallurgist, Second Edition Discovering Metals— A Historical Overview," 2011.

[10] Worldsteel Association, "World Steel in Figures 2019," World Steel Association, Brussels, 2019.

[11] Government of Canada, "Aluminum facts," 27 November 2019. [Online]. Available: https://www.nrcan.gc.ca/our-natural-resources/minerals-mining/minerals-metals-facts/aluminum-facts/20510#L2. [Accessed 25 January 2020].

[12] R. Sefako, K. Sekgarametso and V. Sibanda, "Potential Processing Routes for Recovery of Platinum Group Metals from Southern African Oxidized PGM Ores: A Review," *Journal of Sustainable Metallurgy,* vol. 3, no. 4, pp. 797-807, 2017.

[13] S. Kawatra and T. Eisele, "1 Froth Flotation - Fundamental Principles," *Recovery of Pyrite in Coal Flotation: Entrainment or Flotation,* pp. 1-30, 1992.

[14] N. Rötzer and M. Schmidt, "Decreasing metal ore grades-Is the fear of resource depletion justified?," *Resources,* vol. 7, no. 4, 2018.

[15] P. Hadi, M. Xu, C. S. Lin, C. W. Hui and G. McKay, "Waste printed circuit board recycling techniques and product utilization," *Journal of Hazardous Materials,* vol. 283, pp. 234-243, 2015.

[16] L. Zeng and C. Y. Cheng, "A literature review of the recovery of molybdenum and vanadium from spent hydrodesulphurisation catalysts. Part I: Metallurgical processes," *Hydrometallurgy,* vol. 98, no. 1-2, pp. 1-9, 2009.

[17] D. McBride, J. Gebhardt, N. Croft and M. Cross, "Heap leaching: Modelling and forecasting using CFD technology," *Minerals,* vol. 8, no. 1, 2018.

[18] J. D. Sullivan, "Leaching copper from its ores," *Journal of Chemical Education,* vol. 8, no. 5, pp. 829-847, 1931.

[19] M. L. Free, Hydrometallurgy: Fundamentals and Applications, John Wiley & Sons, 2013.

[20] Solvay, "CYANEX 923," 2020. [Online]. Available: https://www.solvay.com/en/product/cyanex-923. [Accessed 27 January 2020].

[21] H. Dong, H. Du, S. R. Wickramasinghe and X. Qian, "The Effects of chemical substitution and polymerization on the pK a values of sulfonic acids," *Journal of Physical Chemistry B,* vol. 113, no. 43, pp. 14094-14101, 2009.

[22] M. EIGEN and R. G. WILKINS, "The Kinetics and Mechanism of Formation of Metal Complexes," in *Mechanisms of <bold>Inorganic Reactions</bold>*, vol. 49, AMERICAN CHEMICAL SOCIETY, 1965, pp. 55-80.

[23] A. M. Wilson, P. J. Bailey, P. A. Tasker, J. R. Turkington, R. A. Grant and J. B. Love, "Solvent extraction: The coordination chemistry behind extractive metallurgy," *Chemical Society Reviews,* vol. 43, no. 1, pp. 123-134, 2014.

[24] T. S. Anirudhan, S. Jalajamony and S. S. Sreekumari, "Adsorption of heavy metal ions from aqueous solutions by amine and carboxylate functionalised bentonites," *Applied Clay Science,* Vols. 65-66, pp. 67-71, 2012.

[25] M. A. Atieh, O. Y. Bakather, B. Al-Tawbini, A. A. Bukhari, F. A. Abuilaiwi and M. B. Fettouhi, "Effect of carboxylic functional group functionalized on carbon nanotubes surface on the removal of lead from water," *Bioinorganic Chemistry and Applications,* vol. 2010, 2010.

[26] B. Gao, Y. Gao and Y. Li, "Preparation and chelation adsorption property of composite chelating material poly(amidoxime)/SiO2 towards heavy metal ions," *Chemical Engineering Journal,* vol. 158, no. 3, pp. 542-549, 2010.

[27] S. M. Kraemer, S. F. Cheah, R. Zapf, J. Xu, K. N. Raymond and G. Sposito, "Effect of hydroxamate siderophores on Fe release and Pb(II) adsorption by goethite," *Geochimica et Cosmochimica Acta,* vol. 63, no. 19-20, pp. 3003-3008, 1999.

[28] D. Satapathy and G. S. Natarajan, "Surface modification of granular activated carbon by nitric acid for the enhancement of copper adsorption," *Indian Journal of Chemistry - Section A Inorganic, Physical, Theoretical and Analytical Chemistry,* vol. 45, no. 9, pp. 2011-2016, 2006.

[29] P. Ghosh, B. Chattopadhyay and A. K. Sen, "Modification of low density polyethylene (LDPE) by graft copolymerization with some acrylic monomers," *Polymer,* vol. 39, no. 1, pp. 193-201, 1998.

[30] J. Okamoto, T. Sugo, A. Katakai and H. Omichi, "Amidoxime-group-containg adsorbents for metal ions synthesized by radiation-induced grafting," *Journal of Applied Polymer Science,* vol. 30, no. 7, pp. 2967-2977, 1985.

[31] J. L. White and A. Sasaki, "Free radical graft polymerization," *Polymer - Plastics Technology and Engineering,* vol. 42, no. 5, pp. 711-735, 2003.

[32] W. Wang, L. Wang, C. L. Wang, T. X. Sun, H. J. Yu and T. Chen, "Study on the surface grafting of polypropylene fibers," *Journal of Applied Polymer Science,* vol. 99, no. 3, pp. 734-737, 2006.

[33] C. Cai, Q. Shi, L. Li, L. Zhu and J. Yin, "Grafting acrylic acid onto polypropylene by reactive extrusion with pre-irradiated PP as initiator," *Radiation Physics and Chemistry,* vol. 77, no. 3, pp. 370-372, 2008.

[34] H. Kubota and Y. Shigehisa, "Introduction of amidoxime groups into cellulose and its ability to adsorb metal ions," *Journal of Applied Polymer Science,* 1995.

[35] W. Li, R. Liu, H. Kang, Y. Sun, F. Dong and Y. Huang, "Synthesis of amidoxime functionalized cellulose derivatives as a reducing agent and stabilizer for preparing gold nanoparticles," *Polymer Chemistry,* 2013.

[36] R. Saliba, H. Gauthier, R. Gauthier and M. Petit-Ramel, "Adsorption of copper (II) and chromium (III) ions onto amidoximated cellulose," *Journal of Applied Polymer Science,* 2000.

[37] S. Camero, E. S. Puchi and G. Gonzalez, "Effect of 0.1% vanadium addition on precipitation behavior and mechanical properties of Al-6063 commercial alloy," *Journal of Materials Science,* vol. 41, no. 22, pp. 7361-7373, 2006.

[38] B. I. Whittington and J. R. Anderson, "Nature and activity of some vanadium catalysts," *Journal of Physical Chemistry,* vol. 97, no. 5, pp. 1032-1041, 1993.

[39] Roskill, "Vanadium - Outlook to 2029, 18th Edition," Roskill, Wimbledon, 2020.

[40] Aerospace & Defense, "Vanadium: A green metal critical to aerospace and clean energy," August 2020. [Online]. Available:

https://www.aerodefensetech.com/component/content/article/adt/features/articles/37376. [Accessed 25 September 2020].

[41] C. X. Li, C. Wei, Z. G. Deng, M. T. Li, X. B. Li and G. Fan, "Recovery of vanadium from black shale," *Transactions of Nonferrous Metals Society of China (English Edition),* vol. 20, no. SUPPL.1, pp. s127-s131, 2010.

[42] P. Hu, Y. Zhang, J. Huang, T. Liu, Y. Yuan and N. Xue, "Eco-Friendly Leaching and Separation of Vanadium over Iron Impurity from Vanadium-Bearing Shale Using Oxalic Acid as a Leachant," *ACS Sustainable Chemistry and Engineering,* vol. 6, no. 2, pp. 1900-1908, 2018.

[43] D. G. Nejad, A. R. Khanchi and M. Taghizadeh, "Recovery of Vanadium from Magnetite Ore Using Direct Acid Leaching: Optimization of Parameters by Plackett–Burman and Response Surface Methodologies," *Jom,* vol. 70, no. 6, pp. 1024-1030, 2018.

[44] X. Zhang, D. Fang, S. Song, G. Cheng and X. Xue, "Selective leaching of vanadium over iron from vanadium slag," *Journal of Hazardous Materials,* vol. 368, no. October 2018, pp. 300-307, 2019.

[45] X. Y. Chen, X. Z. Lan, Q. L. Zhang, H. Z. Ma and J. Zhou, "Leaching vanadium by high concentration sulfuric acid from stone coal," *Transactions of Nonferrous Metals Society of China (English Edition),* vol. 20, no. SUPPL.1, pp. s123-s126, 2010.

[46] C. G. Anderson, R. C. Dunne and J. L. Uhrie, MIneral Processing and Extractive Metallurgy - 100 Years of Innovation, Englewood: Society for Mining, Metallurgy and Exploration, 2014.

[47] R. R. Langeslay, D. M. Kaphan, C. L. Marshall, P. C. Stair, A. P. Sattelberger and M. Delferro, "Catalytic Applications of Vanadium: A Mechanistic Perspective," *Chemical Reviews,* vol. 119, no. 4, pp. 2128-2191, 2019.

[48] M. Rychcik and M. Skyllas-Kazacos, "Characteristics of a new all-vanadium redox flow battery," *Journal of Power Sources,* vol. 22, no. 1, pp. 59-67, 1988.

[49] S. Ubaldini, I. Zinicovscaia, I. Povar, O. Spinu and B. Pintilie, "Revised Poubaix diagrams for the vanadium – water system," *Journal of Electrochemical Science and Engineering,* 2019.

[50] L. R. Frederick Tim J.; Mitchell, Melvin G.; Partin, "PROCESS FOR PREPARATION OF CELLULOSE ACETATE FILTERS FOR USE N PAPER MAKıng," *United States Patent,* Vols. 5,662,773, no. 1993, 1997.

[51] M. I. H. Mondal, M. S. Yeasmin and M. S. Rahman, "Preparation of food grade carboxymethyl cellulose from corn husk agrowaste," *International Journal of Biological Macromolecules,* vol. 79, pp. 144-150, 2015.

[52] A. C. O'sullvian, "Cellulose: the structure slowly unravels," *Cellulose,* vol. 4, no. 3, pp. 173-207, 1997.

[53] J. Credou and T. Berthelot, "Cellulose: From biocompatible to bioactive material," *Journal of Materials Chemistry B,* vol. 2, no. 30, pp. 4767-4788, 2014.

[54] R. Saliba, H. Gauthier and R. Gauthier, "Adsorption of Heavy Metal Ions on Virgin and Chemically-Modified Lignocellulosic Materials," *Adsorption Science & Technology,* 2005.

[55] K. S. Low, C. K. Lee and S. M. Mak, "Sorption of copper and lead by citric acid modified wood," *Wood Science and Technology,* vol. 38, no. 8, pp. 629-640, 2004.

[56] J. C. Melo, E. C. Silva Filho, S. A. Santana and C. Airoldi, "Synthesized cellulose/succinic anhydride as an ion exchanger. Calorimetry of divalent cations in aqueous suspension," *Thermochimica Acta,* vol. 524, no. 1-2, pp. 29-34, 2011.

[57] M. Bilal, J. A. Shah, T. Ashfaq, S. M. H. Gardazi, A. A. Tahir, A. Pervez, H. Haroon and Q. Mahmood, "Waste biomass adsorbents for copper removal from industrial wastewater - A review," *Journal of Hazardous Materials,* vol. 263, no. 2, pp. 322-333, 2013.

[58] M. Geay, V. Marchetti, A. Clément, B. Loubinoux and P. Gérardin, "Decontamination of synthetic solutions containing heavy metals using chemically modified sawdusts bearing polyacrylic acid chains," *Journal of Wood Science,* vol. 46, no. 4, pp. 331-333, 2000.

[59] M. Liu, H. Zhang, X. Zhang, Y. Deng, W. Liu and H. Zhan, "Removal and Recovery of Chromium(III) from Aqueous Solutions by a Spheroidal Cellulose Adsorbent," *Water Environment Research,* vol. 73, no. 3, pp. 322-328, 2001.

[60] M. Liu, Y. Deng, H. Zhan and X. Zhang, "Adsorption and desorption of copper(II) from solutions on new spherical cellulose adsorbent," *Journal of Applied Polymer Science,* vol. 84, no. 3, pp. 478-485, 2002.

[61] L. V. A. Gurgel, O. K. Júnior, R. P. d. F. Gil and L. F. Gil, "Adsorption of Cu(II), Cd(II), and Pb(II) from aqueous single metal solutions by cellulose and mercerized cellulose chemically modified with succinic anhydride," *Bioresource Technology,* vol. 99, no. 8, pp. 3077-3083, 2008.

[62] W. Zhang, C. Li, M. Liang, Y. Geng and C. Lu, "Preparation of carboxylate-functionalized cellulose via solvent-free mechanochemistry and its characterization as a biosorbent for removal of Pb 2+ from aqueous solution," *Journal of Hazardous Materials,* vol. 181, no. 1-3, pp. 468-473, 2010.

[63] X. Yu, S. Tong, M. Ge, L. Wu, J. Zuo, C. Cao and W. Song, "Adsorption of heavy metal ions from aqueous solution by carboxylated cellulose nanocrystals," *Journal of Environmental Sciences (China),* vol. 25, no. 5, pp. 933-943, 2013.

[64] M. Lu, Y. M. Zhang, X. H. Guan, X. H. Xu and T. T. Gao, "Thermodynamics and kinetics of adsorption for heavy metal ions from aqueous solutions onto surface amino-bacterial cellulose," *Transactions of Nonferrous Metals Society of China (English Edition),* vol. 24, no. 6, pp. 1912-1917, 2014.

[65] X. Yu, S. Tong, M. Ge, L. Wu, J. Zuo, C. Cao and W. Song, "Synthesis and characterization of multi-amino-functionalized cellulose for arsenic adsorption," *Carbohydrate Polymers,* vol. 92, no. 1, pp. 380-387, 2013.

[66] R. R. Navarro, K. Sumi, N. Fujii and M. Matsumura, "Mercury Removal From Wastewater Using Porous Cellulose carrier Modified with Polyethyleneimine," *Science,* vol. 30, no. 10, pp. 2488-2494, 1996.

[67] X. Sun, L. Yang, Q. Li, J. Zhao, X. Li, X. Wang and H. Liu, "Amino-functionalized magnetic cellulose nanocomposite as adsorbent for removal of Cr(VI): Synthesis and adsorption studies," *Chemical Engineering Journal,* vol. 241, pp. 175-183, 2014.

[68] Y. Tian, M. Wu, R. Liu, D. Wang, X. Lin, W. Liu, L. Ma, Y. Li and Y. Huang, "Modified native cellulose fibers-A novel efficient adsorbent for both fluoride and arsenic," *Journal of Hazardous Materials,* vol. 185, no. 1, pp. 93-100, 2011.

[69] S. Hokkanen, E. Repo, T. Suopajärvi, H. Liimatainen, J. Niinimaa and M. Sillanpää, "Adsorption of Ni(II), Cu(II) and Cd(II) from aqueous solutions by amino modified nanostructured microfibrillated cellulose," *Cellulose,* vol. 21, no. 3, pp. 1471-1487, 2014.

[70] M. Monier, A. A. Ibrahim, M. M. Metwally and D. S. Badawy, "Surface ion-imprinted amino-functionalized cellulosic cotton fibers for selective extraction of Cu(II) ions," *International Journal of Biological Macromolecules,* vol. 81, pp. 736-746, 2015.

[71] Z. Dong, J. Liu, W. Yuan, Y. Yi and L. Zhao, "Recovery of Au(III) by radiation synthesized aminomethyl pyridine functionalized adsorbents based on cellulose," *Chemical Engineering Journal,* vol. 283, pp. 504-513, 2016.

[72] B. Ram and G. S. Chauhan, "New spherical nanocellulose and thiol-based adsorbent for rapid and selective removal of mercuric ions," *Chemical Engineering Journal,* vol. 331, no. September 2017, pp. 587-596, 2018.

[73] L. Chai, Q. Li, Y. Zhu, Z. Zhang, Q. Wang, Y. Wang and Z. Yang, "Synthesis of thiol-functionalized spent grain as a novel adsorbent for divalent metal ions," *Bioresource Technology,* vol. 101, no. 15, pp. 6269-6272, 2010.

[74] Z. Wu, Z. Cheng and W. Ma, "Adsorption of Pb(II) from glucose solution on thiol-functionalized cellulosic biomass," *Bioresource Technology,* vol. 104, pp. 807-809, 2012.

[75] R. Yang, K. B. Aubrecht, H. Ma, R. Wang, R. B. Grubbs, B. S. Hsiao and B. Chu, "Thiol-modified cellulose nanofibrous composite membranes for chromium (VI) and lead (II) adsorption," *Polymer,* vol. 55, no. 5, pp. 1167-1176, 2014.

[76] Z. Zhang, Y. Cao, L. Chen and Z. Huang, "Preparation of thiol-functionalized cellulose and its application to the removal of hg (II) from water environment," *Cellulose Chemistry and Technology,* vol. 51, no. 5-6, pp. 559-567, 2017.

[77] M. Anbia and F. Rahimi, "Adsorption of platinum(IV) from an aqueous solution with magnetic cellulose functionalized with thiol and amine as a nano-active adsorbent," *Journal of Applied Polymer Science,* vol. 134, no. 39, pp. 1-8, 2017.

[78] H. Y. Choi, J. H. Bae, Y. Hasegawa, S. An, I. S. Kim, H. Lee and M. Kim, "Thiol-functionalized cellulose nanofiber membranes for the effective adsorption of heavy metal ions in water," *Carbohydrate Polymers,* vol. 234, no. January, p. 115881, 2020.

[79] C. Ruan, M. Strømme and J. Lindh, "A green and simple method for preparation of an efficient palladium adsorbent based on cysteine functionalized 2,3-dialdehyde cellulose," *Cellulose,* vol. 23, no. 4, pp. 2627-2638, 2016.

[80] L. Rong, Z. Zhu, B. Wang, Z. Mao, H. Xu, L. Zhang, Y. Zhong and X. Sui, "Facile fabrication of thiol-modified cellulose sponges for adsorption of Hg2+ from aqueous solutions," *Cellulose,* vol. 25, no. 5, pp. 3025-3035, 2018.

[81] E. Graf, Ullmann's Encyclopedia of Industrial Chemistry, Weinheim: Wiley-VCH, 1987.

[82] C. Bernido, H. Omichi, A. Katakai and J. Okamoto, "Use of Amidoxime-Group-Containing Adsorbent for the Recovery of Uranium and Other Elements from Phosphoric Acid Solution," *Separation Science and Technology,* vol. 23, no. 1-3, pp. 35-47, 1988.

[83] R. Qu, Y. Zhang, W. Qu, C. Sun, J. Chen, Y. Ping, H. Chen and Y. Niu, "Mercury adsorption by sulfur- and amidoxime-containing bifunctional silica gel based hybrid materials," *Chemical Engineering Journal,* vol. 219, pp. 51-61, 2013.

[84] Y. Wang, X. Ma, Y. Li, X. Li, L. Yang, L. Ji and Y. He, "Preparation of a novel chelating resin containing amidoxime-guanidine group and its recovery properties for silver ions in aqueous solution," *Chemical Engineering Journal,* vol. 209, pp. 394-400, 2012.

[85] Z. Zhao, X. Li, Y. Chai, Z. Hua, Y. Xiao and Y. Yang, "Adsorption Performances and Mechanisms of Amidoxime Resin toward Gallium(III) and Vanadium(V) from Bayer Liquor," *ACS Sustainable Chemistry and Engineering,* 2016.

[86] T. SUZUKI, K. SAITO, T. SUGO, H. OGURA and K. OGUMA, "Fractional Elution and Determination of Uranium and Vanadium Adsorbed on Amidoxime Fiber from Seawater," *Analytical Sciences,* vol. 16, no. 4, pp. 429-432, 2000.

[87] S. Kyoichi, U. Kazuya, T. Hori, S. Furusaki, T. Sugo and J. Okamoto, "Recovery of uranium from seawater using amidoixme hollow fibers," *AlChE Journal,* vol. 34, no. 3, pp. 411-416, 1988.

[88] K. Schwochau, "Extraction of Metals from Sea Water," *Inorganic Chemistry,* vol. 124, pp. 91-133, 1984.

[89] H. Omichi, A. Katakai, T. Sugo and J. Okamoto, "A New Type of Amidoxime-Group-Containing Adsorbent for the Recovery of Uranium from Seawater," *Separation Science and Technology,* vol. 20, no. 2-3, pp. 163-178, 1 4 1985.

[90] P. A. Kavakli, N. Seko, M. Tamada and O. Güven, "Adsorption efficiency of a new adsorbent towards uranium and vanadium ions at low concentrations," *Separation Science and Technology,* vol. 39, no. 7, pp. 1631-1643, 2004.

[91] A. S. Ivanov, C. J. Leggett, B. F. Parker, Z. Zhang, J. Arnold, S. Dai, C. W. Abney, V. S. Bryantsev and L. Rao, "Origin of the unusually strong and selective binding of vanadium by polyamidoximes in seawater," *Nature Communications,* 2017.

[92] B. F. Parker, S. Hohloch, J. R. Pankhurst, Z. Zhang, J. B. Love, J. Arnold and L. Rao, "Interactions of vanadium(iv) with amidoxime ligands: Redox reactivity," *Dalton Transactions,* 2018.

[93] S. O. Kang, S. Vukovic, R. Custelcean and B. P. Hay, "Cyclic imide dioximes: Formation and hydrolytic stability," *Industrial and Engineering Chemistry Research,* 2012.

[94] A. Nilchi, R. Rafiee and A. A. Babalou, "Adsorption behavior of metal ions by amidoxime chelating resins," *Macromolecular Symposia,* vol. 274, no. 1, pp. 101-108, 2008.

[95] A. S. El-Khouly, Y. Takahashi, A. A. Saafan and Y. A. Hafiz, "Study of Heavy Metal Ion Adsorbance by Amidoxime Group Introduced to Cellulose-Graft-Polyacrylonitrile," *Journal of Applied Polymer Science,* vol. 120, no. 5, pp. 866-873, 2010.

[96] R. R. Mohamed and M. W. Sabaa, "Graft Copolymerization of Acrylonitrile and its Amidoxime Derivative onto Chitosan," *Journal of Applied Polymer Science,* vol. 116, no. 5, pp. 2658-2667, 2010.

[97] L. Bretherick, Handbook of Reactive Chemical Hazards: An Indexed Guide to Published Data, Elsevier, 2017.

[98] T. Budtova and P. Navard, "Cellulose in NaOH–water based solvents: a review," *Cellulose,* vol. 23, no. 1, pp. 5-55, 2016.

[99] R. Sescousse, R. Gavillon and T. Budtova, "Wet and dry highly porous cellulose beads from cellulose-NaOH-water solutions: Influence of the preparation conditions on beads shape and encapsulation of inorganic particles," *Journal of Materials Science,* vol. 46, no. 3, pp. 759-765, 2011.

[100] N. Reddy and Y. Yang, "Introduction to Regenerated Cellulose Fibers BT - Innovative Biofibers from Renewable Resources," N. Reddy and Y. Yang, Eds., Berlin, Heidelberg, Springer Berlin Heidelberg, 2015, pp. 51-54.

[101] E. C. VIGLIANI, "Carbon disulphide poisoning in viscose rayon factories.," *British journal of industrial medicine,* vol. 11, no. 4, pp. 235-244, 1954.

[102] B. Morgenstern and H.-W. Kammer, "Solvation in Cellulose-LiCl-DMAc Solutions," *Trends in Polymer Science,* vol. 4, no. 3, pp. 87-91, 1996.

[103] S. Köhler and T. Heinze, "New solvents for cellulose: Dimethyl sulfoxide/ammonium fluorides," *Macromolecular Bioscience,* vol. 7, no. 3, pp. 307-314, 2007.

[104] J. Trygg, P. Fardim, M. Gericke, E. Mäkilä and J. Salonen, "Physicochemical design of the morphology and ultrastructure of cellulose beads," *Carbohydrate Polymers,* vol. 93, no. 1, pp. 291-299, 2013.

[105] M. Gericke, J. Trygg and P. Fardim, "Functional cellulose beads: Preparation, characterization, and applications," *Chemical Reviews,* vol. 113, no. 7, pp. 4812-4836, 2013.

[106] J. A. Davis and J. O. Leckie, "Effect of Adsorbed Complexing Ligands on Trace Metal Uptake by Hydrous Oxides," *Environmental Science and Technology,* vol. 12, no. 12, pp. 1309-1315, 1978.

[107] R. L. Tseng, F. C. Wu and R. S. Juang, "Effect of complexing agents on liquid-phase adsorption and desorption of copper(II) using chitosan," *Journal of Chemical Technology and Biotechnology,* vol. 74, no. 6, pp. 533-588, 1999.

[108] J. M. Tobin, D. G. Cooper and R. J. Neufeld, "Influence of anions on metal adsorption by Rhizopus arrhizus biomass," *Biotechnology and Bioengineering,* vol. 30, no. 7, pp. 882-886, 1987.

[109] C. Escudero, C. Gabaldón, P. Marzal and I. Villaescusa, "Effect of EDTA on divalent metal adsorption onto grape stalk and exhausted coffee wastes," *Journal of Hazardous Materials,* vol. 152, no. 2, pp. 476-485, 2008.

[110] Y. Liu, Z. Lou, Y. Sun, X. Zhou, S. A. Baig and X. Xu, "Influence of complexing agent on the removal of Pb(II) from aqueous solutions by modified mesoporous SiO2," *Microporous and Mesoporous Materials,* vol. 246, pp. 1-13, 2017.

[111] K. Foo and B. Hameed, "Insights into the modeling of adsorption isotherm systems," *Chemical Engineering Journal,* vol. 156, no. 1, pp. 2-10, 2010.

[112] Springer Nature Limited, "A Nobel Prizer for Dr. Irving Langmuir," *Nature,* p. 768, 19 November 1932.

[113] B. Meroufel, O. Benali, M. Benyahia, Y. Benmoussa and M. Zenasni, "Adsorptive removal of anionic dye from aqueous solutions by Algerian kaolin: Characteristics, isotherm, kinetic and thermodynamic studies," *Journal of Materials and Environmental Science,* vol. 3, no. 4, pp. 482-491, 2013.

[114] H. Freundlich, Kapillarchemie, eine Darstellung der Chemie der Kolloide und verwandter Gebiete, Akademische Verlagsgesellschaft, 1922.

[115] R. Sips, "On the Structure of a Catalyst Surface," *Journal of Chemical Physics,* vol. 5, no. 16, pp. 490-495, 1948.

[116] J. Skopp, "Derivation of the Freundlich Adsorption Isotherm from Kinetics," *Journal of Chemical Education,* vol. 86, no. 11, pp. 1341-1343, 2009.

[117] G. Sposito, "Derivation of the Freundlich Equation for Ion Exchange Reactions in Soils," *Soil Science Society of America Journal,* vol. 44, no. 3, pp. 652-654, 1980.

[118] C. H. Bolster and G. M. Hornberger, "On the Use of Linearized Langmuir Equations," *Soil Science Society of America Journal,* vol. 71, no. 6, pp. 1796-1806, 2007.

[119] Y.-S. Ho, "Isotherms for the Sorption of Lead onto Peat: Comparison of Linear and Non-linear methods," *Polish Journal of Environmental Studies,* vol. 15, no. 1, pp. 81-86, 2006.

[120] National Center for Biotechnology Information, "Acrylonitrile," 2019. [Online]. Available: https://pubchem.ncbi.nlm.nih.gov/compound/Acrylonitrile. [Accessed 13 February 2020].

[121] D. M. Levine, P. P. Ramsey and R. K. Smidt, Applied Statistics for Engineers and Scientists, Upper Saddle River: Prentice-Hall Inc. , 2001.

[122] VWR Canada, "VWR Signature™ Ergonomic High Performance Single-Channel Variable Volume Pipettors," 2020. [Online]. Available: https://ca.vwr.com/store/product/en/4698601/vwr-signaturetm-ergonomic-high-performance-single-channel-variable-volume-pipettors. [Accessed 13 March 2020].

[123] J. Burgess, Metal Ions in Solution, New York: Chichester, 1978.

[124] IPCS INCHEM, "Acrylonitrile," WHO, March 2001. [Online]. Available: http://www.inchem.org/documents/icsc/icsc/eics0092.htm. [Accessed 20 March 2020].

[125] A. Buchter and P. H, "Clinical toxicology of acrylonitrile," *G Ital Med Lav,* vol. 6, pp. 6-83, 1984.

[126] J. Zhou and L. Zhang, "Solubility of cellulose in NaOH/Urea Aqueous Solution," *Polymer Journal,* vol. 32, no. 10, pp. 866-870, 2000.

[127] B. Duchemin, "Mercerisation of cellulose in aqueous NaOH at low concentrations," *Green Chemistry,* vol. 17, no. 7, pp. 3941-3947, 2015.

[128] B. S. Rabinovitch and C. A. Winkler, "Kinetics of the alkaline hydrolysis of propionitrile," *Canadian Journal of Research,* vol. 20b, no. 9, pp. 185-188, 1942.

[129] A. R. Forrester, H. Irikawa, R. H. Thomson, S. O. Woo and T. J. King, "Iminyls. Part 8. Intramolecular addition to nitrile groups," *Journal of the Chemical Society, Perkin Transactions 1,* pp. 1712-1720, 1981.

[130] J. A. Elvidge, R. P. Linstead and A. M. Salaman, "37. Heterocyclic imines and amines. Part IX. Glutarimidine and the imidine from α-phenylglutaronitrile," *Journal of the Chemical Society (Resumed),* vol. 0, no. 0, pp. 208-215, 1959.

[131] F. Eloy and R. Lenaers, "The chemistry of amidoximes and related compounds," *Chemical Reviews,* vol. 62, no. 2, pp. 155-183, 1962.

[132] F. H. Fry, B. A. Dougan, N. McCann, C. J. Ziegler and N. E. Brasch, "Characterization of novel vanadium(III)/acetate clusters formed in aqueous solution," *Inorganic Chemistry,* vol. 44, no. 15, pp. 5197-5199, 2005.

[133] S. Salehi and A. Mansoor, "Performance comparison of chitosan-clinoptilolite nanocomposites as adsorbents for vanadium in aqueous media," *Cellulose,* vol. 26, pp. 5321-5345, 2019.

[134] M. Jansson-Charrier, E. Guibal, J. Roussy, B. Delanghe and P. Le Cloirec, "Vanadium (IV) sorption by chitosan: Kinetics and equilibrium," *Water Research,* vol. 30, no. 2, pp. 467-475, 1996.

[135] T. Roberto Santana Cadaval Jr., G. Luiz Dotto, E. Rosa Seus, N. Mirlean and L. Antonio de Almeida Pinto, "Vanadium removal from aqueous solutions by adsorption onto chitosan films," *Desalination and Water Treatment,* vol. 57, no. 35, pp. 16583-16591, 2016.

[136] T. Wang, Z. Cheng, B. Wang and W. Ma, "The influence of vanadate in calcined Mg/Al hydrotalcite synthesis on adsorption of vanadium (V) from aqueous solution," *Chemical Engineering Journal,* Vols. 181-182, pp. 182-188, 2012.

[137] A. Naeem, P. Westerhoff and S. Mustafa, "Vanadium removal by metal (hydr)oxide adsorbents," *Water Research,* vol. 41, no. 7, pp. 1596-1602, 2007.

[138] N. H. Mthombeni, S. Mbakop, A. Ochieng and M. S. Onyango, "Vanadium (V) adsorption isotherms and kinetics using polypyrrole coated magnetized natural zeolite," *Journal of the Taiwan Institute of Chemical Engineers,* vol. 66, pp. 172-180, 2016.

[139] C. Namasivayam and D. Sangeetha, "Removal and recovery of vanadium(V) by adsorption onto ZnCl2 activated carbon: Kinetics and isotherms," *Adsorption,* vol. 12, pp. 103-117, 2006.

[140] D. M. Manohar, B. F. Noeline and T. S. Anirudhan, "Removal of Vanadium(IV) from Aqueous Solutions by Adsorption Process with Aluminum-Pillared Bentonite," *Ind. Eng. Chem. Res.,* vol. 44, no. 17, pp. 6676-6684, 2005.

[141] S. C. Chang and G. A. Jeffrey, "The crystal structure of a basic chromium acetate compound, [OCr3(CH3COO)6.3H2O] + Cl-.6H2O, having feeble paramagnetism," *Acta Crystallographica Section B Structural Crystallography and Crystal Chemistry,* vol. 26, no. 6, pp. 673-683, 1970.

[142] W. L. McCabe, J. C. Smith and H. Peter, Unit Operations of Chemical Engineering, New York: McGraw-Hill, 2005.

[143] M. Rhodes, Introduction to Particle Technology, John Wiley & Sons, 2008.

Appendix A – Permissions

For figures that were reproduced and were not classified under designation of Creative Commons, permissions were obtained.

The permission associated with Figure 9 is shown below.

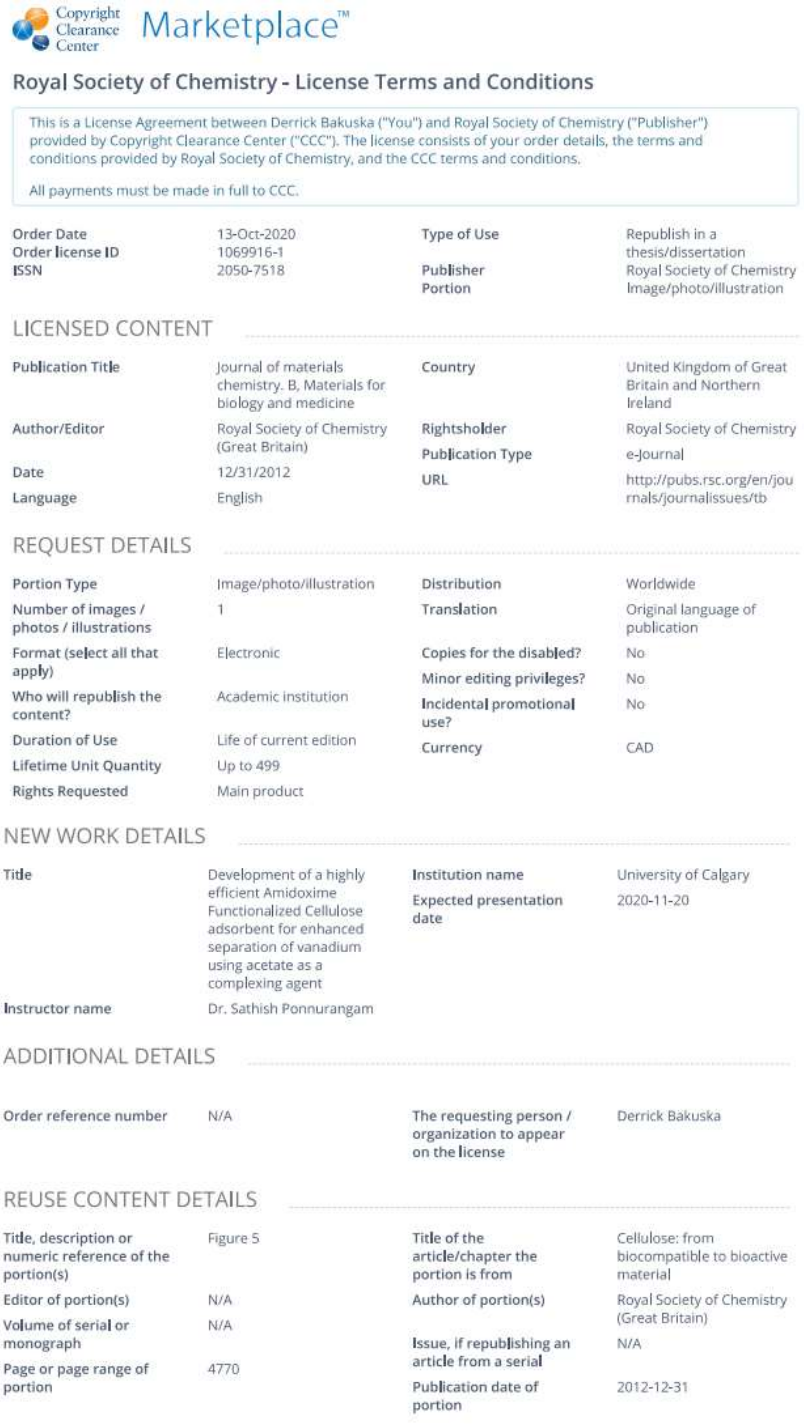

Copyright Clearance Center Marketplace™

Royal Society of Chemistry - License Terms and Conditions

This is a License Agreement between Derrick Bakuska ("You") and Royal Society of Chemistry ("Publisher") provided by Copyright Clearance Center ("CCC"). The license consists of your order details, the terms and conditions provided by Royal Society of Chemistry, and the CCC terms and conditions.

All payments must be made in full to CCC.

Order Date	13-Oct-2020	Type of Use	Republish in a thesis/dissertation
Order license ID	1069916-1		
ISSN	2050-7518	Publisher	Royal Society of Chemistry
		Portion	Image/photo/illustration

LICENSED CONTENT

Publication Title	Journal of materials chemistry. B, Materials for biology and medicine	Country	United Kingdom of Great Britain and Northern Ireland
Author/Editor	Royal Society of Chemistry (Great Britain)	Rightsholder	Royal Society of Chemistry
		Publication Type	e-Journal
Date	12/31/2012	URL	http://pubs.rsc.org/en/journals/journalissues/tb
Language	English		

REQUEST DETAILS

Portion Type	Image/photo/illustration	Distribution	Worldwide
Number of images / photos / illustrations	1	Translation	Original language of publication
Format (select all that apply)	Electronic	Copies for the disabled?	No
		Minor editing privileges?	No
Who will republish the content?	Academic institution	Incidental promotional use?	No
Duration of Use	Life of current edition	Currency	CAD
Lifetime Unit Quantity	Up to 499		
Rights Requested	Main product		

NEW WORK DETAILS

Title	Development of a highly efficient Amidoxime Functionalized Cellulose adsorbent for enhanced separation of vanadium using acetate as a complexing agent	Institution name	University of Calgary
		Expected presentation date	2020-11-20
Instructor name	Dr. Sathish Ponnurangam		

ADDITIONAL DETAILS

Order reference number	N/A	The requesting person / organization to appear on the license	Derrick Bakuska

REUSE CONTENT DETAILS

Title, description or numeric reference of the portion(s)	Figure 5	Title of the article/chapter the portion is from	Cellulose: from biocompatible to bioactive material
Editor of portion(s)	N/A	Author of portion(s)	Royal Society of Chemistry (Great Britain)
Volume of serial or monograph	N/A	Issue, if republishing an article from a serial	N/A
Page or page range of portion	4770	Publication date of portion	2012-12-31

The permission associated with Figure 30 is shown below.